

การพัฒนาระบบจัดเก็บฝุ่นสำหรับโรงสีข้าว โดยใช้ชั้นแกลบ



นาย ศิระ ศรีนิเวศน์

สถาบันวิทยบริการ

จุฬาลงกรณ์มหาวิทยาลัย

วิทยานิพนธ์นี้เป็นส่วนหนึ่งของการศึกษาตามหลักสูตรปริญญาวิศวกรรมศาสตรมหาบัณฑิต

สาขาวิชาวิศวกรรมเคมี ภาควิชาวิศวกรรมเคมี

คณะวิศวกรรมศาสตร์ จุฬาลงกรณ์มหาวิทยาลัย

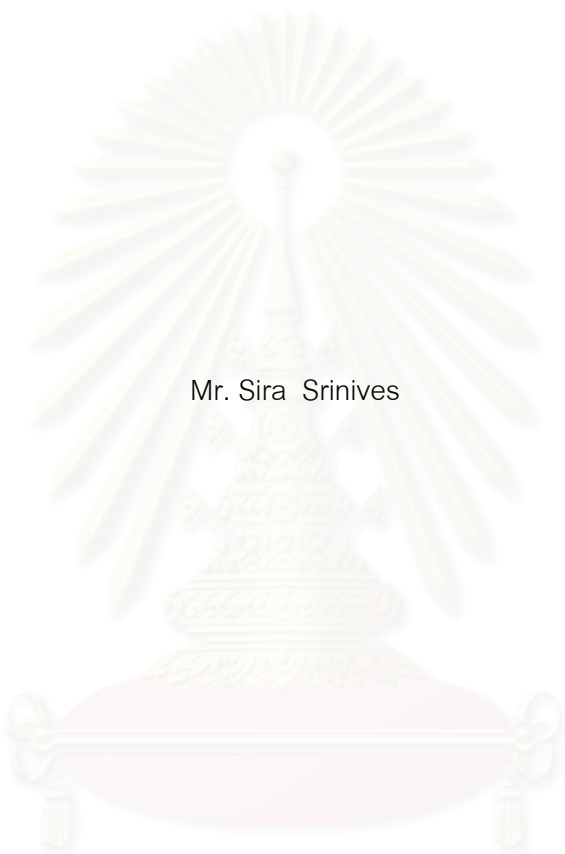
ปีการศึกษา 2548

ISBN 974-53-2828-6

ลิขสิทธิ์ของจุฬาลงกรณ์มหาวิทยาลัย

DEVELOPMENT OF RICE MILL DUST COLLECTION SYSTEM
USING RICE HUSK BED

Mr. Sira Srinives



สถาบันวิทยบริการ
จุฬาลงกรณ์มหาวิทยาลัย

A Thesis Submitted in Partial Fulfillment of the Requirements
for the Degree of Master of Engineering Program in Chemical Engineering

Department of Chemical Engineering

Faculty of Engineering

Chulalongkorn University

Academic Year 2005

ISBN 974-53-2828-6

ศิระ ศรีนิเวศน์ : การพัฒนาระบบจับเก็บฝุ่นสำหรับโรงสีข้าว โดยใช้ชั้นแกลบ

(DEVELOPMENT OF RICE MILL DUST COLLECTION SYSTEM USING RICE

HUSK BED) อ. ที่ปรึกษา: รศ.ดร. ธวัชชัย ชรินพานิชกุล, อ. ที่ปรึกษาร่วม: ศ. ดร. วิวัฒน์

ดิษฐ์พานิชกุล จำนวนหน้า 121 หน้า.

ISBN 974-53-2828-6

วัสดุเหลือใช้หรือของเสียทางการเกษตรที่มีลักษณะรูปร่างเป็นแผ่นบาง เป็นเม็ด หรือเป็นเส้นใย อาจมีศักยภาพในการเป็นวัสดุกรองประสิทธิภาพสูงได้ ในงานวิจัยนี้ทางนักวิจัยได้ทำการออกแบบอุปกรณ์จับเก็บฝุ่นรูปร่างคล้ายไซโลขึ้น โดยอาศัยหลักการการกรองฝุ่นด้วยชั้นกรองอัด และทำการทดลองเพื่อสนับสนุนแนวคิดในการออกแบบ ในเบื้องต้น ทดลองนำเอาแกลบมาเป็นวัสดุกรอง และเสนอให้นำอุปกรณ์จับเก็บฝุ่นดังกล่าวไปใช้ในการกรองลมฝุ่นที่รั่วไหลออกมาจากโรงสีข้าว อุปกรณ์จับเก็บฝุ่นที่ออกแบบได้ มีประโยชน์ไม่ใช่ว่าเพียงเพื่อดักจับฝุ่นละอองเท่านั้น แต่ยังทำหน้าที่เป็นภาชนะบรรจุแกลบ เก็บรักษาแกลบจากฝนและลมได้อีกด้วย ในการทดลอง ทางนักวิจัยได้ทำการศึกษาประสิทธิภาพการกรองของชั้นอัดของแกลบ ที่ความหนาชั้นอัดที่ 0.125 0.25 และ 0.5 เมตร ตามลำดับ โดยนำเอาชั้นกรองมากรองฝุ่นของแคลเซียมคาร์บอเนต (ขนาดอนุภาคโคโรลัมที่ 1.6 ไมโครเมตร) ออกจากลมฝุ่น ความเร็วการกรองถูกแปรผันอยู่ในช่วง 0.22 0.48 0.63 และ 0.81 เมตรต่อวินาที ประสิทธิภาพการกรองที่ได้ของชั้นอัดของแกลบมีค่าอยู่ในระดับที่น่าพอใจ คือ 87 – 99% โดยน้ำหนัก

สถาบันวิทยบริการ จุฬาลงกรณ์มหาวิทยาลัย

ภาควิชา วิศวกรรมเคมี
สาขาวิชา วิศวกรรมเคมี
ปีการศึกษา 2548

ลายมือชื่อนิสิต..... ศิระ ศรีนิเวศน์
ลายมือชื่ออาจารย์ที่ปรึกษา.....
ลายมือชื่ออาจารย์ที่ปรึกษาร่วม.....

4670521821 : MAJOR ENGINEERING

KEY WORD: RICE HUSK / PACKED BED / DUST COLLECTION / AIR FILTRATION / AIR POLLUTION/ FINE DUST/ SUBMICROMETER PARTICLES

SIRA SRINIVES: DEVELOPMENT OF RICE MILL DUST COLLECTION SYSTEM USING RICE HUSK BED.THESIS ADVISOR: ASSOC. PROF. TAWATCHAI CHARINPANITKUL, THESIS CO-ADVISOR : PROF. WIWUT TANTHAPANICHAKOON, 121 pp. ISBN 974-53-2828-6.

Agricultural residues or waste with grain-like or fibrous shapes has potential to be high-efficiency dust-filtration media. In this research, an innovative dust collecting silo was designed, based on the principle of packed-bed filtration and supported by experimental results. The packed husk filter was employed to clean the dust-laden air, emitted from a rice mill. The proposed system was not only useful in collecting fine dust but also served as husk storage, protecting raw husk from the effect of rain and wind. The dust collection efficiencies of the rice husk bed with a thickness of 0.125, 0.25, and 0.5 meters were investigated by filtrating fine dust of calcium carbonate particles (average size = 1.6 μm .) from dust-laden air. The filtration face velocity was varied from 0.22, 0.48, 0.63 to 0.81 m/s. The observed experimental efficiency lay between 87 – 99%.

สถาบันวิทยบริการ
จุฬาลงกรณ์มหาวิทยาลัย

Department Chemical Engineering

Field of study Chemical Engineering

Academic year 2005

Student's signature..... *Sira Srinives*

Advisor's signature..... *T. Charinpanitkul*

Co-advisor's signature..... *W. Tanthapanichakoon*

ACKNOWLEDGEMENTS

This research has been well supported by Chulalongkorn University-Industry Collaborative Research Fund, Radchadapisek Sompoch Fund and MTEC Technology Unit Fund. Also, Assoc. Prof. Tawatchai Charinpanitkul and Prof. Wiwut Tanthapanichakoon received partial support from TRF-RTA Project (2002-2005).

Moreover, the author would like to thank you Mr. Mongkol Kaewmaha, legal officer of Chulalongkorn University Intellectual Property Institute, for his kind help in patent registration, Mahanakorn Tanyakit Co., Ltd. for their grateful support about rice husk material and information of rice mill processes, and Department of Mining & Petroleum Engineering for lending us the opacity meter.

Personally, the author would like to thank his beloved father and mother for all grateful advises and full support they always give, professor Wiwut, professor Tawatchai, professor Vichitra, and professor Jirdsak for their hospitality and understanding, and all CEPT members for their kind help.



สถาบันวิทยบริการ
จุฬาลงกรณ์มหาวิทยาลัย

CONTENTS

	Page
ABSTRACT IN THAI	iv
ABSTRACT IN ENGLISH	v
ACKNOWLEDGEMENT	vi
CONTENT	vii
LIST OF TABLES	x
LIST OF FIGURES	xi
NOMENCLATURE	xiv

CHAPTER

I INTRODUCTION

1.1 Literature reviews.....	2
1.2 Present status in a rice mill	
1.2.1 Rice mill process.....	10
1.2.2 Components of a rice grain.....	12
1.2.3 Data measured from line of treated air.....	13
1.2.4 Porosity of rice husk packed bed.....	15
1.2.5 Equivalent diameter of rice husk.....	15
1.3 Problem Identification.....	19

II OBJECTIVE AND SCOPE OF RESEARCH

2.1 Objectives.....	22
2.2 Scope.....	22
2.3 Expected benefit.....	22

III FUNDAMENTAL THEORY

3.1 Dust collection mechanisms.....	23
3.1.1 Interception.....	24
3.1.2 Inertial impaction.....	25
3.1.3 Diffusion.....	27
3.1.4 Gravitational settling.....	27
3.1.5 Electrostatic.....	28
3.2 Overall dust collection efficiency.....	28

IV LABORATORY SCALE UNIT, DESIGN AND EXPERIMENT

4.1 Laboratory Scale System Design.....	31
4.2 Experimental Procedures and Results.....	42
4.2.1 Experimental procedures.....	42
4.2.2 Experimental results and discussions.....	44
4.3 Comparing of pressure drop results gained from experiments and calculation of Ergun equation.....	52
4.4 Comparison of Dust collection efficiency measured from the experiments and results estimated by the theory of deposition mechanism.....	56
4.5 Conclusions.....	62

V DESIGN OF RICE MILL DUST COLLECTION SYSTEM

5.1 Calculation of required thickness of rice-husk filter media.....	63
5.1.1 Face velocity and filtration area.....	63
5.1.2 Minimum require of media thickness.....	64
5.2 Dimension designations.....	70
5.2.1 Dimension of effluent pipe.....	71
5.2.2 Appropriated thickness of media filter and void spaces.....	71
5.2.3 Dimension of storey of media filter.....	73
5.2.4 Dimension of silo.....	76
5.3 Calculation of pressure drop.....	79
5.3.1 Pressure drop due to the effect of pipe line system.....	80
5.3.2 Pressure drop due to the effect of clean rice husk media.....	85
5.3.3 Pressure drop due to the effect of dust cake layer.....	86
5.4 The maximum dust collection efficiency.....	89

REFERENCES.....	91
APPENDICES.....	93
APPENDIX A1 Properties of rice husk sample (Tested by Powder Tester).....	94
APPENDIX A2 Properties of rice mill dust particles (Tested by Powder Tester).....	96
APPENDIX A3 Properties of Turbo 1 dust particles (Tested by Powder Tester).....	98

APPENDIX B Method of finding equivalent diameter based on terminal velocity.....	99
APPENDIX C1 Distribution curve of rice mill dust particle Tested by Mastersizer.....	102
APPENDIX C2 Distribution curve of Turbo 1 dust particles Tested by Mastersizer.....	103
APPENDIX D1 Minimum fluidization velocity.....	104
APPENDIX D2 Calculation procedure related to saturated zone.....	105
VITA.....	107



สถาบันวิทยบริการ
จุฬาลงกรณ์มหาวิทยาลัย

LIST OF TABLES

		Page
Table 1.1	Estimated percentages of mass decrease of rice grain in each stage of rice mill processes.....	13
Table 1.2	Air velocity measured at the sampling point.....	14
Table 1.3	Results of equivalent diameter from three methods of calculation....	19
Table 4.1	Operating conditions for laboratory-scale system.....	43
Table 4.2	Equivalent Diameters calculated by four methods.....	53
Table 4.3	Initial experimental versus predicted pressure drops obtained from calculations, using the equivalent diameters in Table 4.2.....	53
Table 4.4	Calculation results of pressure drop corresponding to $D_{EV} = 1.593$ mm.....	55
Table 4.5	Calculation results of pressure drop corresponding to $D_{EV}^* = 0.421$ mm.....	55
Table 4.6	Calculated results of filtration efficiency corresponding to equivalent diameter appeared in Table 4.2.....	56
Table 4.7	Accurate calculated results of filtration efficiency corresponding to $D_{EV} = 1.593$ mm.....	59
Table 4.8	Comparison of experimental and calculated results when the saturated zone was included. ($D_{EV} = 1.593$ mm.).....	60
Table 5.1	Required thicknesses of filter media corresponding to each size of rice mill dust particles.....	69
Table 5.2	Overall dust collection efficiencies, corresponding to 1 meter of media filter	70
Table 5.3	The maximum dust collection efficiencies of the rice-husk packed bed dust collection system.....	90

LIST OF FIGURES

	Page
Figure 1.1	Collection efficiency measured as a function of aerosol particle diameter and face velocity. 2
Figure 1.2	Effect of particle number ratio on pressure drop change and cake height increase 3
Figure 1.3	Comparison of collection efficiencies of particles by fibrous filters as predicted by the moment method and direct integration method ... 5
Figure 1.4	Panel bed filter with “Puff back” renewal of filtration surfaces..... 6
Figure 1.5	Arrangement for study of puff back..... 6
Figure 1.6	Diagram showing three steps of dust formation..... 7
Figure 1.7	Pressure drop versus specific density of fly ash deposits laid down at room temperature..... 8
Figure 1.8	Fractional penetration of 1.1 μm . monodisperse aerosol through 6.3 cm. bed of 0.3-0.42 mm. sand with fly ash deposit. 9
Figure 1.9	Flow chart illustrating the rice mill process..... 11
Figure 1.10	Rice grain compositions..... 12
Figure 1.11	Cross-sectional area of pipe line..... 13
Figure 1.12	Isokinetic Sampling System..... 14
Figure 1.13	A simple system for measuring bed porosity..... 15
Figure 1.14	2.3-meter-high pipe was used to measure the terminal velocity of rice husk particle..... 16
Figure 1.15	Geometric model of rice husk particle..... 17
Figure 1.16	Geometric model of rice husk particle (2)..... 18
Figure 1.17	Size distribution curve of rice husk..... 19
Figure 1.18	Fine dust particles from rice husk..... 20
Figure 1.19	Schematic diagram of laboratory-scale system..... 21
Figure 3.1	Path way of a particle, collected by a medium filter due to the effect of interception mechanism..... 24
Figure 3.2	Path way of a particle, collected by a medium filter due to the effect of inertial impaction mechanism..... 25

	Page
Figure 3.3	Relations of η_1 against $Stk^{1/2}$ 26
Figure 3.4	Brownian motion of very small particles due to diffusion deposition mechanism..... 27
Figure 3.5	Model for mass balance..... 28
Figure 3.6	Model of an observed unit volume..... 29
Figure 4.1	Turbo 1 calcium carbonate dust particle..... 32
Figure 4.2	Schematic diagram of laboratory-scale system..... 32
Figure 4.3	A picture shot from the laboratory-scale unit..... 33
Figure 4.4	A photo of Blower..... 33
Figure 4.5	Calibration curve of air flow rate to pressure drop across the orifice meter..... 34
Figure 4.6	Calibration curve of accurate feeder with Turbo 1..... 35
Figure 4.7	Column and glass bead..... 35
Figure 4.8.1	Front part: Air Inlet..... 36
Figure 4.8.2	Middle part: rice husk media container..... 36
Figure 4.8.3	Rare part: treated air outlet..... 37
Figure 4.9	The combination of three parts..... 37
Figure 4.10	The net screen..... 38
Figure 4.11	Cyclone Dimension..... 39
Figure 4.12	Opacity Meter..... 40
Figure 4.13	HEPA Filter..... 41
Figure 4.14	Vacuum Pump..... 41
Figure 4.15	Well packed rice husk media filter in the media box..... 44
Figure 4.16	Correlation of Pressure Drop with Operation Time..... 44
Figure 4.17(a)	Dust cake formation [After 2 hours of operation, $U = 0.63$ m/s, thickness of media = 0.25 m.]..... 46
Figure 4.17(b)	The enlarged picture of dust cake layer..... 46
Figure 4.18	Dust cake formation (2) [After 2 hours of operation, $U = 0.63$ m/s, thickness of media = 0.5 m.]..... 47
Figure 4.19	Dust cake formation (3) [After 2 hours of operation, $U = 0.81$ m/s, thickness of media = 0.5 m.]..... 47

	Page
Figure 4.20	From a front view of filtration area [After 2 hours of operation, $U = 0.63$ m/s, thickness of media = 0.125 m.]..... 47
Figure 4.21	Relation of Dust Collection Efficiency with Operation Time..... 48
Figure 4.22	Packed bed of dust cake..... 49
Figure 4.23	Dust particles (smaller) fulfilling empty spaces between rice husk particles (bigger)..... 49
Figure 4.24	Correlation of Dust Collection Efficiency with Operation Time at 0.125 m. Media thickness..... 50
Figure 4.25	Correlation of Dust Collection Efficiency with Operation Time at 0.25 m. Media thickness..... 51
Figure 4.26	Correlation of Dust Collection Efficiency with Operation Time at 0.5 m. Media thickness..... 51
Figure 4.27	The model illustrating Saturated zone and clean zone in packed bed..... 60
Figure 5.1	Schematic diagram of the dust collector..... 71
Figure 5.2	Schematic diagram of the dust collector (2)..... 72
Figure 5.3	One storey of media filter..... 73
Figure 5.4	Dimensions of one storey of media..... 74
Figure 5.5	Eight pieces of dust inlet vane are arranged in octagonal shape..... 75
Figure 5.6	Model for the calculation of inlet vane..... 75
Figure 5.7	Model for the calculation of trapezium sheet..... 76
Figure 5.8	Dimension of gas inlet vanes and trapezium sheet..... 77
Figure 5.9	Schematic diagram of the dust collector (3)..... 78
Figure 5.10	Model for the calculation of bottom part and rice husk storage part..... 78
Figure 5.11	Model for the calculation of distance between rice husk storage and filtration zone..... 79
Figure 5.12	Schematic diagram of the dust collector with dimensions..... 79
Figure 5.13	Top view of perforated pipe..... 80
Figure 5.14	Line of exhausted pipe..... 83

NOMENCLATURES

A_F	Filtration area of media [m^2]
a	Coefficient of diffuse reflection
B	Ratio of slit width to the perimeter of pipe [-]
C	Orifice coefficient [-]
C_C	Cunningham correction factor [-]
C_{in}	Dust concentration in influent stream [g/m^3]
C_{out}	Dust concentration in effluent stream [g/m^3]
D	Particle Diffusion Coefficient [m^2/s]
D_E	Equivalent diameter [m]
D_{ES}	Equivalent in surface area of particle [m]
D_{ET}	Equivalent diameter based on the terminal velocity [m]
D_{ER}	Equivalent diameter based on the trials and errors (compared with experimental data) [m]
D_{EV}	Equivalent in volume of particle [m]
D_F	Diameter of perforated pipe [m]
D_p	The dust particle diameter [m]
D_m	The medium body diameter [m]
d_f	Diameter of fiber collector [m]
d_m	Diameter of media particle [m]
d_p	Diameter of dust particle [m]
F	Fanning factor [-]
Ku	Kuwabara hydrodynamic factor [-]
$N _x$	Concentration of dust in dust-laden air coming into the control volume at point x [g/m^3]
$N _{x+\Delta x}$	Concentration of dust in dust-laden air going out of the control volume at point $x+\Delta x$ [g/m^3]
N_{Re}	Dimensionless Reynolds number [-]
n_m	Amount of media particle appeared in a projected area of media filter [Particles]
P	Penetration ratio [-]

Pe	Dimensionless Peclet number [-]
Q	Flow rate of dust-laden air [m^3/s]
R	Interception dimensionless parameter [-]
S_p	Surface area of a media particle [m^2]
Stk	Stokes number [-]
t	The minimum required thickness of filter media [m]
U_o	Face velocity [m/s]
U	Filtration velocity, Air velocity [m/s]
V_p	Volume of a media particle [m^3]
ϵ	Porosity [-]
α	Solidity [-]
ΔP	Pressure drop [Pa]
ΔP_m	Pressure drop across the media filter [Pa]
ΔP_c	Pressure drop across the cake layer [Pa]
$\eta_{Media\ Particle}$	The total single-particle coefficient [-]
η_D	Individual efficiency contributed by diffusion [-]
η_E	Individual efficiency contributed by diffusion electrostatic [-]
η_G	Individual efficiency contributed by gravitational settling [-]
η_I	Individual efficiency contributed by inertial impaction [-]
$\eta_{Overall}$	The overall dust collection efficiency [-]
η_R	Individual efficiency contributed by interception [-]
λ	Gas mean free path [m]
ρ	Density of air [kg/m^3]
ρ_p	Density of dust particle [kg/m^3]
μ	Viscosity of air [kg/ms]

CHAPTER 1

INTRODUCTION

One of the most serious environmental concerns is recently focused on air pollution problem, caused by effects of aerosol, toxic gas, and green house gas etc. Especially, suspended particulate matter (SP) generated from both human activities and natural phenomena, such as fly ash and fine metallic particles, is not only harmful to human's respiratory system but also promote the amount of solar radiation reaching and burning the surface of the earth, which worsens global climate situation [1].

In the rice milling process, rice husk and rice kernel are separated from each other, and, as a result, tons of coarse and fine dust are generated, and emitted from rice mill site. The use of cyclone as a dust collecting system is widely accepted among rice mill owners, since it is easy to maintain, requires not much space, and is suitable for continuous processing. However, the cyclone could efficiently collect only dust particles that are larger than 3-5 micrometers [2], and a lot of fine dust still escapes and goes annoying people living in nearby area. Since high efficiency dust collectors, such as Bag filter and Electrostatic Precipitator (ESP), are too expensive for Thai rice mill to invest and operate, it is crucial to develop alternative secondary dust collector that could capture fine dust with lower fixed and operating costs.

Generally, most of the rice husk, separated from rice grain, will be collected and used as fuel material for the rice mill itself. However, in Thailand, the rice husk could also be used in other applications, for example; added as filler in promoting cement properties [3], used as adsorbent for waste water treatment [4, 5], or even used as a silica resource for synthesizing nanomaterials [4]. The use of natural fibers and particles as aerosol filtration media is quite well-known for a long time, and some published journal articles even mention the use of rice husk bed as a filter media. However, reliable data on the dust collection efficiency of rice husk bed are still not available. In this research, a laboratory-scale system is established to determine the dust collection efficiency of rice husk media, with respect to three variables, namely media thickness, face velocity, and dust cake layer thickness.

1.1 Literature review

M.T. Guise et al. [6] did research on applying packed bed silica aerogel microspheres (average diameter = 120 micrometers) to capture aerosol particles, ranging between 20 – 2000 nm. in size. The face velocity was varied from 3.4 to 20 and to 40 cm./s, which corresponded to the minimum size with minimum dust collection efficiency of 93%, 76% and 64%, respectively. Therefore collection efficiency would be increased with the decrease in filtration velocity. Moreover, according to figure 1.1, when the face velocity was raised from 3.4, to 20, and to 40 cm./s, the minimum size of particle responding to the minimum dust collection efficiency was shifted from 570 to 315 and to 300 nm., respectively. The minimum dust collection efficiency happened at the transition region, in which dust particles became too big to be captured by the diffusion mechanism and other deposition mechanisms, such as interception and inertia impaction, became more important. Obviously, when filtration velocity increased, the transition point appeared at a bigger particle size.

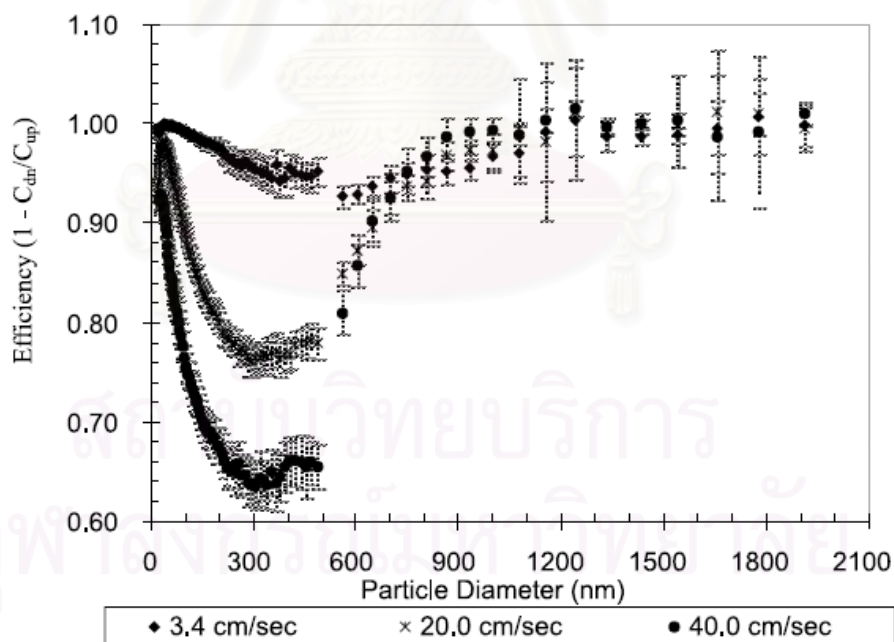


Figure 1.1 Collection efficiency measured as a function of aerosol particle diameter and face velocity. [6]

In conclusion, diffusion, direct interception, and inertia impaction were three major deposition mechanisms, by which aerosol particles were captured theoretically.

Roughly, for particle smaller than 0.5 micrometers, diffusion mechanism played its major role in collecting dust particles. And for dust particle bigger than 0.5 micrometers, effect of inertial impaction and interception mechanisms became predominated in dust collection efficiency.

Yoshiyuki Endo et al. [7] observed formation of dust cake, accumulated from “bimodal aerosol” which was a mixture of two types of dust particles with two different log-normal size distributions, Arizona road dust particles (average diameter = 2 micrometers, density = 265 g/cm³) and alumina particles (average diameter = 0.7 micrometers, density = 2.42 g/cm³). According to figure 1.2, effects of dust mass loading and number ratio of Arizona road dust particle to alumina particle were revealed in pressure drop across the glass fiber filter and dust cake, and cake height. Since Arizona road dust particle was nearly three times bigger than alumina particle, it contributed less effect to pressure drop, but more effect to the height of dust cake layer. The increase in number ratio of alumina particles to Arizona road dust particles increased the slopes of pressure drop curves; on the other hand, the said ratio provided just a small effect to the cake height. However, once both kinds of dust particle mixed equally, the fine particles (alumina) would fill in the inter-particle spaces, thereby not contributing to the increase in the height of cake layer.

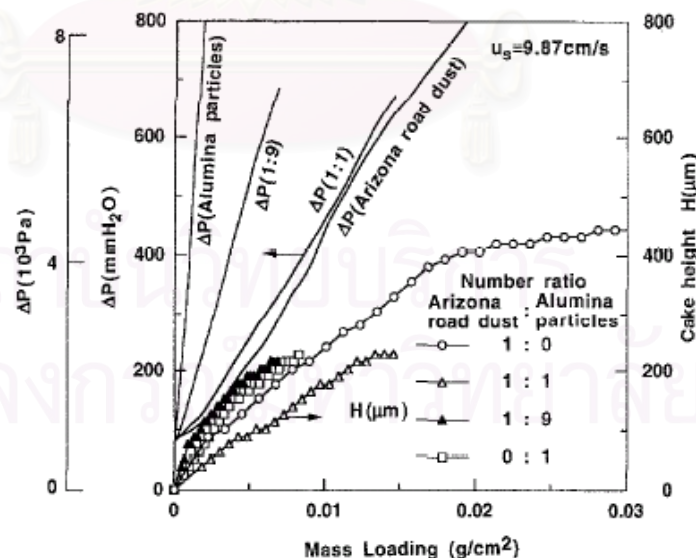


Figure 1.2 Effect of particle number ratio on pressure drop change and cake height increase [7]

Yoshiyuki Endo et al. [8] modified the Kozeny-Carman equation, used in predicting permeation resistance for fluid passing through particle layers in Stokes regime, by two ways of derivation, Channel theory and Drag theory. Among those two modified equations, the equation obtained from the Drag theory was found to be more useful than that from the Channel theory, since parameters involved in the former, such as the dynamic shape factor (κ) was more definitely stated than those in the latter, such as shape factor (Φ_S) and volume factor (Φ_V) which strongly rely on the figure of the particle. Nevertheless, both equations obtained show improvement over conventional Kozeny-carman equation, by including the effect of particle polydispersivity and non-spherical shape into the calculation.

H T Kim et. al. [9] focused on diffusional filtration efficiencies of polydispersed particles on fibrous and packed bed filters, based on an approximation method including integration of lognormal function moments, and another method, direct numerical integration of the penetration equation. Generally, Brownian diffusion is the dominant filtration mechanism for particles whose radius is smaller than 0.01 micrometers. In this kind of mechanism, the fact that the diffusion coefficient is inversely proportional to the size of dust particles means that smaller particles would rapidly be captured while bigger particles may pass farther through the packed bed column before being collected. In reality, aerosols are always polydispersed to a certain degree, and their size distribution is changing while being filtered, which offer high impact to the overall filtration efficiency. The filtration efficiencies predicted by the moment method are compared with those obtained by the direct numerical integration, as illustrated in Figure 1.3.

สถาบันวิทยบริการ
จุฬาลงกรณ์มหาวิทยาลัย

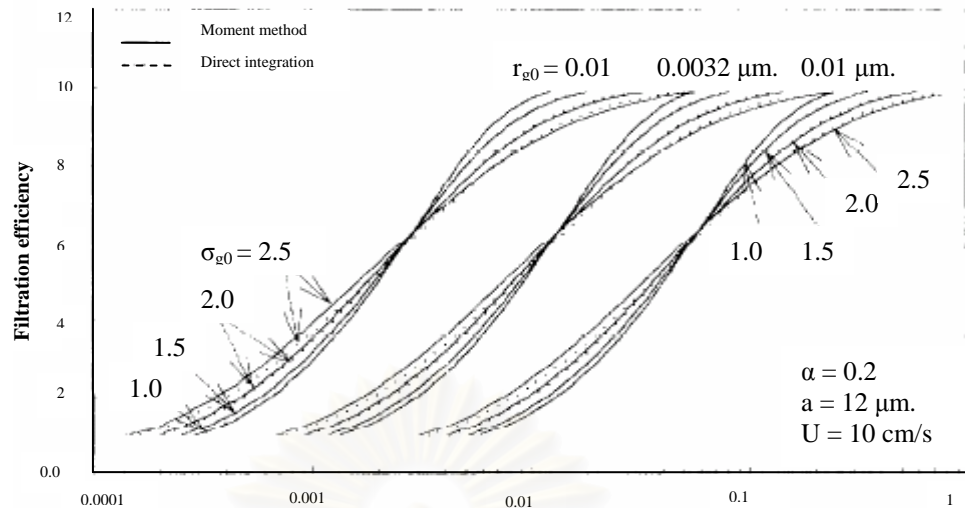


Figure 1.3 Comparison of collection efficiencies of particles by fibrous filters as predicted by the moment method and direct integration method. [8]

In both cases, at the early stage of filtration, the filtration efficiency responded to polydispersed aerosol ($\sigma_{g0} = 1.5, 2.0,$ and 2.5) would initially increase with the higher rate, along the length of the column, than that resulted from the monodispersed aerosol ($\sigma_{g0} = 1$). Anyway, since polydispersed aerosol contains both of small and large particles, after small particles are quickly deposited on filters at the early state of filtration the filtration efficiencies will be gradually retarded and therefore less than those of monodispersed aerosol. In figure 1.3, all curves are intersected in the same region, in which the filtration efficiency is about 0.6. Likewise, the moment method used in estimating the filtration efficiency of fibrous filters in the previous section could be applied to the packed bed. It is revealed that, as the polydispersed aerosol passes through the packed bed, the standard deviation of particle size distribution will decrease and the mean radius of the particles increases. In conclusion, the moment approximation method is shown to predict filtration efficiency for fibrous and packed-bed filters with an acceptable tolerance.

K.-C. Lee et al. [10, 11, 12] brought out a series of impressive research, including 5 serial papers, dealing with granular-bed filtration assisted by filter-cake formation. In the first paper of this series, a new soil failure mechanism, caused by sharp reversing puff of gas, was introduced. It was explained that the particles captured on gas entry surface of the granular bed would accumulated and boosted up

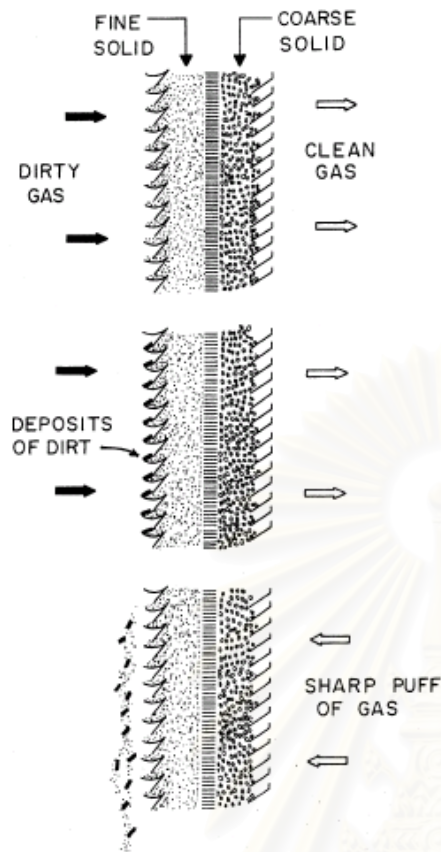


Figure 1.4 Panel bed filter with “puffback” renewal of filtration surfaces

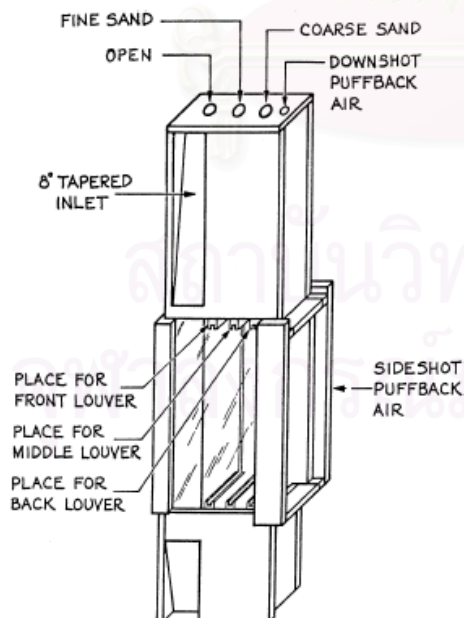


Figure 1.5 Arrangement for study of puffback.

the overall pressure drop across the bed. Up to one point, the cleaning stage would be initiated whereby the flow of dusty gas would be interrupted and a reverse flow, the so-called “puffback”, would cause the filter cake with surface layers of the media to fall out from the gas entry surfaces, thus renewing the surface of the granular-bed for another cycle of filtration. The 3 steps of puff back renewal of filtration surfaces were shown in Figure 1.4. Conventionally, the granular bed filtrates dust-laden air by “deep bed” dust capture mechanism, in which dust would accumulate deep inside the granular bed, not upon the gas-entry surface. So, it was unlikely for a deep-bed filtration device to collect lots of particles smaller than $5\ \mu\text{m}$. in size. However, a cake-forming granular bed filter was capable of achieving higher filtration efficiencies than the granular bed itself. An arrangement was settled and illustrated in Figure 1.5. Sand grain was sieved and grain size was controlled to use as a media filter, packing in an enclosed transparent box, held by louvers. In the second paper of this series [11], three kinds of dust, namely coal fly ash from Commonwealth Edison and Con Edison, and Portland cement dust, were used as aerosols and tested in the filtration

arrangement. The conclusion was that the pressure drop across the media just before the puffback exploit, gas face velocity and puffback intensity could affect the filtration efficiencies of the system. At low face velocity (7.75 and 11.1 cm/s), filtration efficiencies would not strongly vary with the puffback intensity, as they only changed in the range of 99.94 to 99.99%. Anyway, at the higher face velocity (17.2 cm/s), it was assumed that dust particles penetrate so deeply in the media filter that higher puffback intensity must be applied to spill larger amount of sand than the other two experiments. It was also revealed that 11.1 cm/s of face velocity was suitable for using in a commercial scale. Moreover, K.-C. Lee et al. found out that there were three steps of dust cake formation, as shown in Figure 1.6. Freshly sand media was filled shortly after the start of filtration. (On the left of Figure 1.6) This cake would become support for other particles to form cake layer. Up to this point, filtration efficiency was improved and dust cake penetrated deep into the surface of granular bed. These cakes penetrate too deeply for a puffback to spill them all out together with the sand, so they were left as “roots”, or permanent cake in the media filter. (On the center of Figure 1.6) Then, when the cake layer was too thick, the pressure drop across the cake became so large that parts of it broke away, and straight through, or pinholes, were formed, which would re-increase penetration of the system. (On the right hand side of Figure 1.6)

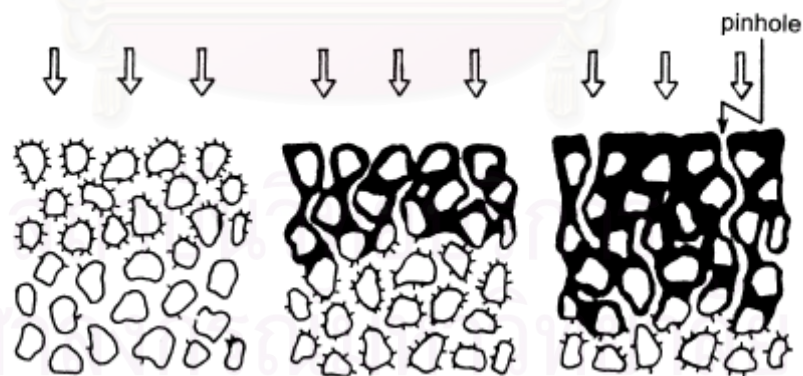


Figure 1.6 Diagram showing three steps of dust formation

The third paper in this series [12] is the last one to mention here. It concentrated on the filtration of 1.1 μm monodispersed aerosol with dust cake resting upon surfaces of three types of granular bed, including sand, silicon carbide and copper shot. K.-C. Lee went on his research and revealed that tensile strength of dust

cake layer increased monotonically from atmospheric temperature to 700 degree Celsius, and some kind of dust cake even showed major change in mechanical properties, when it was slowly heated to a critical temperature. Peukert [12] cited his PHD thesis and reported that granular particles larger than 1 mm. would usually not allow dust cake formation at an elevated temperature, which concurred with Lee's experiment, shown in Figure 1.7.

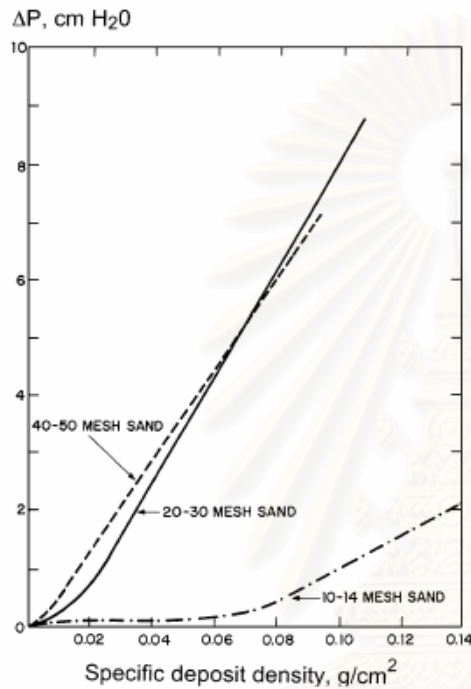


Figure 1.7 Pressure drop versus specific density of fly ash deposits laid down at room temperature. Air superficial velocity was set steady at 5.5 cm/s. It should be noted that 10–14 mesh = 1.4-2.0 mm., 20-30 mesh = 0.59-0.84 mm., and 40-50 mesh = 0.3-0.42 mm.

In Figure 1.7, when the size of sand reached 1.4-2 mm., the relation of specific deposit density, equal to mass of dust cake captured on filtration surface per filtration area, with pressure drop across the dust cake layer itself could easily be distinguished from the other two experiments, and agreed with Peukert's report. In addition, it was also noted that some types of granular bed might not able to capture some kinds of aerosol particles, if the aerosol possessed low cohesivity and low adhesivity toward the granular bed. Another interesting research, developed by Lee et al., concentrated on the fractional penetration of the filtration of 1.1 μm monodispersed fly-ash aerosol with 0.3-0.42 mm. sand at room temperature. Thickness of the sand granular bed was set at 6.3 cm, and by fly ash deposited upon the filtration surface as an initial cake.

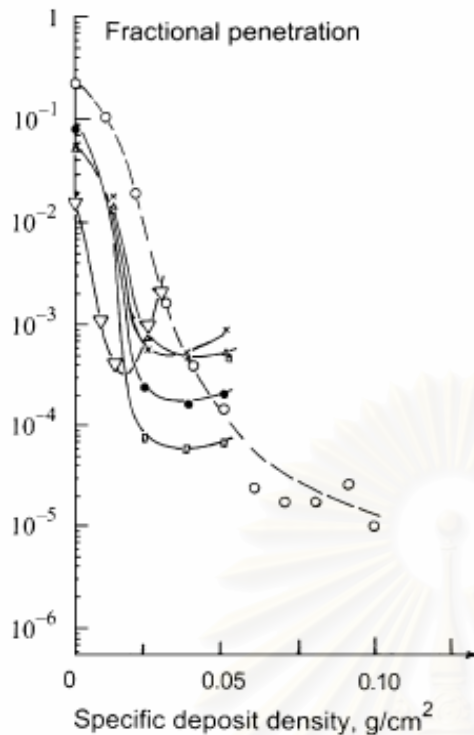


Figure 1.8 Fractional penetration of 1.1 μm . monodisperse aerosol through 6.3 cm. bed of 0.3-0.42 mm. sand with fly ash deposit. \circ = air at 15.24 cm./s, initial $\Delta P = 9.1 \text{ cmH}_2\text{O}$; Δ , \times , \square , and \bullet = air at 30.5 cm/s with initial $\Delta P = 26.0, 28.9, 31.3$ and $28.6 \text{ cmH}_2\text{O}$ respectively; ∇ = air at 45.7 cm/s, initial $\Delta P = 20.2 \text{ cm. H}_2\text{O}$.

For cake free sand, it appeared that dust penetration would decrease with an increase in filtration velocity beyond about 10 cm/s. In Figure 1.8, in the condition that face velocity was 30.5 and 45.7 cm/s, penetration would decrease with first addition of fly ash, but bottomed out and increased with later additions. It was explained that pinhole defects, developed in fly ash cake, would boost up the penetration of aerosol.

G.W. Carter et al. [3] did some research on another application of rice husk, being an additive material in brick making process. Combination of clay and rice husk provides bricks with light weight characteristic and, above all, save cost of raw material input and number of breaking brick. In this research, the ratio of rice husk contained in bricks was varied from 0 to 70% by mass. While the percent moisture content in bricks would gradually be increased with the rise in rice husk ratio, on the other hand, the density of brick and its compressive strength would be decreased with the increase in rice husk ratio. However, since the minimum acceptable compressive strength was generally set around 5 MPa, up-to 50% by mass of rice husk ratio could be added into the bricks with an acceptable quality.

1.2 Present status in a rice mill

1.2.1 Rice mill process

Thailand was one of the leaders in rice exporting for years, judging from 7.6 millions tones and 10.1 million tones of rice exported in 2003 and 2004 respectively (The Nation, Thursday, August 11, 2005). Although technologies of Thai rice-mill industries have continually been developed for a long time, their milling processes are generally based on the same three major steps, cleaning, husking & husk separation, and polishing.

Cleaning is the first step in rice mill. Fine and coarse impurities as well as gravel and sand are separated and removed within this unit sector. Since gravel and sand are very harmful to rubber rolls used in huskers, his cleaning step will help prolong the life-time of rubber rolls.

The next step is husking and husk separation, in which rubber roll huskers are applied in cracking husk from rice paddy to gain brown rice kernels. The rubber rolls must be carefully adjusted, so that the breakage of rice is minimized during the process. The un-husked paddy will be recovered in the paddy separator and returned to the rubber roll husker.

Finally, the polishing stage is applied to whiten the brown rice. In this step, abrasive stones are used to clean off rice bran from brown rice. Thus, the white rice is obtained as product, and rice bran gained as a by product. Normally, to minimize the percentage of broken rice, brown rice must be carefully treated, and no more than 3 stages of whitening processes are used.

A suitable rice mill was surveyed and the process flowchart was made, as shown in Figure 1.9.

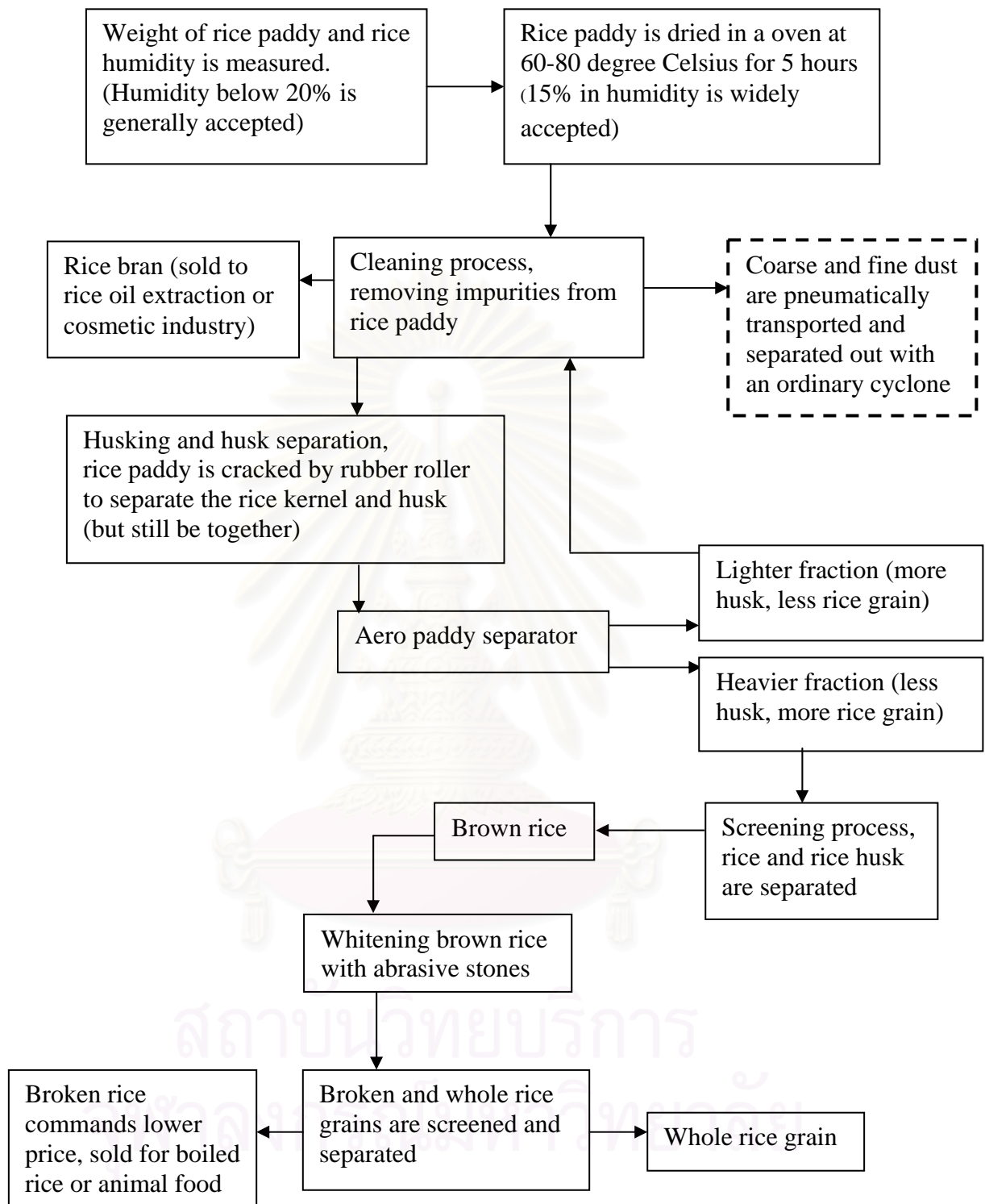
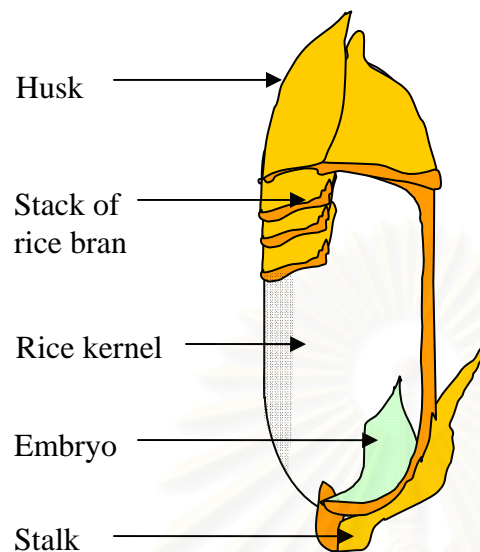


Figure 1.9 Flow chart illustrating the rice mill process

1.2.2 Components of a rice grain

Figure 1.10 Rice grain compositions



Rice Husk

According to Figure 1.10, rice husk is the outer part of a rice grain, loosely enveloping the brown rice and combining with lots of “soft hair” which is the major source of fine dust.

Generally, rice husk is sold or used as a fuel for electricity generation or in the power station of rice mill itself. Husk ash can be used as an additive to asphalt.

Rice bran

The outer part of brown rice, so-called rice bran, is rich in Thiamin, niacin, vitamin B-6, iron, phosphorus, magnesium, potassium, and fiber. It is the raw material for the rice oil extraction industry and also used as part of human and animal food, or even in cosmetic industry.

Rice kernels

Rice kernels or head rice is the edible part, containing mostly starch.

Embryo

Embryo is a high nutrient part of the rice grain, and is an important factor in comparing product’s quality between rice mills. However, the embryo can cause stale smell in rice kernel.

1.2.3 Data measured from the line of treated air

Table 1.1 Estimated percentages of mass decrease in each stage of rice mill processes.*

Process	Percentages Loss (by mass)	Percentages Left (by mass)
Dried paddy		100%
Cleaning	3%	97%
Husking	20%	77%
Polishing	10%	67%
1/4 Brokens	2%	65%
1/2 Brokens	5%	60%
3/4 Brokens	8%	52%
Whole rice kernel, Head rice		52%

* More information is available at www.ricemilling.com.

Records obtained from the observed rice mill revealed that the average amount of dried paddy fed into the milling process was about 200 tons per day (averaged from workdays only). It can be concluded that dust load carried from the cleaning process to the dust collector can be calculated from the percentage losses in Table 1.1 as about 6 tons per day.

Air flow rate and dust concentration in the pipe line, carrying dust particle to cyclone, were measured. Four spots were identified in the cross section of the 0.4-meter-wide circular pipe that make a good representation of air velocity in the pipe, as shown in Table 1.2, and Figure 1.11.

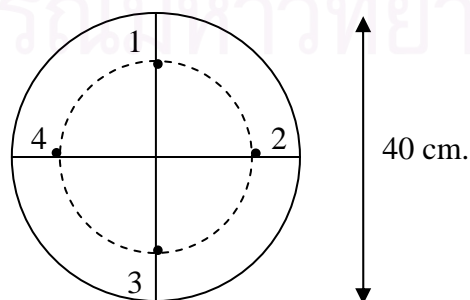


Figure 1.11 Cross-sectional area of pipe line

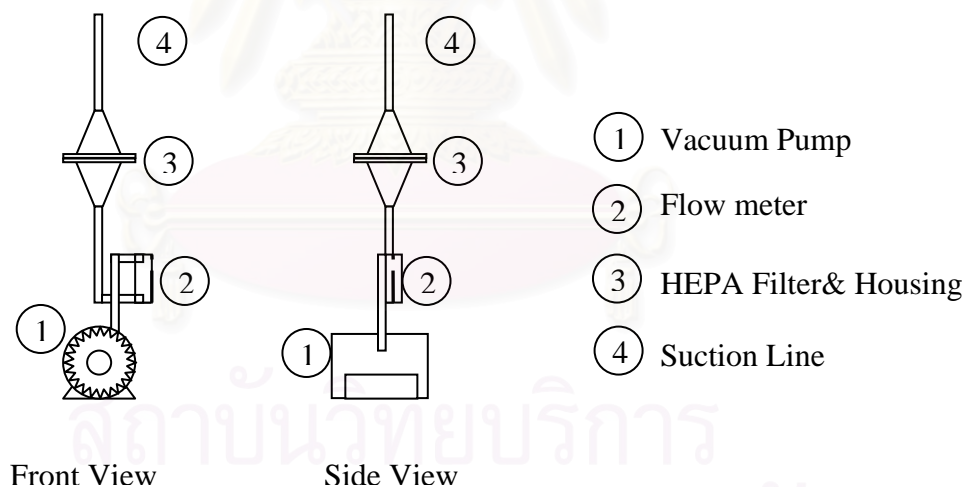
Table 1.2 Air velocity measured at the sampling point

Measurement	Spot 1	Spot 2	Spot 3	Spot 4
First time (m./s)	10.6	8.4	8.6	12.1
Second time (m./s)	10.8	6.9	7.5	10.1
Average data (m./s)				9.38

Due to the average linear velocity, obtained from Table 1.2, the flow rate of dust-laden air passing through the pipe line was

$$\pi*(0.4/2)^2*9.38 = 1.18 \text{ m}^3/\text{s}.$$

The measurement of dust concentration in the pipe line relied on the principle of “Isokinetic”, by which dust particle suspended as aerosol in dust-laden air would be collected with the same air velocity as it was in the pipe line. According to Table 1.2, the isokinetic sampling system, as shown in Figure 1.12, was managed to collect rice mill dust particles at the rate of 9.38 m /s of air velocity.

**Figure 1.12** Isokinetic Sampling System

In Figure 1.12, the vacuum pump would generate suction force of air flow rate, while the flow meter was controlling velocity of air at 9.38 m/s. HEPA Filter was an effective filter sheet, functioning as absolute dust collector in capturing dust particle from the sample of dust-laden air.

The measured results, collected by isokinetic system in Figure 1.12, revealed that the *dust concentration of load in pipe line, detected from the observed rice mill, was around 1.353 g/m^3* . However, the dust concentration based on the information of percentage loss in the cleaning process of Table 1.1 was 55.91 g/m^3 . So, it could be implied that not all losses in the cleaning process was carried out of the rice mill plant as aerosol.

1.2.4 Porosity of packed bed of rice husk

Porosity of packed bed was defined as the percentage of void space in the porous bed. So, porosity of rice husk packed bed could be measured by dividing the volume of its void spaces with the total volume of the bed. In practice, a 500-cm^3 of beaker was packed with 250 cm^3 of rice husk as shown in Figure 1.13.

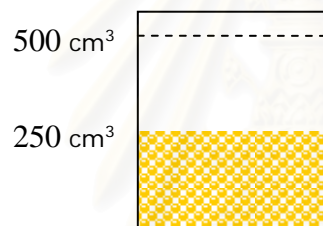


Figure 1.13 A simple system for measuring bed porosity

While the height of packed rice husk bed was kept constant, water was filled to occupy void spaces in packed bed until the water level reached the same level as the rice husk bed. Volume of water, filling up the empty space, was recorded as volume of the void space at 150 cm^3 . Based on the definition, the porosity of rice husk bed was obtained by dividing the volume of water pouring in (150 cm^3) with the volume of packed rice husk bed (250 cm^3). *Porosity of rice husk bed was equal to 0.60.*

1.2.5 Equivalent diameter of rice husk

To determine the dust collection efficiency of, or pressure drop across the packed bed of a media, the shape of media particle would be assumed as spherical. However, since rice husk particle was, in reality, of flake-like shape, light weight, and flat, an effective method for the calculation of equivalent diameter of rice-husk would depend on the purpose in using this equivalent diameter.

- Equivalent diameter from terminal velocity (D_{ET})

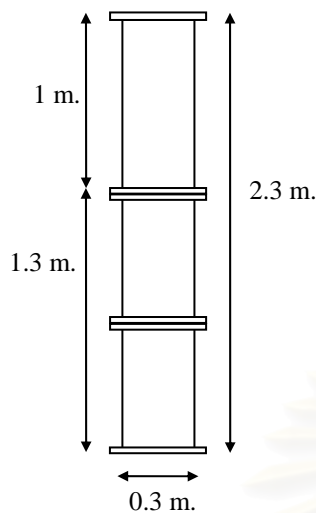


Figure 1.14 2.3-meter-high pipe was used to measure the terminal velocity of rice husk particle

Firstly, an equivalent diameter based on the terminal velocity (D_{ET}) could be determined. A simple system was consisted of a 2.3-meter-long pipe, made of three transparent pipes, as shown in Figure 1.14.

Rice husk particle was dropped in free fall from the top of the first section of the pipe for 1 meter. Once the particle reached the second section, it was assumed to have achieved its terminal velocity. The period of time required by the particle to fall from the top of section two to the end section three was measured and the terminal velocity was calculated.

All data gained from this experiment were listed in Appendix B.

The average terminal velocity was 1.605 m/s, which is equivalent to a sphere of 237 μm . in diameter by iteration method. (Page 55 of [13])

- Equivalent diameter from surface area of a particle (D_{ES})

Another type of equivalent diameter was calculated by the surface-area-equivalent method, in which an expanded area of rice husk particle was assumed to be geometrically a flat sheet, as shown in Figure 1.15.

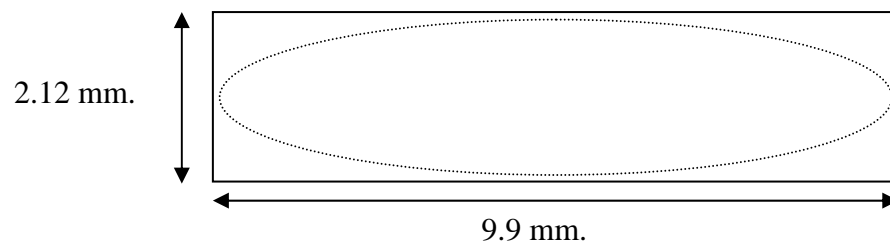


Figure 1.15 Geometric model of rice husk particle

In the calculation, expanded area of rice husk flat sheet was assumed to be so thin that surface area of each edge could be neglected.

$$\begin{aligned}
 \text{So, Surface Area} &= \frac{3}{4} * 2 * 2.12 * 9.9 \\
 &\text{(Including 2 sides of surface area)} \\
 &= 30.21 \text{ mm}^2 \quad (1.1)
 \end{aligned}$$

Meantime, surface area of a sphere was calculated by equation (1.2)

$$\text{Surface Area of sphere} = \pi * (D_{ES})^2 \quad (1.2)$$

From equation (1.1) and (1.2),

$$\begin{aligned}
 30.21 &= \pi * (D_{ES})^2 \\
 D_{ES} &= 3.101 \text{ mm.}
 \end{aligned}$$

The equivalent diameter, obtained from the method of equivalent-surface-area was 3.101 mm.

- Equivalent diameter from the volume of a particle. (D_{EV})

Rice husk particle was considered as an expanded sheet. Rice husk dimensions were measured and averaged as illustrated in Figure 1.15 and 1.16, and were applied in calculation of the equivalent diameter based on volume basis.

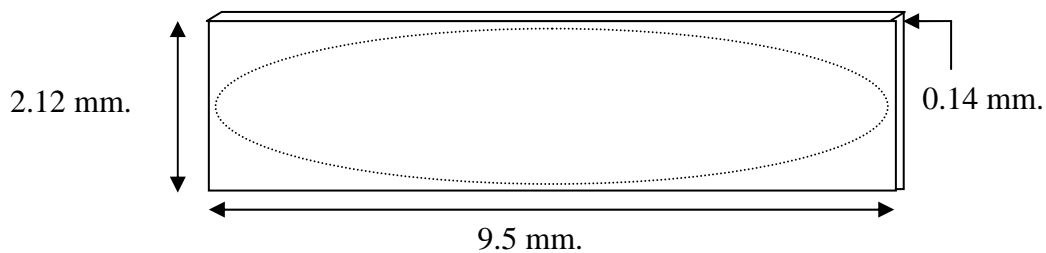


Figure 1.16 Geometric model of rice husk particle (2)

$$\begin{aligned} \text{Volume of a rice husk particle} &= (3/4) * 2.12 * 9.5 * 0.14 \\ &= 2.115 \text{ mm.}^3 \end{aligned}$$

$$\text{Where the volume of spherical shape was defined as} = \frac{\pi}{6} D_{EV}^3 \quad (1.3)$$

$$\text{So, volume of a rice husk particle} = 2.115 = \frac{\pi}{6} D_{EV}^3$$

$$\text{, or } D_{EV} = 1.593 \text{ mm.}$$

The equivalent diameter, obtained from the method of equivalent-volume was 1.593 mm.

- Equivalent diameter from sieve mesh. (D_{EM})

5 sets of sieve mesh were set in position by putting bigger size of sieve mesh over a smaller one. 1 kg. of rice husk was screened and separated to several groups of size range. The size distribution curve of rice husk was made as shown in Figure 1.16 Judging by area enclosing, it was clear that average diameter size of rice husk was 2 mm.

สถาบันวิทยบริการ
จุฬาลงกรณ์มหาวิทยาลัย

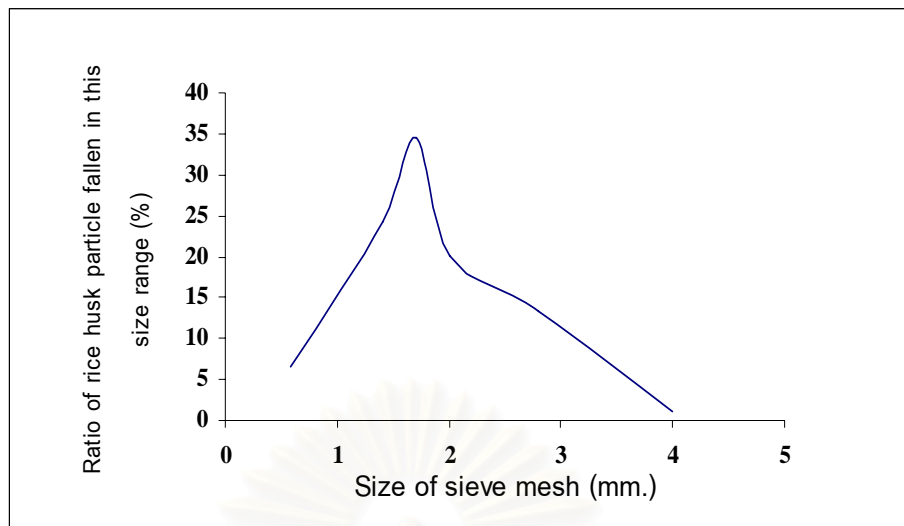


Figure 1.17 Size distribution curve of rice husk

In conclusion, the equivalent diameters gained from the four different methods were shown in Table 1.3.

Table 1.3 Results of equivalent diameter from four methods of calculation.

Methods	Equivalent diameter (mm.)
Equivalent in terminal velocity (D_{ET}) (Stokes diameter)	0.237
Equivalent in surface area of particle (D_{ES})	3.101
Equivalent in volume of particle (D_{EV})	1.593
Equivalent diameter from sieve mesh (D_{EM})	2.000

It was believed that equivalent diameter in volume of particle was suitable in representing physical properties of particles, including pressure drop of particle stack. [14] This topic would be further analyzed in Chapter 4.

1.3 Problem Identification

Referring to the flow chart in figure 1.9, coarse and fine dust, generated in the cleaning process, would continuously be collected in a cyclone dust collector located outside the building. However, since only dust particle bigger than 3-5 μm . can

significantly be collected, most of the fine dust still escapes and annoys people living in nearby area. So, another supplementary dust collection system should be developed and applied.

Rice husk dust particles that escaped from the cyclone in the observed rice mill were collected and tested by Powder Tester and analyzed by Mastersizer S long bed Ver. 2.11. The full test results were given in Appendix C.

Since dust particles emitted from rice mill plant are mostly “the soft hair” detached from the surface of rice husk itself, (Photos of rice husk dust particles was shown in figure 1.18), it is practical to study the application of rice husk as a filter media.

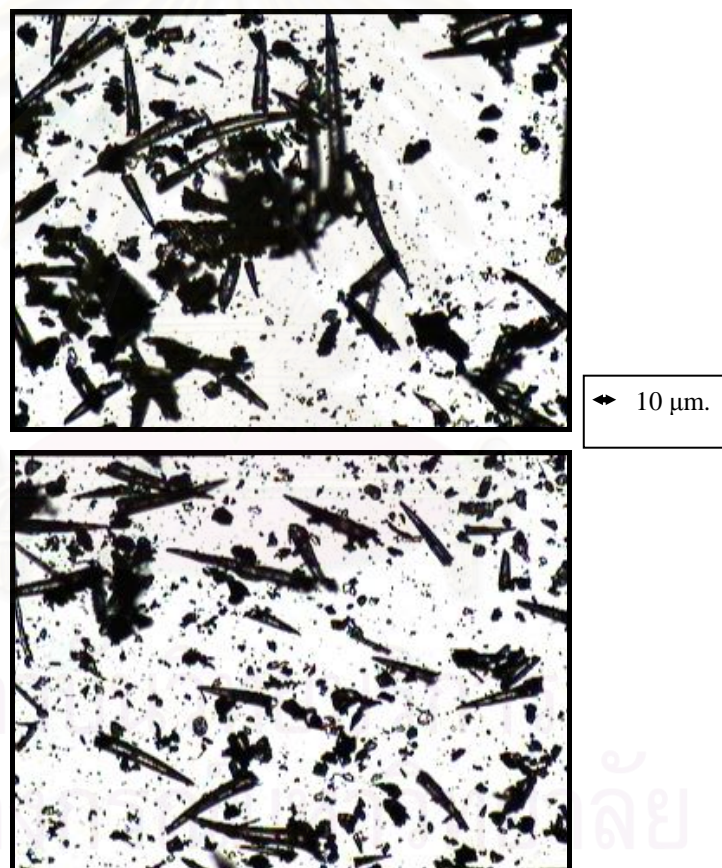


Figure 1.18 Fine dust particles from rice husk

A laboratory-scale dust collection system was set up to determine the dust collection efficiency of rice husk media (as shown in Figure 1.19). In this experiment, rice husk was moderately packed in a rectangular box to serve as packed bed filter.

According to Figure 1.19, air flow generated from a blower (number 1) would mix with dust particles fed out by an accurate feeder (number 4), and then it became dust-laden air. While passing through packed-rice-husk media, dust-laden air was filtrated and consequently transferred to dust collector unit (number 7) before being released to atmosphere. Sample of treated air would intermittently be collected for determination of dust collection efficiency every 30 minutes of operation time. Meanwhile, changes in light intensity were detected by an opacity meter (number 11) to monitor the instantaneous dust concentration in the treated air behind the filter media.

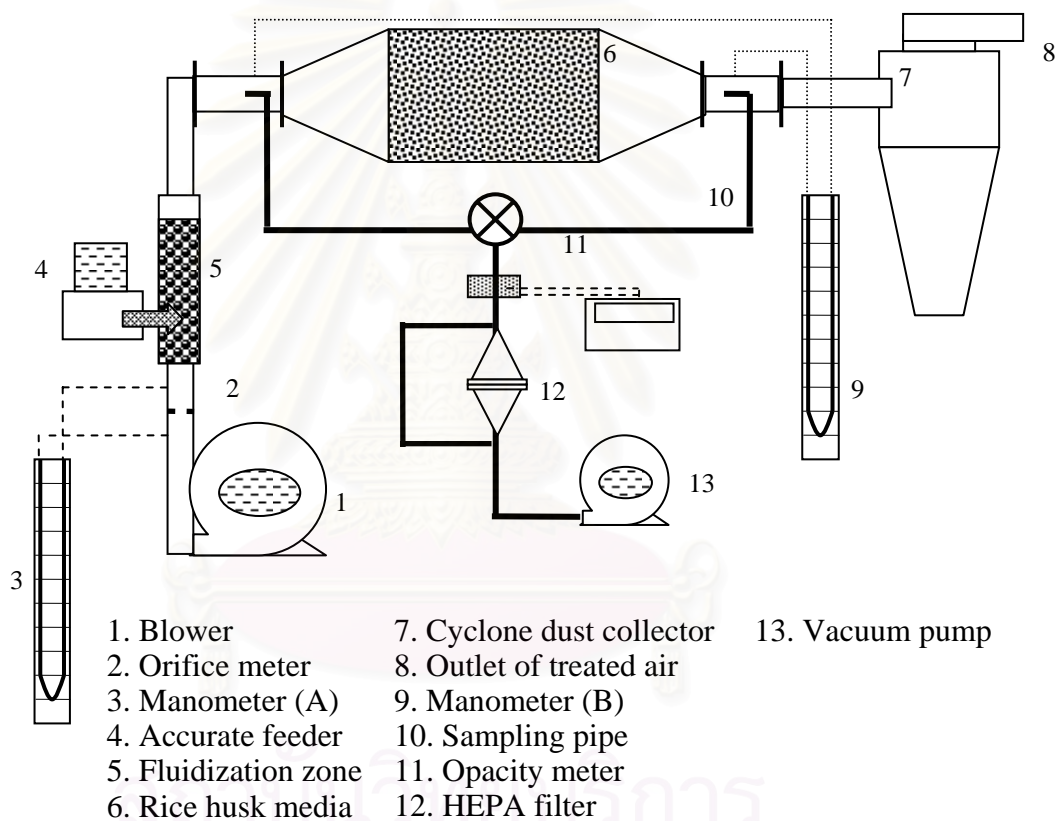


Figure 1.19 Schematic diagram of laboratory-scale system

It is now clear from the experiments that the dust collection efficiencies of rice husk media were in several cases higher than 90% for dust particles which are only 1.6 μm . in average size. Additional information of laboratory-scale system and experimental results is available in Chapter 4.

CHAPTER 2

OBJECTIVE AND SCOPE OF RESEARCH

2.1 Objectives

- To develop and design an economical simple-structure dust collection system for a rice mill.
- To test the filtration efficiency of rice husk media.

2.2 Scope

1. Design system for rice husk storage and dust collection that is capable of capturing particles smaller than 3 micrometers.
2. Test the dust collection efficiency of rice husk in the laboratory-scale system. Investigate the effect of media thickness, filtration time, filtration velocity, and dust load on the filtration efficiency and pressure drop.

2.3 Expected benefit

1. The drawing and dimensions of the economical dust collection system will be determined that has high dust collection efficiency at reasonable fixed and operation cost.
2. Dust collection efficiency of rice husk bed is demonstrated and confirmed by the laboratory-scale system.

CHAPTER 3

FUNDAMENTAL THEORY

Although the use of natural fibers and particles as aerosol filtration media is quite well-known for a long time in industrial society, experimental data on dust collection efficiency of rice husk bed are still not available. Before testing the real performance of packed-bed media, and designing the dust collector, the fundamental theory of aerosol deposition mechanism, the process in which dust particles are captured by a single media particle, and theory of packed bed filtration, including flow resistance and basic rule of thumb, could be used to predict the filtration efficiency and pressure difference across the packed-bed media.

3.1 Dust-collecting efficiency of a single particle

There are five basic mechanisms by which an aerosol particle can be deposited onto a fiber in an air filter. [1, 13, 15]

1. Interception
2. Inertial impaction
3. Diffusion
4. Gravitational settling
5. Electrostatic deposition

The first three mechanisms are short-range mechanisms. That is, particles must be carried close enough to the media, in order that they would be collected. The last two terms are considered as external forces, which will affect dust collection efficiency conditionally. Individual efficiency of each mechanism is contributed by interception, η_R , inertial impaction, η_I , gravitational settling, η_G , diffusion, η_D , and electrostatic deposition, η_E . [15] Although the combination of two or more of these short-range or external-force mechanisms have not yet been well developed on a comprehensive basis, in most cases, it is found that only one or two mechanisms would predominate in a system. Generally, inertial impaction and interception would predominate for particles in micron-size range, while diffusion mechanism becomes more important for the collection of sub-micrometer particles.

3.1.1 Interception

When a particle with an identified size follows through a certain gas streamline and approaches within one particle radius of the medium surface, it is often collected on the surface of the medium by the effect of interception. In other words, interception deposition mechanism must be considered where the particle has relatively large size, even without mass. [13]

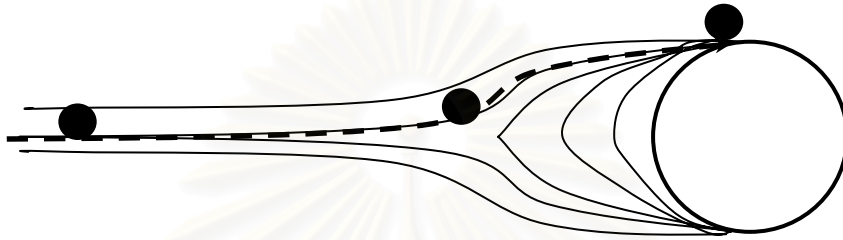


Figure 3.1 Pathway of an aerosol particle, collected by a medium particle due to the effect of interception mechanism.

Interception is characterized by a dimensionless parameter R , defined as

$$R = d_p/d_m \quad (3.1),$$

where d_p and d_m are the dust particle diameter and medium body diameter respectively. If an air stream could be characterized by potential flow [4], then

$$\eta_C = 1 + R - \frac{1}{(1 + R)} \quad (\text{cylindrical collector}) \quad (3.2).$$

$$\eta_C = (1 + R)^2 - \frac{1}{(1 + R)} \quad (\text{spherical collector}) \quad (3.3).$$

It must be noted that filtration efficiency is not more than 1.

There is another method applied for predicting η_C of cylindrical or fibrous collector in Kuwabara flow, as shown in equation (3.4).

$$\eta_C = \frac{(1 - \alpha)R^2}{Ku (1 + R)} \quad (\text{cylindrical collector}) \quad (3.4)$$

Where Ku : Kuwabara hydrodynamic factor:

$$K_u = -\frac{\ln \alpha}{2} - \frac{3}{4} + \alpha - \frac{\alpha^2}{4} \quad (3.5)$$

α : Solidity of filter media (-)

From Equations 3.2 – 3.4, it is clear that η_c increases with increasing R, but could not exceed the maximum theoretical value of 1 (based on the definition of single-fiber efficiency). Moreover, interception is the only mechanism that does not directly depend on filtration velocity (U_0).

3.1.2 Inertial impaction

A particle with a finite mass may be able to deviate from a curved streamline because of its inertia, and collide with the medium filter. The inertial impaction increases with an increase in the particle's size and air velocity. External forces such as gravity could assist in or act against this. [13]

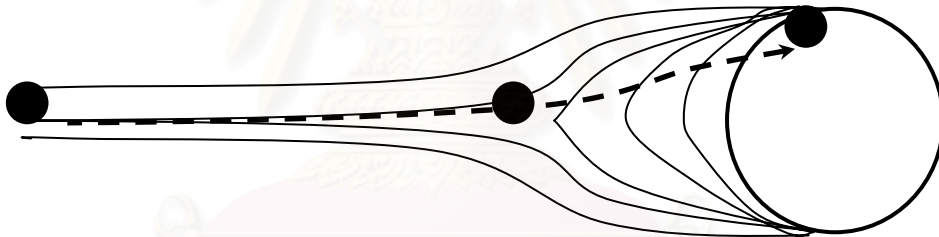


Figure 3.2 Pathway of an aerosol particle, collected by a medium filter particle due to the effect of inertial impaction mechanism.

The governing parameter of this mechanism is Stokes number, Stk , defined as

$$Stk = \frac{C_c \rho_p U_0 d_p^2}{(18 \mu d_f)} \quad (3.6)$$

Where C_c : Cunningham correction factor:

$$C_c = 1 + \left(\frac{2\lambda C}{d_p} \right) * [0.7004 * ((2 * a) - 1)] \quad (3.7)$$

λ : Gas mean free path (m.)

d_p : Diameter of dust particle (m.)

U_0 : Filtration velocity (m/s)

ρ_p : Density of dust particle (kg/m^3)

μ : Viscosity of air (kg/ms)

d_f : Diameter of fiber collector (m)

This dimensionless number represents the ratio of “persistence” of particle to the size of the target. η_I increases with an increasing value of Stokes number, because of greater particle inertia (greater d_p or ρ_p), greater particle velocity, or more abrupt curvature of streamlines. Thus, single-particle efficiency due to inertial impaction, η_I can be read from Figure 3.3.

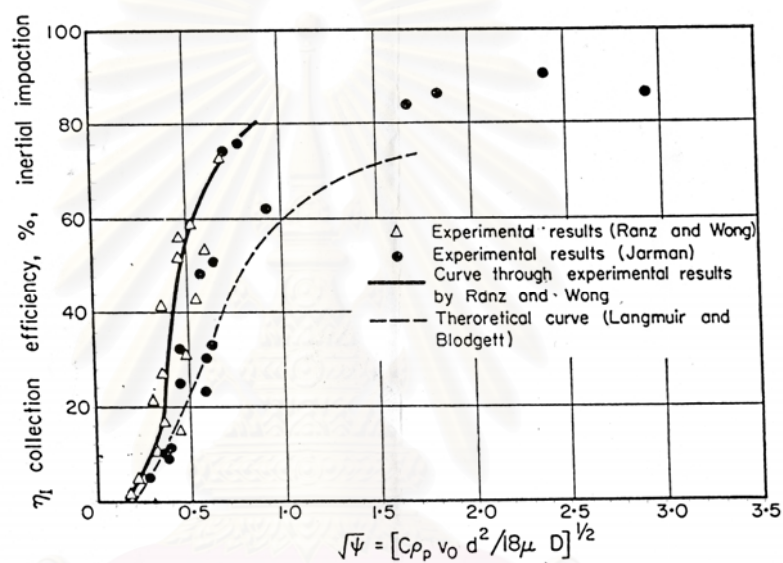


Figure 3.3 relations of η_I against $\text{Stk}^{1/2}$ (Spherical collector)

Alternatively, η_I for cylindrical shape of media particle could be found in Equation 3.8 [15]

$$\eta_I = \frac{(\text{Stk}) * J}{2 * \text{Ku}^2} \quad (\text{Cylindrical Collector}) \quad (3.8)$$

$$\text{Where } J = (29.6 - 28\alpha^{0.62})R^2 - 27.5R^{2.8} \quad \text{for } R < 0.4$$

There is no simple equation to calculate J , when $R > 0.4$. However, it could approximately be set equal to 2 for $R > 0.4$.

As expected, impaction is the most important deposition mechanism for a large particle. However, it must be noted that such particles could also be significantly

captured by interception deposition mechanism. The summation of η_C and η_I should not exceed the theoretical maximum of 1.

3.1.3 Diffusion mechanism

For a very submicrometer particle, its motion in a gas becomes irregular and known as Brownian diffusion, which results in enhancing the probability of the particle to hit on a medium filter randomly. [15] This is a special case of diffusion to a medium's surface which depends on a dimensionless Peclet number, Pe.

$$Pe = \frac{d_p U_o}{D} \quad (3.9)$$

Where D is the particle diffusion coefficient.

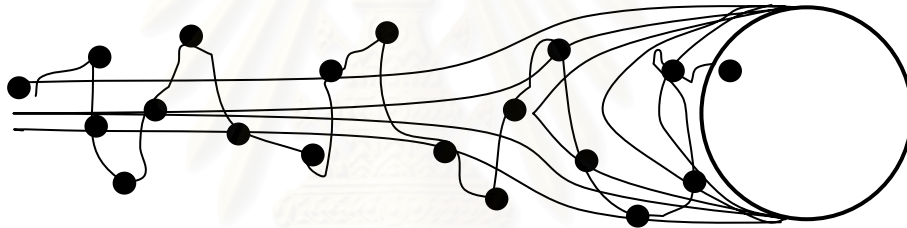


Figure 3.4 Brownian motion of submicrometer particles due to diffusional deposition mechanism.

The single-particle efficiency due to the diffusion mechanism is given by

$$\eta_D = 2Pe^{-\frac{2}{3}} \quad (\text{Cylindrical collector})^{[1]} \quad (3.10)$$

$$\eta_D = \left(\frac{8}{3\pi} \right) \left(\frac{2}{Pe} \right)^{\frac{1}{2}} \quad (\text{Spherical collector})^{[4]} \quad (3.11)$$

It could be clearly seen that the single-particle efficiency increases with a decrease in Peclet number. And η_D is the only on deposition mechanism that decreases as d_p increases.

3.1.4. Gravitational settling

Gravitational settling mechanism becomes important, once the particle is large enough (bigger than 10 microns) and air velocity is lower than 0.1 m/s. This deposition mechanism is the effect of gravity force, considered as external force, acting vertically on a particle, which has no effect on the efficiency of this system.

3.1.5. Electrostatic deposition

This deposition mechanism is another form of external force, based on the understanding of electrical charges on the particles, and often is neglected, unless the particle is electrically charged in some quantifiable way. A charged dust particle is attracted to the oppositely charged medium due to columbic forces. Since there is no electrical charging of particles in this system, electrostatic deposition is assumed negligible.

3.2 Overall dust collection efficiency

To determine the total single-particle coefficient, each single-particle deposition mechanism must be correctly combined by Equation 3.12. [13]

$$\eta_{\text{Media Particle}} = 1 - (1 - \eta_I)(1 - \eta_C)(1 - \eta_D)(1 - \eta_G) \quad (3.12).$$

Next, to find the overall dust collection efficiency, mass balance over a infinitely small thickness of media filter must be done, as follows.

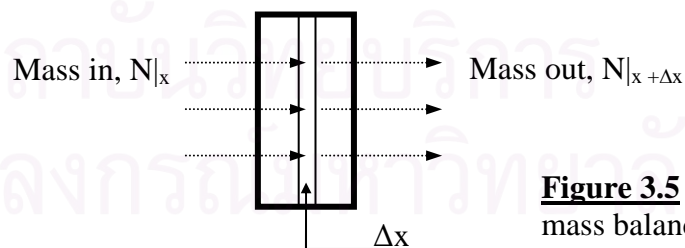


Figure 3.5 Model for mass balance

A media control volume, whose thickness is Δx , makes up part of the whole bed volume, as illustrated in Figure 3.5. Dust particles come in at point x , and go out at point $x + \Delta x$. The balance of mass coming in and out of this control volume is given by

$$[N|_x - N|_{x+\Delta x}] * A_F = - n_m * (\eta_{\text{Media Particle}}) * (N|_x) * (\pi d_m^2) / 4 \quad (3.13)$$

where $N|_x$: Concentration of dust in dust-laden air coming into the control volume at point x

$N|_{x+\Delta x}$: Concentration of dust in dust-laden air going out of the control volume at point $x+\Delta x$

A_F : Filtration area of media

n_m : Amount of media particle appeared in a projected area of media filter. It could be found by the definition of packing density (α).

Based on the definition, α is a ratio of the control volume to the volume of media particle. In other words,

$$\alpha = \left(\frac{n_m * \pi * D_m^3}{6 * (A_F * \Delta x)} \right) \quad (3.14)$$

By rearranging Equation (3.14), we obtained

$$n_m = \left(\frac{6 * \alpha * A_F * \Delta x}{\pi * D_m^3} \right) \quad (3.15)$$

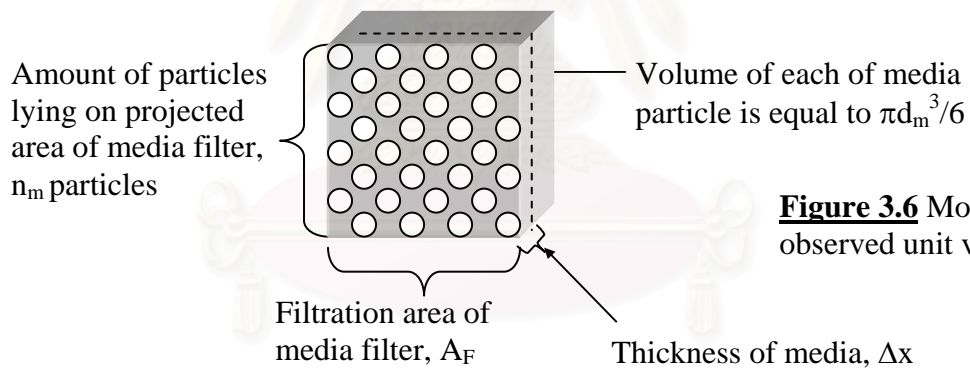


Figure 3.6 Model of an observed unit volume

Substitute n_m from (3.15) into (3.13) to obtain

$$\begin{aligned} [N|_x - N|_{x+\Delta x}] * A_F &= - \left(\frac{6 * \alpha * A_F * \Delta t}{\pi * D_m^3} \right) * \left(\frac{\eta_{MediaParticle} * N|_x * (\pi * d_m^2)}{4} \right) \\ \left(\frac{N|_x - N|_{x+\Delta x}}{\Delta t} \right) &= - (3/2) * \left(\frac{\alpha}{d_m} \right) * \eta_{Media Particle} * N|_x \end{aligned} \quad (3.16)$$

Take $\lim_{\Delta x \rightarrow 0}$ on both sides of Equation (3.16) and get

$$\lim_{\Delta x \rightarrow 0} \left(\frac{N|_x - N|_{x+\Delta x}}{\Delta t} \right) = - \lim_{\Delta x \rightarrow 0} (3/2) * \left(\frac{\alpha}{d_m} \right) * \eta_{Media Particle} * N|_x \quad (3.17)$$

Here $\lim_{\Delta x \rightarrow 0} \left(\frac{N|_x - N|_{x+\Delta x}}{\Delta t} \right)$ could be estimated as $-\left(\frac{dN}{dx} \right)$

So, Equation (3.17) becomes

$$\left(\frac{dN}{N} \right) = - (3/2) * \left(\frac{\alpha}{d_m} \right) * \eta_{\text{Media Particle}} dx \quad (3.18)$$

Integrate both sides of Equation (3.18) to obtain

$$\ln \left(\frac{N_{\text{OUT}}}{N_{\text{IN}}} \right) = - (1.5) * \left(\frac{\alpha}{d_m} \right) * \eta_{\text{Media Particle}} * x \quad (3.19)$$

, where N_{IN} and N_{OUT} is the mass flux of dust particles moving in and out of the media filter respectively.

However, it is known from the definition that the ratio of N_{OUT} to N_{IN} (P), or, in other words, the ratio of dust particles escaping from the media filter.

$$P = \left(\frac{N_{\text{OUT}}}{N_{\text{IN}}} \right) \quad (3.20)$$

The overall dust collection efficiency (E) is defined as

$$E = \left(\frac{N_{\text{IN}} - N_{\text{OUT}}}{N_{\text{IN}}} \right) = 1 - P \quad (3.21)$$

According to Equations (3.19), and (3.21), it could be rearranged that

$$P = 1 - E = e^{\left(-1.5 * \left(\frac{\alpha * t}{d_m} \right) * \eta_{\text{Media Particle}} \right)} \quad (3.22)$$

Equation (3.22) is a correlation between the parameters and overall dust collection efficiency of the media filter,

where

P : Penetration (-)

E : Overall dust collection efficiency (-)

$\eta_{\text{Medium Particle}}$: Dust collection efficiency of a single particle: (-)

t : Minimum required thickness of filter media (m.)

d_m : Equivalent diameter of a single media particle: (m)

CHAPTER 4

DUST COLLECTION EFFICIENCY OF A LABORATORY SCALE UNIT

The full-scale dust collection system was designed using published correlations and described in Chapter 5. Meantime, a laboratory-scale unit of the dust collection system was designed and constructed to demonstrate and determine the real performance of rice husk media in filtering fine dust particles diffused in dust-laden air. Results on pressure drop gained from these experiments would also be compared with the calculated values from Ergun equation in 4.3, so that the reliability of the experimental results would be confirmed.

4.1 Design of laboratory-scale dust collection system

Test rice husk was provided by Mahanakorn Tanyakit Company, located in outer Bangkok area. Properties of rice husk, tested with a Powder Tester instrument, were shown in Appendix A. Rice husk generally has in a flake-like shape, with an equivalent diameter (based on terminal velocity) of only 0.237 millimeters. Porosity of rice husk bed is about 0.6, and 80% of screened rice husk would lie between 0.8 to 3.2 millimeters sieve meshes.

The laboratory-scale system was set up in Chulalongkorn University. Calcium carbonate dust particle, with the size range of 0.2 - 9 micrometers in diameter (Average size 2 micrometer, and commercial name Turbo 1), was bought from Silathipsaraburi Co. Ltd. It was used to represent of the aerosol particles in this experiment, since it was not possible to collect enough amount of fine rice husk dust particle from the rice mill. Moreover, the white calcium carbonate dust particles could easily be differentiated from the rice husk, once they form dust cake in front of the filtering media.



Figure 4.1 Turbo 1 calcium carbonate dust particle

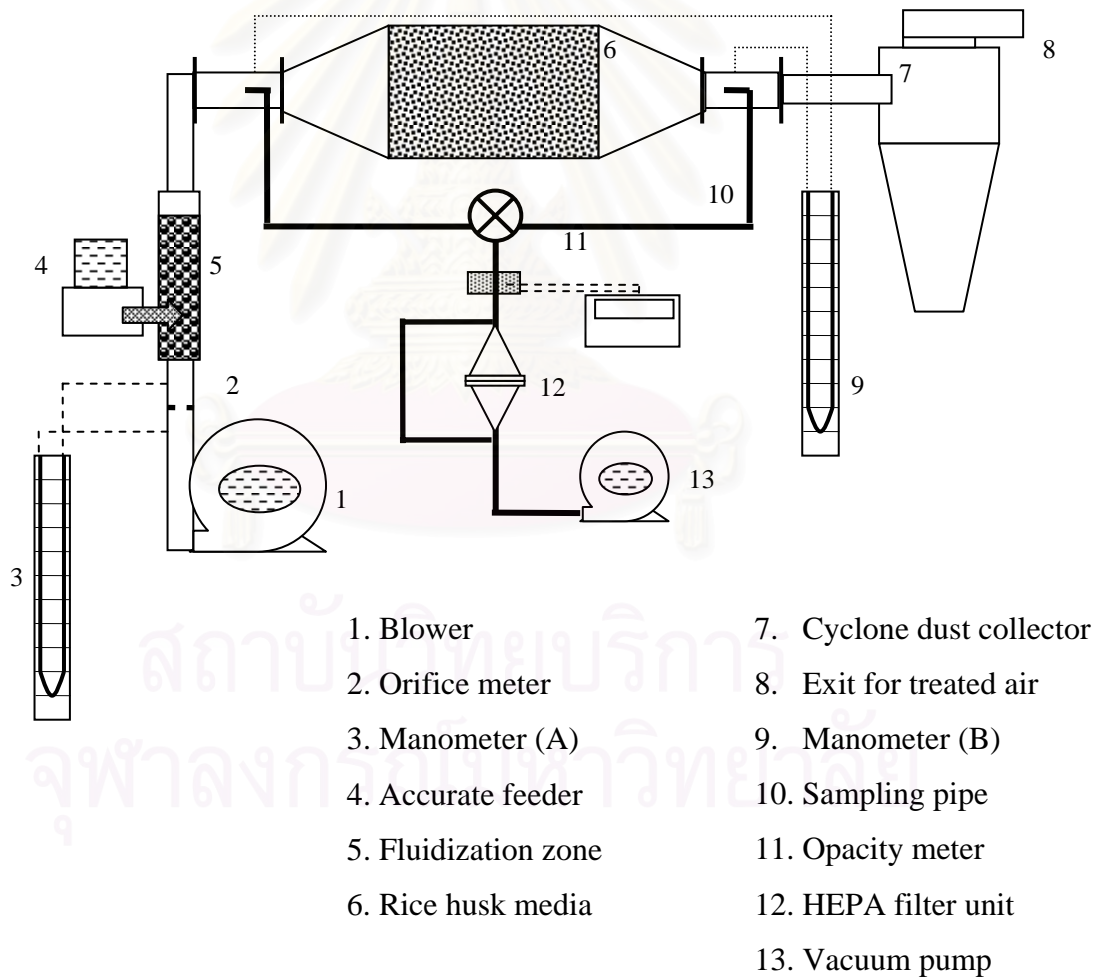


Figure 4.2 Schematic diagram of laboratory-scale system

In figure 4.2, after the blower (1) was turned on and the flow rate became steady, calcium carbonate particles were fed in through the accurate feeder (4). Next, the dust and were well mixed and became dust-laden air in the fluidization zone (5), in which 0.5-mm. glass beads were used as fluidizing media. The dust-laden air would be filtered by the rice husk media, contained in a media box (6), and then sent forward through an air cyclone (7) before being released to the atmosphere (8). Key pieces of equipments were listed below.



Figure 4.3 A photo of the side view of the laboratory-scale unit. The media box, lies on left side of the rectangular box, in the center.



Blower

AHD – 324 Blower, made by Tungpiriya Engineering, was used in this experiment. (Shown as number 1 in figure 4.2) The rated maximum flow rate was about $20 \text{ m}^3/\text{min}$ at a static head of 580 millimeters of water.

Figure 4.4 A photo of blower

Orifice meter

An orifice meter (number 2 in figure 4.2), a circular metal sheet with a central hole, was located between the blower and accurate feeder and equipped with a manometer (number 3 in figure 4.2). It measured the pressure drop across the orifice meter in millimeters of water. By calibrating the pressure drop data against the air velocity measured by a hot-wire anemometer, a calibration curve was obtained and plotted in Figure 4.5.

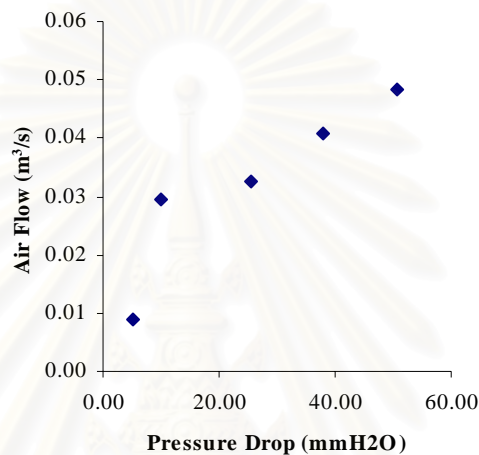


Figure 4.5 Calibration curve between air flow rate and pressure drop across the orifice meter

Accurate feeder

An accurate feeder (number 4 in Figure 4.2) made by KURIMOTO Ltd. was suitable for feeding dry small particles of any shape, such as granular, flake, and sphere. It consisted of a combination of PVC hopper, which has a moving part to break dust particle agglomerates, and a Helix screw. It provided 0.000707 to 336.026 cm³/s of feed flow rate, which can be adjusted by setting a dimensionless number between 0 and 999. When calibrated with Turbo 1, the accurate feeder possessed the calibration curve shown in figure 4.6.

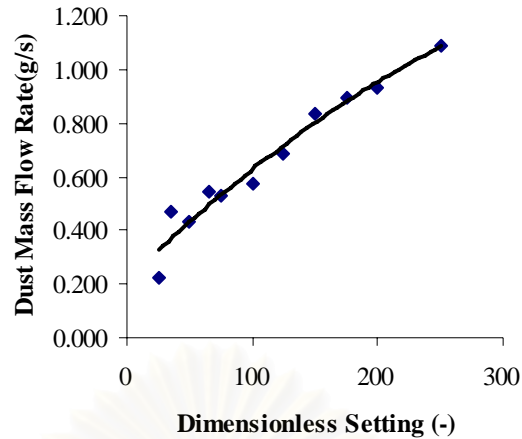


Figure 4.6 Calibration curve of the accurate feeder with Turbo 1.

Fluidized bed column

Spherical glass beads (number 5 in Figure 4.2), 0.5 millimeters in diameter, were filled in the fluidized bed column to a depth of 3 centimeters. The minimum fluidization velocity of these glass beads were 0.3 meter per second. The calculation of minimum fluidization velocity was illustrated in Appendix D1. Generally, the fluidization velocity should be 10-20 times the minimum velocity. So the proper operation range lay between 3-6 m/s of velocity in the fluidization column, which is equivalent to 0.8 – 1.6 m/s of face velocity in front of the media filter.

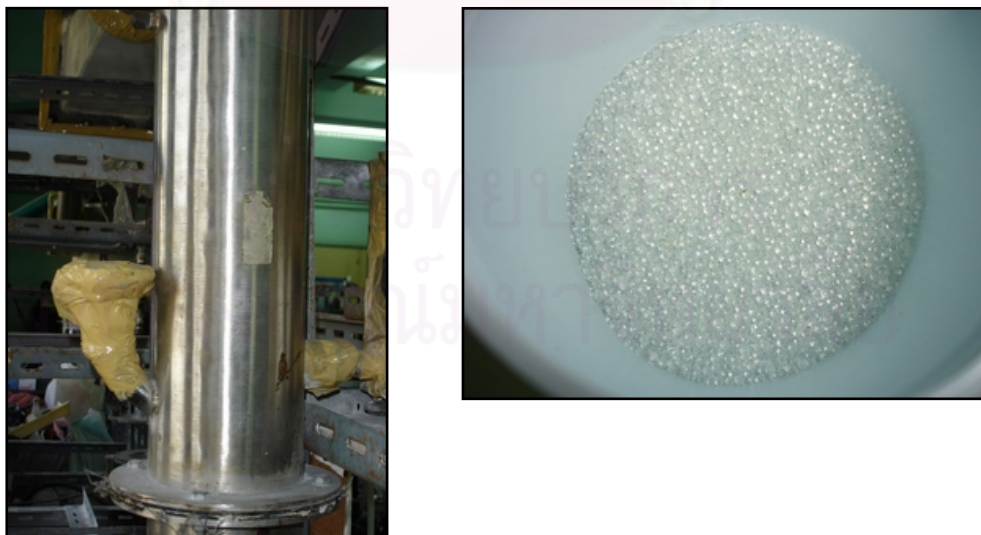


Figure 4.7 A photo of column (left) containing 0.5 mm. diameter of glass bead (right) inside

Media box

This transparent acrylic box was the zone that dust filtration took place (Shown as number 6 in Figure 4.2), since it was packed with rice husk media up to the derived length. Its dimensions were shown in figure 4.8. Moreover, to keep the packed media steady, two net screens were inserted as shown in figure 4.10. Dust-laden air would be forced to move only through the active area (20x20 cm.).

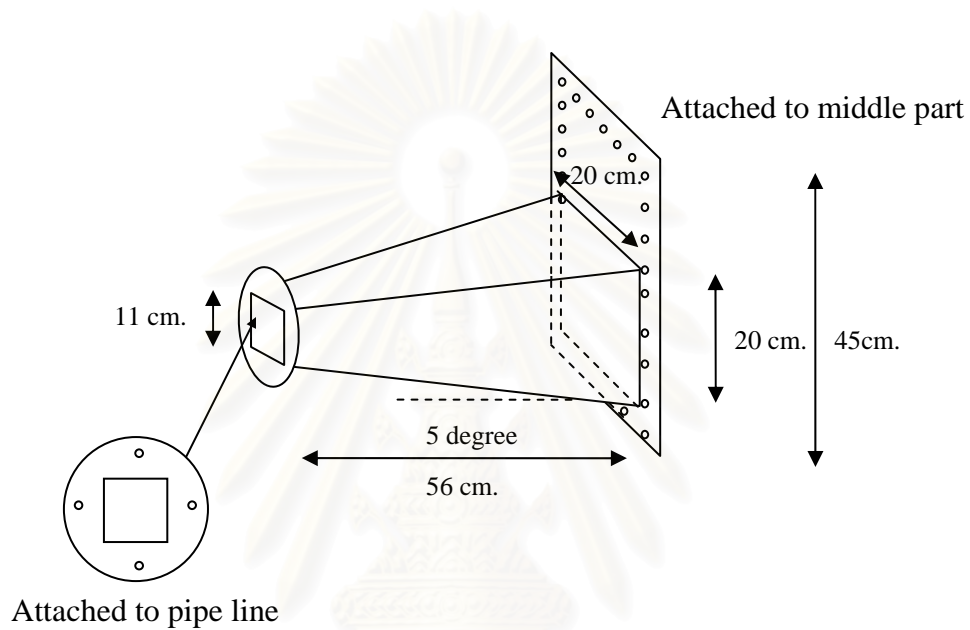


Figure 4.8.1 Front part: Air Inlet

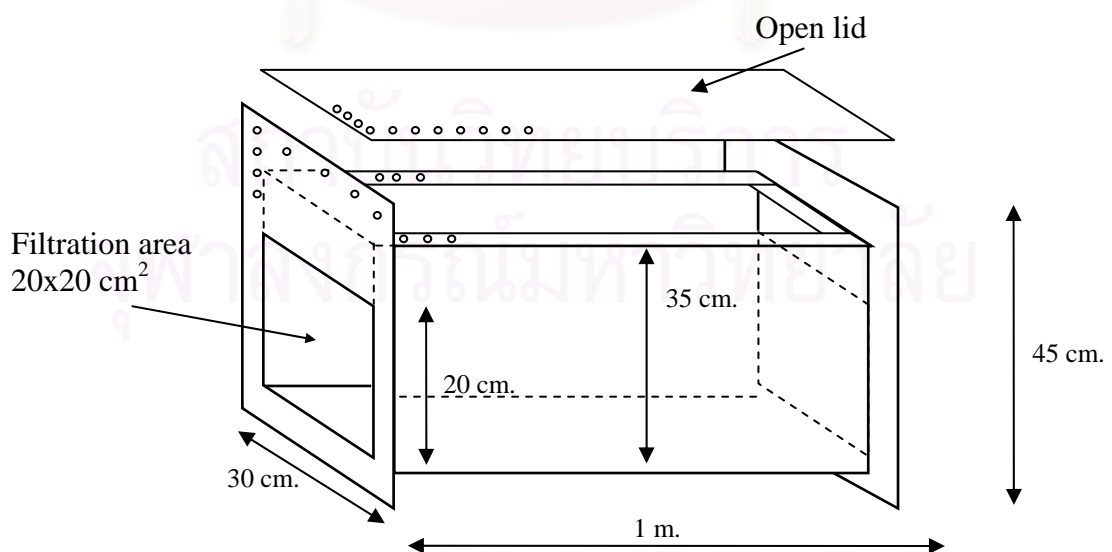


Figure 4.8.2 Middle part: rice husk media container

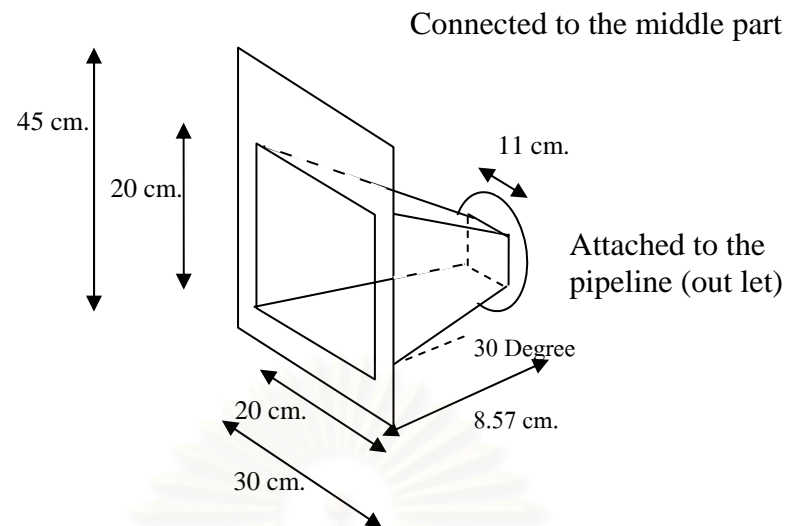


Figure 4.8.3 Rear part: treated air outlet

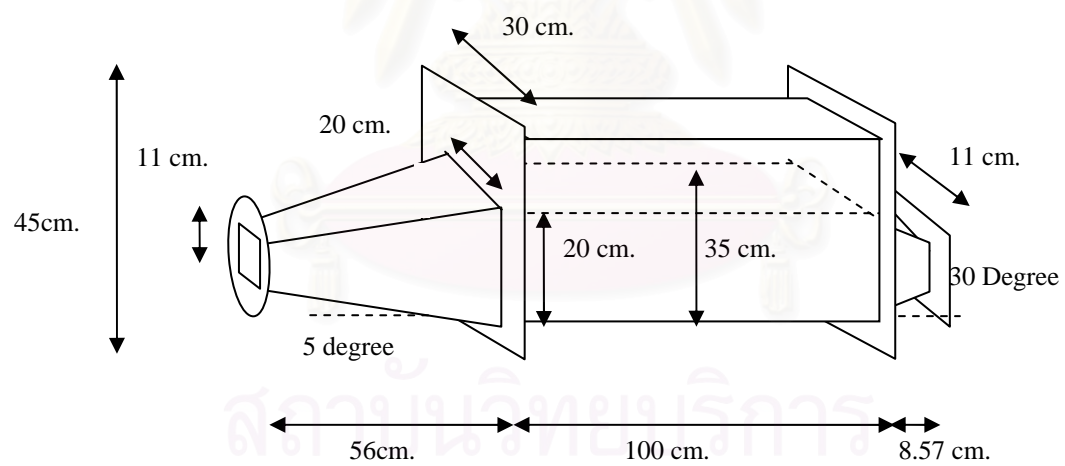
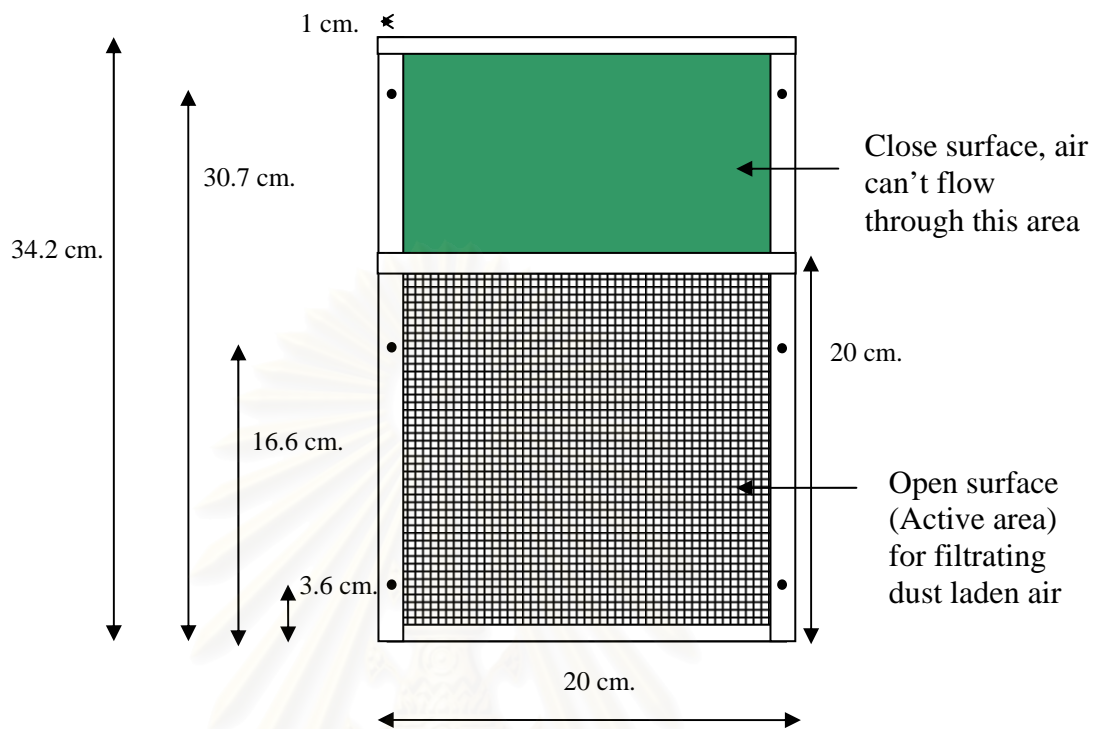


Figure 4.9 The combination of the three parts

Figure 4.10 The net screen



Cyclone Dust Collector

A cyclone dust collector was equipped as a safety system (number 7 in Figure 4.1), although it obviously was not efficient to collect escaping calcium carbonate particles, smaller than 5 micrometers in size. The designed influent air velocity was 15 m/s. According to standard ratios of dimension of a cyclone [2], the dimensions were shown in Figure 4.11.

สถาบันวิทยบริการ
จุฬาลงกรณ์มหาวิทยาลัย

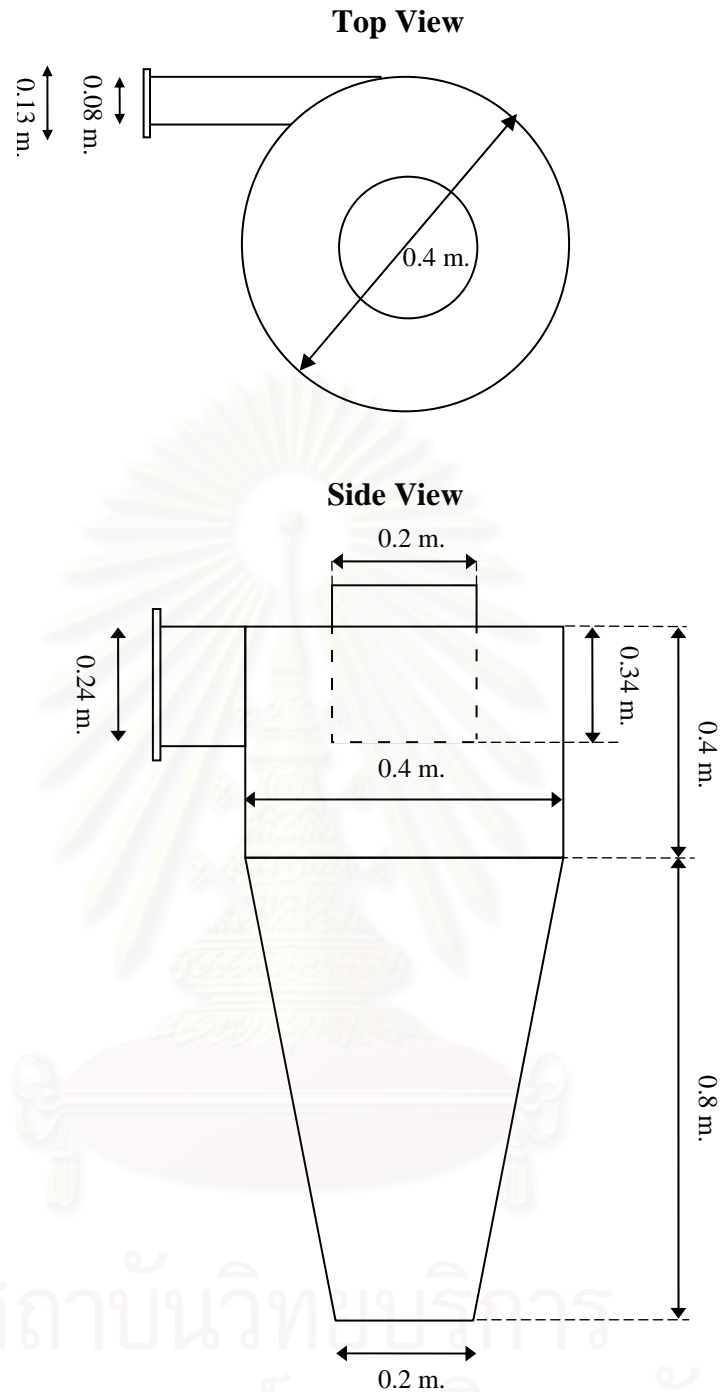


Figure 4.11 Cyclone Dimension

Opacity Meter

A Smoke Meter or Opacity meter (the WAGER Model 6500) ,borrowed from department of Mining & Petroleum Engineering, Chulalongkorn University, was used to monitor the air borne dust concentration by detecting changes in the transmitted

light intensity. It was calibrated with the dust concentration suspended in air flow to make a calibration curve. However, the opacity meter was not sensitive enough to detect changes of transmitted light intensity in the treated air coming out of the media box.



Figure 4.12 Opacity Meter

HEPA filter unit

HEPA Filter, or High Efficiency Particulate Air Filter, was a kind of air filter sheet, which provided more than of 99.97% by number of dust collection efficiency for particles bigger than 0.3 μm . In this experiment, the HEPA filter unit played its role as an important part of the sampling line in collecting calcium carbonate particles left in treated air.

สถาบันวิทยบริการ
จุฬาลงกรณ์มหาวิทยาลัย



Figure 4.13 HEPA Filter

Vacuum pump

A vacuum pump (Model 0523-V103/(101Q)-G21DX), produced by GAST Manufacturing Co. Ltd., a rotary non-lubricant type with maximum suction capacity about $0.1 \text{ m}^3/\text{min}$ at $635 \text{ mmH}_2\text{O}$, was used to continuously draw the air sample at the desired flow rate.



Figure 4.14 Vacuum pump

4.2 Experimental procedure and results

4.2.1 Experimental procedure

1. Prepare the media filter by packing rice husk fully but not too tightly in the media box. (Figure 4.9)
2. Turn on the blower, adjust the air flow rate to get the desired face velocity, and wait until it become steady.
3. Monitor the air flow rate by watching the pressure drop across the orifice during the operation time.
4. Feed in calcium carbonate dust particles from the accurate feeder.
5. Turn on the vacuum pump to begin sampling calcium carbonate particles from pipe line.
6. Change the HEPA filter sheet every 30 minutes without stopping the experiment to estimate the amount of escaped dust particles collected in a 30-minutes period.
7. Measure and record the pressure drop over across the rice husk media continually.
8. After reaching 2 hours, turn off the accurate feeder first, and then shut down the vacuum pump and blower consecutively.
9. Calcium carbonate particles collected in HEPA filter during each 30 minutes was weighed and dust collection efficiency of each elapse time was calculated with Equation 4.1.

$$\eta_{\text{Overall}} = [C_{\text{in}} - C_{\text{out}}]/C_{\text{in}} \quad (4.1)$$

η_{Overall} : The overall dust collection efficiency: (-)

C_{in} : Dust concentration in influent stream: (g/m³)

C_{out} : Dust concentration in effluent stream: (g/m³)

From the calibration results, all process limitations were considered and proper experimental conditions were selected. 3 media thicknesses and 4 face velocities were varied to give 12 experimental conditions as shown in Table 4.1.

Table 4.1 Summary of experimental conditions

Condition	Media thickness [m]	Face velocity [m/s]	Inlet dust concentration [g/m ³]
1	0.125	0.22	1.89*
2	0.125	0.48	1.2126
3	0.125	0.63	1.03
4	0.125	0.81	0.7856
5	0.25	0.22	1.89*
6	0.25	0.48	1.2126
7	0.25	0.63	1.03
8	0.25	0.81	0.7856
9	0.5	0.22	1.89*
10	0.5	0.48	1.2126
11	0.5	0.63	1.03
12	0.5	0.81	0.7856

* Air velocity in the pipeline for conditions 1, 5, and 9 was so low that calcium carbonate particles can not be well mixed with air in fluidization zone (due to effect of minimum fluidization velocity, as shown in Appendix D1). Consequently, it was necessary to decrease the feed mass flow rate of dust particles.

สถาบันวิทยบริการ
จุฬาลงกรณ์มหาวิทยาลัย

4.2.2 Experimental Results and Discussion



Figure 4.15 Well packed rice husk media filter in the media box.

Effect of filtration time on the increase of pressure drop was measured and presented in Figure 4.16. Meanwhile, dust particles collected by HEPA filter were weighed, and dust collection efficiencies during each 30 minutes of operation were calculated.

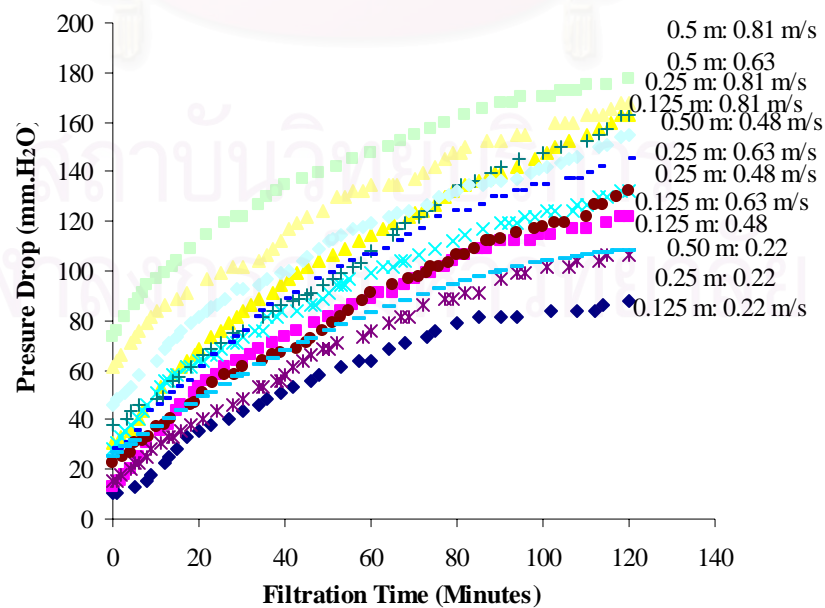


Figure 4.16 Correlation of pressure drop with filtration time (bed thickness: face velocity)

According to Figure 4.16, the pressure drop monotonically rose with the filtration time. On the other hand, the slope of each curve gently decreased with time. In the case of surface filtration, such as bag filtration, a distinct layer of dust cake would be formed and the rate of pressure drop rise should be constant as filtration time increased, unless compaction of the cake layer occurred. [10] With compaction, the rate of pressure drop rise would become faster and not slower. In the case of high-efficiency air filtration, particles would penetrate only a small distance into the filter mat. As particles continued to deposit and accumulate in this zone, the collection efficiency and the pressure drop would rise at a faster and faster rate until clogging of the filter occurred. This scenario assumed that there would be negligible re-entrainment or detachment of captured particles.

In the present experiments, the size of rice husk or filter media was much larger than the dust particles and the adhesion forces between rice husk and dust particles as well as the cohesion forces between dust particles themselves were not very strong. *This means that dust particles would penetrate a significant distance, say several ten to hundred millimeters before being mostly captured. Note that the overall penetration rate for the entire bed was as high as 15% and not less than a few percents.* As particles continued to deposit and accumulate in the front end of the bed, the bed porosity would decrease and the collection efficiency increased. So would the pressure drop and the interstitial gas velocity increase. Because of relatively weak adhesion and cohesion forces, however, clogging would not occur but a point would come when fracture of the deposited structure occurred, and the bed porosity rebounded slightly. After this point of time, re-entrainment of excess particles would limit any new net deposition of particles in this “saturated” zone. This is the reason why the rate of pressure drop rise becomes slower as filtration time increased. The described scenarios could be observed in Figure 4.17 – 4.19. By comparing the data in Figure 4.16 with those in Figure 4.21, it was clear that dust collection efficiency did not vary proportionally with the pressure drop.



Figure 4.17 (a) Dust particles deposited, accumulated, and formed a non-uniform patchy dust cake layer while penetrating and partially passing through the bed [A photo taken after 2 hours of operation, at 0.63 m/s of face velocity, when thickness of media filter was 0.25 m.]



Figure 4.17 (b) A zoomed-up photo of dust cake layer was revealed. Obviously, the layer was a nonuniform patchy combination of calcium carbonate dust and rice husk particles.



Figure 4.18 Another photo illustrating the formation of dust cake layer as well as dust penetration. [Taken after 2 hours of operation, at 0.63 m/s of face velocity, and 0.5 m. of media thickness]



Figure 4.19 Front view of the filtration area showing the formation of patchy dust cake layer (The net screen is clearly visible) [Taken after 2 hours of operation, at 0.81 m/s of face velocity, and 0.5 m. of media thickness]



Figure 4.20 Another front view of the inlet filtration area showing the formation of non-uniform dust cake layer (The net screen is clearly visible) [Taken after 2 hours of operation, at 0.63 m/s of face velocity, and 0.125 m. of media thickness]

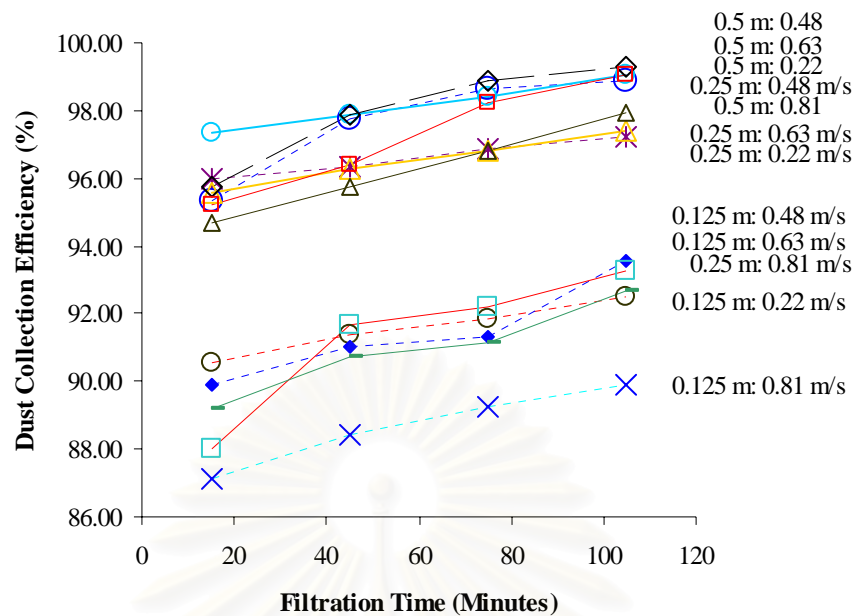


Figure 4.21 Relation of dust collection efficiency with filtration time

In Figure 4.21, there are 12 curves representing 12 conditions of experiment. These curves revealed that the dust collection efficiency was definitely a function of the filtration time with media thickness and face velocity as parameters. Since the filtration time was closely related to the dust load and thickness of dust cake layer, the dust collection efficiency could be expressed as a function of the dust load instead of the filtration time. While an increase in the media thickness and dust load would result in a corresponding increase in the dust collection efficiency, an increase in face velocity would result instead in a decrease in the dust collection efficiency. In addition, it could be concluded that *the media thickness and dust load played major roles, whereas the face velocity played a minor role in affecting the dust collection efficiency.*

The conclusion that the dust collection efficiency decreased against an increase in the filtration velocity was supported by the experiment results. According to equation (3.11)

$$\eta_D = \left(\frac{8}{3\pi} \right) \left(\frac{2}{Pe} \right)^{\frac{1}{2}} \quad (3.11).$$

Therefore, it could be considered that the diffusion mechanism, by which submicron dust particles deposited on media particle, was a dominant mechanism in this system. Also, interception mechanism, which provided even more effect to filtration efficiency than diffusion mechanism, was predominated in this range of size of dust particle. However, when the size of dust particles was in the range of micrometers, the initial impaction deposition mechanism would gradually become more important. *The dust collection efficiency due to the effect of initial impaction deposition mechanism (η_I) could be found in Figure 3.1*

As mentioned before, a dust cake layer, or stack of screened dust particles, would be generated, thereby reducing the porosity of filter media, and increasing the dust collection efficiency of filter media. If the shape of calcium carbonate dust particles were spherical, the pore size in the dust cake layer would definitely be smaller than that of dust particles themselves, as shown in Figure 4.21. So, the cake layer would possess higher potential in filtrating dust particles from dust-laden air than the clean filter media.

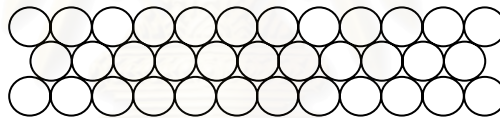


Figure 4.22 Dust cake layer of packed bed

However, as mentioned earlier, dust particles were not really piled up and packed as the stack of dust cake over the rice husk media, but they penetrate and partially filled up the empty spaces in the bed, thereby gradually boosting up the dust collection efficiency. This assumption was supported not only by experimental efficiencies but also by photo taken (Figures 4.17, 4.18, and 4.19), as well as pressure drop measured with respect to filtration time.

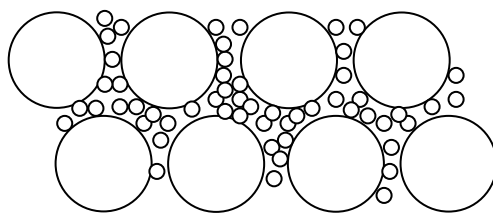


Figure 4.23 Dust particles (smaller) partially filled empty spaces between rice husk particles (bigger) and led to increase in dust collection dust collection efficiency.

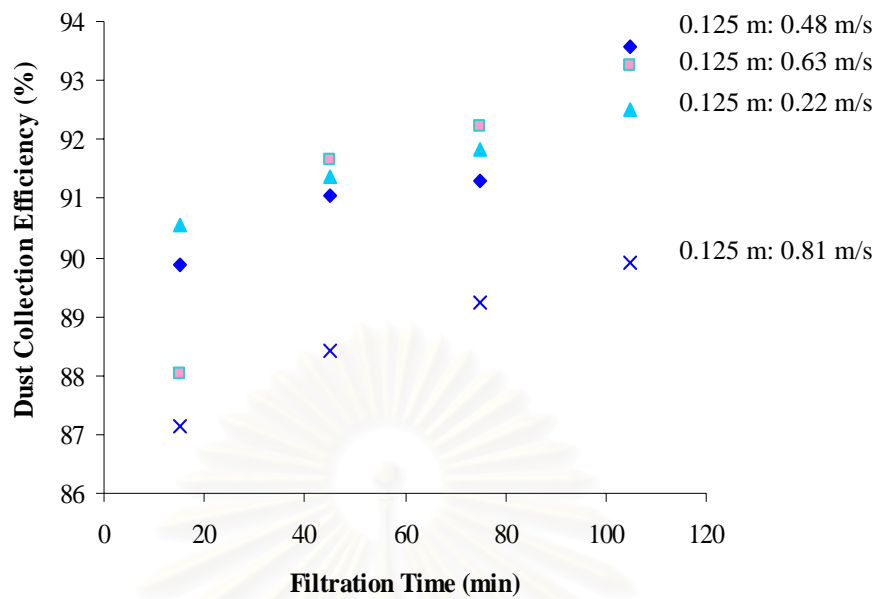


Figure 4.24 Relation of dust collection efficiency with filtration time for 0.125 m. media thickness

In Figure 4.24, dust collection efficiencies in the case of 0.125 m. of media thickness, were plotted against filtration times. Obviously, the dust collection efficiency would be gradually increased due to the effect of dust cake formation. In the early stage of the experiments the dust collection efficiencies for 0.22 m/s of face velocity was greater than those for 0.48, 0.63 and 0.81 m/s of face velocity, respectively, because of the effect of diffusion mechanism. However, since the amount of dust particles fed out from the accurate feeder, in the case of 0.22 m./s face velocity, was less than the 3 other cases, as mentioned in Table 4.1, it was clear that rate of dust cake formation for 0.22 m./s face velocity would be much slower than that of the 3 conditions. Consequently, the increase in rate of dust collection efficiency for 0.22 m/s face velocity was less than that for 0.48 m/s and 0.63 m/s face velocity after a long filtration time. As a result, effect of dust cake layer would finally win over that of face velocity after a long filtration time. Therefore, the dust collection efficiency for 0.48 m/s and 0.63 m/s of face velocity overtakes that for 0.22 m/s.

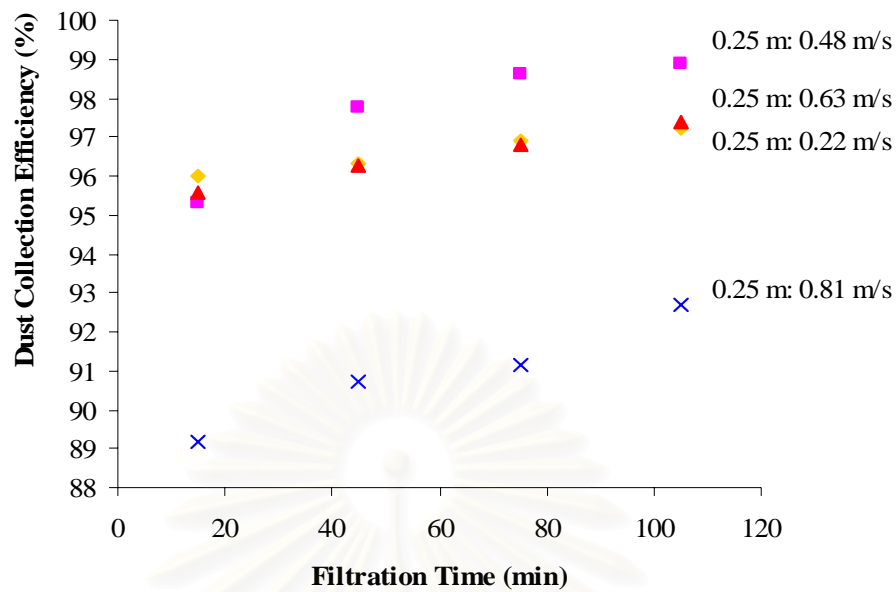


Figure 4.25 Relation of dust collection efficiency with filtration time for 0.25 m. media thickness

In Figure 4.25, the trend of dust collection efficiency for 0.25 m. of media thickness stayed slightly above those for 0.125 m. of media thickness. However, the trend of dust collection efficiency with respect to the media thickness, dust load, and face velocity, were still the same and is not reiterated here. The same comments are also applicable to Figure 4.26.

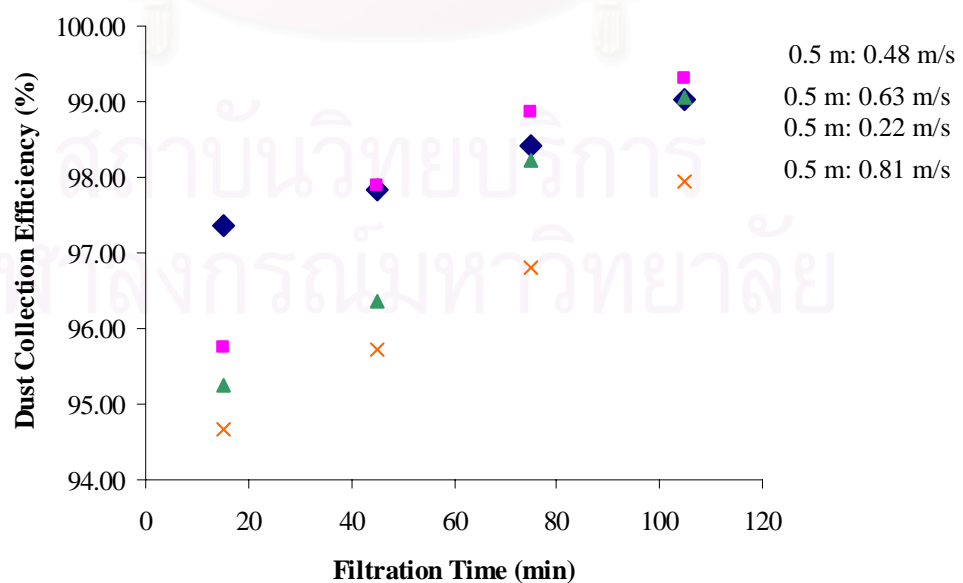


Figure 4.26 Relation of dust collection efficiency with operation time for 0.5 m. media thickness

4.3 Comparison of experimental pressure drop data with those calculated with Ergun equation

To estimate the flow resistance of filter media, it is practical to use the well-known Ergun equation. Ergun equation is an empirical correlation for estimation of pressure drop across a packed bed [16]. It is the combination of two parts of flow resistances, fluid viscosity and kinetic energy, as shown in equation 4.2.

$$\left(\frac{\Delta P_m}{t}\right) = \rho * \left(\frac{S_p}{V_p}\right) * \left(\frac{1-\varepsilon}{\varepsilon^3}\right) * \left[\left[\left(\frac{150 * \mu * U_0 * (1-\varepsilon)}{36}\right) * \left(\frac{S_p}{\rho * V_p}\right)\right] + \left(\frac{1.75 * U_0^2}{6}\right)\right] \quad (4.2)$$

, where

ΔP_m : Pressure drop across the media filter: [Pa]

t : Media thickness: [m.]

μ : Air viscosity: [kg/ms],

(based on the viscosity of clean air at 27° C)

ρ : Air density: 1.3 [kg/m³]

(based on the density of clean air at 27° C)

ε : Porosity of media: [-]

U_0 : Filtration velocity: [m/s]

S_p : Surface area of a media particle: $\pi * (D_m^2)/4$

V_p : Volume of a media particle: $\pi * (D_m^3)/6$

D_m : Equivalent diameter of media particle: [m]

Equation (4.2) was rearranged to give Equation (4.3).

$$\left(\frac{\Delta P_m}{t}\right) = \rho * \left(\frac{1.5}{D_m}\right) * \left(\frac{1-\varepsilon}{\varepsilon^3}\right) * \left[\left[\left(\frac{150 * \mu * U_0 * (1-\varepsilon)}{36}\right) * \left(\frac{1.5}{\rho * D_m}\right)\right] + \left(\frac{1.75 * U_0^2}{6}\right)\right] \quad (4.3)$$

As mention before, filtered dust particles did not form a distinct uniform dust cake layer, but they penetrated and partially filled the empty spaces in the filter media. Therefore, the filtration phenomenon is so complicated that the Ergun equation was not appropriate for predicting the pressure drop in the presence of the dust cake layer. Consequently, the application of Ergun equation here was limited for the calculation of the pressure drop across the clean filter media. Table 4.2 summarizes the equivalent

diameters of rice husk obtained via 4 different methods. Each of those 4 equivalent diameters was substituted into Equation 4.2 to gain the calculated pressure drop.

Table 4.2 Equivalent diameters calculated with four different methods

Methods	Equivalent diameter (mm.)
Equivalent in terminal velocity (D_{ET}) (Stokes diameter)	0.237
Equivalent in surface area of particle (D_{ES})	3.101
Equivalent in volume of particle (D_{EV})	1.593
Equivalent diameter from sieve mesh (D_{EM})	2.000

Table 4.3 Initial experimental versus predicted pressure drops obtained from calculations, using the equivalent diameters in Table 4.2

Case	Media thickness (m)	Face velocity (m/s)	ΔP_E (Pa) [experimental results]	ΔP_1 (Pa) [$D_{ET} = 0.237$ mm]	ΔP_2 (Pa) [$D_{ES} = 3.101$ mm]	ΔP_3 (Pa) [$D_{EV} = 1.593$ mm]	ΔP_4 (Pa) [$D_{EM} = 2.000$ mm]
1	0.125	0.22	99.6	1092.2	14.0	37.8	26.6
2	0.125	0.48	124.5	2660.2	51.7	123.7	90.8
3	0.125	0.63	273.9	3701.5	83.8	193.6	144.1
4	0.125	0.81	298.8	5083.1	132.6	297.1	223.7
5	0.25	0.22	128.0	2184.3	28.0	75.6	53.1
6	0.25	0.48	224.1	5320.5	103.4	247.4	181.7
7	0.25	0.63	273.9	7403.1	167.7	387.2	288.2
8	0.25	0.81	373.5	10166.2	265.2	594.3	447.3
9	0.5	0.22	247.1	4368.7	55.9	151.2	106.3
10	0.5	0.48	448.2	10641.0	206.7	494.9	363.3
11	0.5	0.63	597.7	14806.2	335.5	774.5	576.4
12	0.5	0.81	804.9	20332.4	530.4	1188.5	894.7

From Table 4.3, Equivalent diameter based on the volume of media particle provided the most suitable result in pressure drops, comparing with experimental results. I could be found it research of R. Pan et al. [14] that the equivalent diameter

based on volume equivalent representing good physical properties, including pressure drop, of the packed bed.

It should be noted that the calculated results were relied on Ergun equation, which was generally applied to predict flow resistance provided by the “granular” packed bed, and shape of rice husk particle was clearly a flake-like, not a spherical one. Then, sphericity [16] should adjust to D_{EV} to earn another form of equivalent diameter.

Sphericity was defined as surface-volume ratio for a sphere of diameter D_P divided by the surface-volume ratio for the particle whose nominal size is D_P [16].

Thus,

$$\Phi_S = \frac{\left(\frac{6}{D_P}\right)}{\left(\frac{S_P}{V_P}\right)} \quad (4.5)$$

, where in this case, S_P was defined as specific surface and V_P as specific volume of an observed particle, rice husk. And, it was revealed in Chapter 1 that S_P and V_P of rice husk particle were equal to 30.21 mm^2 and 2.115 mm^3 respectively. By substituting D_P with $D_{EV} = 1.593 \text{ mm}$. into equation 4.5, it would gain that

$$\Phi_S = \frac{\left(\frac{6}{(1.593)}\right)}{\left(\frac{30.21}{2.115}\right)} = 0.264$$

$$\text{Defining that } D_{EV}^* = \Phi_S * D_{EV} \quad (4.6)$$

$$\text{So, } D_{EV}^* = (0.264) * (1.593 * 10^{-3}) = 4.206 * 10^{-4} \text{ m.}$$

Pressure drops corresponding to D_{EV}^* were illustrated in Table 4.5 and compared with those resulted from D_{EV} in Table 4.4. It was obvious that the original equivalent diameter based on volume equivalence ($D_{EV} = 1.593 \text{ mm}$.) providing closer pressure drops to the experimental results than the adjusted equivalent diameter ($D_{EV} = 0.421 \text{ mm}$.). Then, there was no need to adjust the D_{EV} with sphericity.

Table 4.4 Calculation results of pressure drop corresponding to $D_{EV} = 1.593$ mm.

Case	Media thickness (m)	Face velocity (m/s)	ΔP_E (Pa) [experimental results]	ΔP_1 (Pa) [$D_{EV} = 1.593$ mm]	Relative error [%]
1	0.125	0.22	99.6	37.8	62.1
2	0.125	0.48	124.5	123.7	0.6
3	0.125	0.63	273.9	193.6	29.3
4	0.125	0.81	298.8	297.1	0.6
5	0.25	0.22	128.0	75.6	41.0
6	0.25	0.48	224.1	247.4	- 10.4
7	0.25	0.63	273.9	387.2	- 41.4
8	0.25	0.81	373.5	594.3	- 59.1
9	0.5	0.22	247.1	151.2	38.8
10	0.5	0.48	448.2	494.9	- 10.4
11	0.5	0.63	597.7	774.5	- 29.6
12	0.5	0.81	804.9	1188.5	- 47.7

Table 4.5 Calculation results of pressure drop corresponding to $D_{EV}^* = 0.421$ mm.

Case	Media thickness (m)	Face velocity (m/s)	ΔP_E (Pa) [experimental results]	ΔP_1 (Pa) [$D_{EV}^* = 0.421$ mm]	Relative error [%]
1	0.125	0.22	99.6	372.6	- 274.0
2	0.125	0.48	124.5	969.0	- 678.3
3	0.125	0.63	273.9	1390.0	- 407.5
4	0.125	0.81	298.8	1969.6	- 559.1
5	0.25	0.22	128.0	745.2	-482.0
6	0.25	0.48	224.1	1930.0	- 762.2
7	0.25	0.63	273.9	2780.1	- 915.0
8	0.25	0.81	373.5	3939.1	- 954.7
9	0.5	0.22	247.1	1490.3	- 503.1
10	0.5	0.48	448.2	3876.0	- 764.8
11	0.5	0.63	597.7	5560.1	- 830.3
12	0.5	0.81	804.9	7878.2	- 878.8

4.4 Comparison of experimental dust collection efficiencies with those estimated from the theory of deposition mechanism

Although the correlation to predict the filtration efficiency resulted from the combination of dust cake layer and rice husk media could not reliably be developed yet, it was still possible to compare initial filtration efficiency data measured at the beginning of the operation with those calculated by dust deposition mechanisms (Chapter 3). The calculation procedures of dust collection efficiency were accurately explained in Section 5.1.2.

Although it was believed, still, that D_{EV} should provide good prediction for filtration efficiency, calculated results corresponding to those equivalent diameters illustrated in Table 4.2 were compared with experimental result in Table 4.6

Table 4.6 Calculated results of filtration efficiency corresponding to equivalent diameter appeared in Table 4.2

Case	$\eta_{Overall}$ (-) (corresponding to $D_{ET} = 0.237$ mm.)	$\eta_{Overall}$ (-) (corresponding to $D_{ES} = 3.101$ mm.)	$\eta_{Overall}$ (-) (corresponding to $D_{EV} = 1.593$ mm.)	$\eta_{Overall}$ (-) (corresponding to $D_{EM} = 2.000$ mm.)
1	25.1	5.0	17.2	11.4
2	100.0	4.9	16.9	11.1
3	100.0	4.8	16.8	11.1
4	100.0	4.8	16.7	11.0
5	43.9	9.7	31.5	21.5
6	100.0	9.5	30.9	21.0
7	100.0	9.4	30.8	20.9
8	100.0	9.3	30.7	20.8
9	68.5	18.5	53.0	38.3
10	100.0	18.0	52.3	37.6
11	100.0	17.9	52.1	37.5
12	100.0	17.8	52.0	37.3

Due to deposition mechanisms, interception, inertial impaction, and diffusion, individual filtration efficiencies corresponding to each mechanism were combined to earn the single particle efficiency ($\eta_{\text{Media particle}}$), and then overall filtration efficiency (η_{Overall}) respectively (Chapter 3).

From Table 4.6, overall filtration efficiencies related to D_{ET} at 0.22 m/s of face velocity were affected by flow pattern of fluid, in that the viscous flow, appeared at low filtration velocity, provided less capability in capturing dust particles to interception mechanism than did the potential flow. And, in this range, interception mechanism was the most important one predominating to filtration efficiency. So, filtration efficiency at 0.22 m/s of face velocity was quite lower than other cases. However, once the filtration velocity reached 0.48 m/s, flow pattern was transformed into potential flow, which affected more impact to filtration efficiency than viscous flow. In addition, inertial impaction deposition mechanism became more important in those cases and was, therefore, the predominant of deposition mechanisms. This would lead to the fact that filtration efficiencies increased when face velocity increased, which was strongly contrast with experimental results.

On the other hand, D_{ES} , D_{EV} , and D_{EM} provided the same trend, in that filtration efficiency corresponding to these equivalent diameters increased with face velocity decreased, and among those diameters D_{EV} was the most suitable equivalent diameter to use in prediction of filtration efficiency.

It should be noted from Chapter 3 that filtration efficiency dedicated to each deposition mechanism for spherical media were

$$\eta_c = (1 + R)^2 - \frac{1}{(1 + R)} \quad (3.3)$$

, where η_c : the efficiency of collection resulted by interception

R: interception parameter: d_p/d_m (-)

$$\eta_D = \left(\frac{8}{3\pi} \right) \left(\frac{2}{\text{Pe}} \right)^{\frac{1}{2}} \quad (3.11)$$

, where η_D : the efficiency of collection resulted by diffusion

$$\text{Pe: Peclet number: } \text{Pe} = \frac{d_p U_o}{D} \quad (-)$$

and η_I , collection efficiency corresponding to inertial impaction mechanism, could be read from Figure 3.3, as shown below.

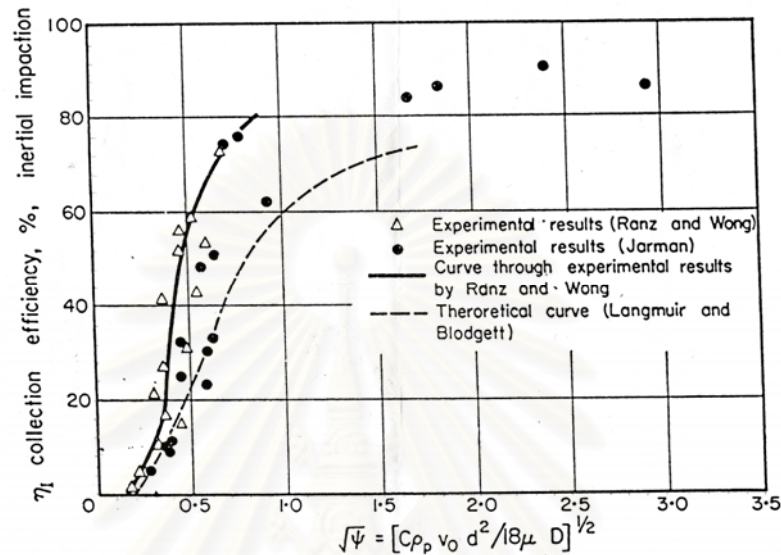


Figure 3.3 relations of η_I against $\text{Stk}^{1/2}$ (Spherical collector)

In brief, η_C was relied on interception parameter, R , which was the ratio of size of dust particle to size of media, not the face velocity. And, it was clear from equation 3.11 and Figure 3.3 that η_I increased when face velocity increased, and η_D increased with the decrease of face velocity. Then, it could be concluded that interception was predominated, and diffusion played its minor role in deposition mechanism.

สถาบันวิทยบริการ
จุฬาลงกรณ์มหาวิทยาลัย

Table 4.7 Accurate calculated results of filtration efficiency corresponding to $D_{EV} = 1.593$ mm.

Case	Media thickness (m)	Face velocity (m/s)	$\eta_{\text{Interception}}$ (-)	$\eta_{\text{Inertial impaction}}$ (-)	$\eta_{\text{Diffusion}}$ (-)	η_{Overall} (-) [experimental results]	η_{Overall} (-) [$D_{ET} = 1.593$ mm]	Relative error [%]
1	0.125	0.22	3.77×10^{-3}	0	2.5×10^{-4}	90.6	17.2	81.0
2	0.125	0.48	3.77×10^{-3}	0	1.7×10^{-4}	89.9	16.9	81.2
3	0.125	0.63	3.77×10^{-3}	0	1.4×10^{-4}	88.0	16.8	80.9
4	0.125	0.81	3.77×10^{-3}	0	1.2×10^{-4}	87.1	16.7	80.8
5	0.25	0.22	3.77×10^{-3}	0	2.5×10^{-4}	96.0	31.5	67.2
6	0.25	0.48	3.77×10^{-3}	0	1.7×10^{-4}	95.3	30.9	67.5
7	0.25	0.63	3.77×10^{-3}	0	1.4×10^{-4}	95.6	30.8	67.8
8	0.25	0.81	3.77×10^{-3}	0	1.2×10^{-4}	89.2	30.7	65.6
9	0.5	0.22	3.77×10^{-3}	0	2.5×10^{-4}	97.4	53.0	45.5
10	0.5	0.48	3.77×10^{-3}	0	1.7×10^{-4}	95.8	52.3	45.4
11	0.5	0.63	3.77×10^{-3}	0	1.4×10^{-4}	95.2	52.1	45.3
12	0.5	0.81	3.77×10^{-3}	0	1.2×10^{-4}	94.7	52.0	45.1

Although an equivalent diameter based on the volume of media particle, D_{EV} , was the best to represent the physical properties of the rice husk in the packed bed, still, the differences of 45 – 81% from experimental results remained. *Most, probably, this was caused by partial agglomeration of feed calcium carbonate dust particles, due to insufficient dispersion in the fluidized bed.*

Moreover, since the initial filtration efficiency was, in reality, based on the filtration efficiency measured over the first 30 minutes of operation, it was possible that some cakes forming could significantly affect filtration efficiency over that time of operation. It was considered here that the filtration efficiency η was separated in two zones, consisting of the saturated zone and the clean media zone (see Figure 4.27). The former zone was the mixing of dust particle and media. And it was assumed that dust particles fulfilling empty spaces between rice husk, while the latter was considered as clean bed providing deep bed filtration. The accurate calculation procedures could be found in Appendix D2.

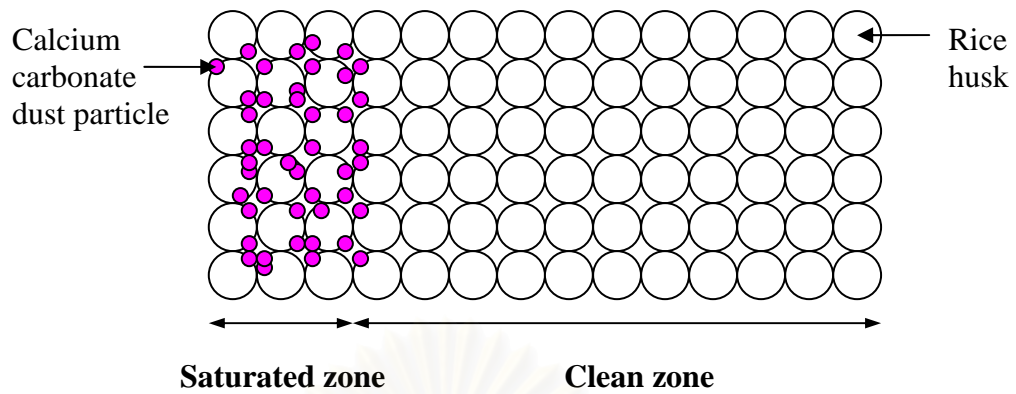


Figure 4.27 The model illustrating Saturated zone and clean zone in packed bed

Table 4.8 Comparison of experimental and calculated results when the saturated zone was included. ($D_{EV} = 1.593$ mm.)

Condition	Media thickness [m]	Face velocity [m/s]	Thickness of saturated zone [m.]	Initial dust collection efficiency, (Experimental) [-]	Initial dust collection efficiency, (Calculated with $D_{EV} = 1.593$ mm.) [-]	Relative error [%]
1	0.125	0.22	0.002	90.56	17.4	80.8
1	0.125	0.22	0.005	90.56	17.4	80.8
1	0.125	0.22	0.010	90.56	17.4	80.8
1	0.125	0.22	0.020	90.56	17.4	80.8
2	0.125	0.48	0.002	89.89	17.1	80.9
2	0.125	0.48	0.005	89.89	17.1	80.9
2	0.125	0.48	0.010	89.89	17.1	80.9
2	0.125	0.48	0.020	89.89	17.1	80.9
3	0.125	0.63	0.002	88.03	17.1	80.6
3	0.125	0.63	0.005	88.03	17.1	80.6
3	0.125	0.63	0.010	88.03	17.1	80.6
3	0.125	0.63	0.020	88.03	17.1	80.6
4	0.125	0.81	0.002	87.14	17.0	80.5
4	0.125	0.81	0.005	87.14	17.0	80.5
4	0.125	0.81	0.010	87.14	17.0	80.5
4	0.125	0.81	0.020	87.14	17.0	80.5
5	0.25	0.22	0.002	96.00	31.6	65.1
5	0.25	0.22	0.005	96.00	31.6	65.1
5	0.25	0.22	0.010	96.00	31.6	65.1

Table 4.8 (continue) Comparison of experimental and calculated results when the saturated zone was included. ($D_{EV} = 1.593$ mm.)

Condition	Media thickness [m]	Face velocity [m/s]	Thickness of saturated zone [m.]	Initial dust collection efficiency, (experimental) [-]	Initial dust collection efficiency, (Calculated with $D_{ET} = 1.593$ mm.) [-]	Relative error [%]
5	0.25	0.22	0.020	96.0	31.6	65.1
6	0.25	0.48	0.002	95.3	31.1	65.4
6	0.25	0.48	0.005	95.3	31.1	65.4
6	0.25	0.48	0.010	95.3	31.1	65.4
6	0.25	0.48	0.020	95.3	31.1	65.4
7	0.25	0.63	0.002	95.6	31.0	64.8
7	0.25	0.63	0.005	95.6	31.0	64.8
7	0.25	0.63	0.010	95.6	31.0	64.8
7	0.25	0.63	0.020	95.6	31.0	64.8
8	0.25	0.81	0.002	89.2	30.9	64.5
8	0.25	0.81	0.005	89.2	30.9	64.5
8	0.25	0.81	0.010	89.2	30.9	64.5
8	0.25	0.81	0.020	89.2	30.9	64.5
9	0.5	0.22	0.002	97.4	53.1	41.4
9	0.5	0.22	0.005	97.4	53.1	41.4
9	0.5	0.22	0.010	97.4	53.1	41.4
9	0.5	0.22	0.020	97.4	53.1	41.4
10	0.5	0.48	0.002	95.8	52.4	41.7
10	0.5	0.48	0.005	95.8	52.4	41.7
10	0.5	0.48	0.010	95.8	52.4	41.7
10	0.5	0.48	0.020	95.8	52.4	41.7
11	0.5	0.63	0.002	95.2	52.3	40.6
11	0.5	0.63	0.005	95.2	52.3	40.6
11	0.5	0.63	0.010	95.2	52.3	40.6
11	0.5	0.63	0.020	95.2	52.3	40.6
12	0.5	0.81	0.002	94.7	52.1	40.2
12	0.5	0.81	0.005	94.7	52.1	40.2
12	0.5	0.81	0.010	94.7	52.1	40.2
12	0.5	0.81	0.020	94.7	52.1	40.2

In Table 4.8, it was clear that dust cake slightly affect filtration efficiency,. However, effect of different thickness of saturated zone could be neglected. Since relative discrepancy gained in Table 4.8 were slightly less than those appeared in Table 4.7, the assumption that there existed the saturated zone, covering in front of the

filter media, was supported. However, thickness of the saturated zone was roughly estimated to be between 0.002 to 0.02 m. from the contacting surface of filter media.

Therefore, rice husk media was quite effective in capturing fine dust particles, judging by its performance of collecting more than 85% by mass of 2-micrometer dust particles. These experimental results revealed potential of rice husk in collecting dust particles, and promised the possibility of using rice husk bed as a media in dust collector.

4.5 Conclusions

1. Media thickness, dust cake layer thickness, and face velocity individually provided effects on filtration efficiency, and pressure drop of the whole system.
2. The increase in media thickness and dust cake layer thickness would strongly convince increasing in filtration efficiency. On the other hand, the increase in face velocity would moderately decrease dust collection efficiency of the filter media.
3. With media thickness, dust cake layer thickness, and face velocity increase, pressure drop across media filter would be increased.
4. Filtration efficiencies, gained from experiments at 0.125, 0.25, 0.5 m. of media thickness, were lying between 87-93%, 89-99%, and 92-99% by mass respectively, which were 40 to 80 % differing from data, predicted by theory of deposition mechanisms (based on $D_{EV} = 1.593$ mm.). The discrepancy between experimental and theoretical results was considered to partial result from the agglomeration of feed calcium carbonate dust particles.
5. Initial pressure drop results gained from experiments could be compared with those predicted by Ergun equation, in which, again, equivalent diameter was set at 1.593 mm., and differences between experimental and calculation results were revealed as $\pm 60\%$.
6. The interception and diffusion mechanisms were the major dust deposition mechanisms, controlling dust collection efficiency in this system.

CHAPTER 5

DESIGN OF RICE MILL DUST COLLECTION SYSTEM

Fine dust particles emitted from the agricultural industry is recently one of the most environmental concerns. Based on the hypothesis that fine dust particles detaching from rice husk could practically be captured by rice husk itself and the impressive performance tested in Chapter 4, a dust collection system made of rice husk media is developed. In this chapter, the design calculation of the rice-husk packed bed dust collection system is clearly explained.

5.1 Calculation of required thickness of rice-husk filter media

5.1.1 Face velocity and filtration area

Face velocity, U_0 , is defined as

$$U_0 = Q/A_F, \quad (5.1)$$

, where Q : Flow rate of dust-laden air (m^3/s)
 A_F : Filtration area (m^2)

And filtration velocity is defined as

$$U = \frac{Q}{(A_F * (1 - \varepsilon))} = \frac{Q}{(A_F * \alpha)} \quad (5.2)$$

, where α : Packing density of packed bed of media filter (-)
 ε : Void fraction of packed bed of media filter (-)

It is noted that $\alpha = 1 - \varepsilon$.

Generally, the suitable face velocity for packed bed filtration is between 0.1 to 0.2 m/s. [2] Two times the amount of the dust-laden air flow rate measured in section 1.2.3 is used in the design calculation as $2.4 m^3/s$. According to equation 5.1, if Q and U_0 is $2.4 m^3/s$ and $0.1 m/s$, respectively, the required filtration area (A_F) becomes at $24 m^2$. In conclusion, *24 square meters of filtration area is needed to filtrate 2.4 cubic meters of dust-laden air at 0.1 meters per second of face velocity.*

5.1.2 Minimum required of media thickness

As mentioned in section 3.1, the deposition mechanisms explain how a dust particle is captured by a media particle. They include interception, inertial impaction, diffusion, and gravitational settling mechanisms. To find the required thickness of filter media, a minimum overall dust collection efficiency of the filter media is first identified at 95% by mass. *It means that 0.95 gram out of 1 gram of influent dust particles, passing through the media, must be captured.* For simplicity, dust collection efficiencies, corresponding to each of the four deposition mechanisms, will be considered individually.

- Dust collection efficiency due to the effect of interception deposition mechanism (η_c)

When a dust particle, moving along with air stream of dust-laden air, comes close enough to a media particle, it would collide and be captured on the surface of that media by virtue of the particle size. This is called interception deposition mechanism. (Section 3.1.1). [13]

First of all, the Reynolds number (N_{Re}) of the flow is calculated to explain the characteristics of fluid flow around a media. In this situation, the Reynolds Number is defined as in equation 5.3 [16]

$$N_{Re} = \frac{\rho_a * d_m * U}{\mu} \quad (5.3).$$

Where ρ_a : Density of air at room temperature (27° C): 1.3 kg/m³

μ : Viscosity of air (27° C): 1.81*10⁻⁵ kg/ms

d_m : Average size of diameter of media particle: $D_{EV} = 1.593$ mm.

U: Filtration velocity of air passing through the media particle:
referring to equation 5.2,

$$U = \frac{2.4}{[24 * (0.6)]} = 0.17 \text{ m/s}$$

$$\text{Then, } N_{Re} = \frac{(1.3) * (1.593 * 10^{-3}) * (0.17)}{(1.81 * 10^{-5})}$$

$$N_{Re} = 19.45 \gg 1$$

, the flow pattern is potential flow. [13]

However, as this dust collector is targetted at capturing fine dust of rice mill particles, diameter of dust, assumed in design process, is defined at *10 micrometers* (In the first assumption, targetted size of rice mill dust is used. Filtration efficiencies corresponding to other sizes of dust are illustrated in Table 5.5). Size distribution curve of rice-husk dust particle is shown in Appendix C1.

Referring to equation 3.3, the dust collection efficiency of a media particle due to effect of Interception deposition mechanism is shown below.

$$\eta_c = (1 + R)^2 - \frac{1}{(1 + R)} \quad (3.3)^{[13]}$$

Where

R: Interception parameter: $R = d_p/d_m$

d_p : Identified diameter of finedust particle: 10 μm .

d_m : Equivalent diameter of media particle: 1.593 mm.

(referring to section 1.2.5)

$$R = \frac{(10 * 10^{-6})}{(1.593 * 10^{-3})} = 6.277 * 10^{-3}$$

Then,

$$\eta_c = (1 + (6.277 * 10^{-3}))^2 - \frac{1}{(1 + (6.277 * 10^{-3}))}$$

$$\eta_c = 1.883 * 10^{-2} \quad (5.4)$$

- Dust collection efficiency due to the effect of Inertial Impaction Deposition

Mechanism (η_i)

The dust collection efficiency corresponding to this deposition mechanism is a function of Stokes number (Stk).

$$Stk = \frac{C_c \rho_p U_0 d_p^2}{(18 \mu d_m)} \quad (3.6)^{[13]}$$

Where C_c : Cunningham correction factor:

$$C_c = 1 + \left(\frac{2 * \lambda}{d_p} \right) * [0.7004 * ((2 * a) - 1)] \quad (3.7)^{[13]}$$

λ : Mean Free Path: 3.7×10^{-10} m.

a : coefficient of diffuse reflection :

$a = 0.9$ (assume a rigid body)

$$C = 1 + \left(\frac{2 * 3.7 * 10^{-10}}{10 * 10^{-6}} \right) * [0.7004 * ((2 * 0.9) - 1)]$$

$$C \approx 1$$

ρ_p : Density of dust particle: $2,330 \text{ kg/m}^3$ (assume pure silica)

U_0 : Face velocity: 0.1 m/s

$$\text{From equation (3.6), } \text{Stk} = \frac{1 * 2,330 * 0.1 * (10 * 10^{-6})^2}{(18 * 1.81 * 10^{-5} * 1.593 * 10^{-3})}$$

$$\text{Stk} = 4.489 * 10^{-2}$$

The dust collection efficiency ascribed to inertial impaction deposition mechanism (η_I) is a function of $\text{Stk}^{1/2}$ and can be read from Figure 3.3

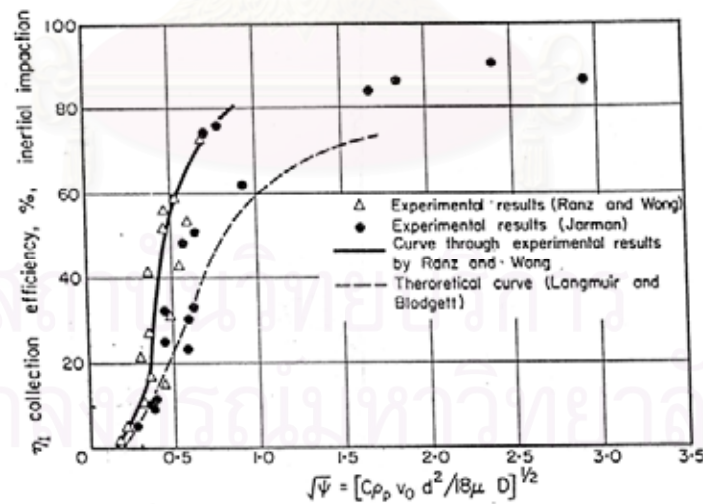


Figure 3.3 Correlations of $\text{Stk}^{1/2}$ and η_I [13]

It is gained from Figure 3.3 that

$$\eta_I = 5.00 * 10^{-3} \quad (5.5).$$

- Dust collection efficiency due to the effect of Diffusion Deposition Mechanism (η_D)

Fine particles, submicrons or nanometers in size, would diffusively move in dust-laden air. This kind of motion is called “Brownian motion”, in which movements of particles are random.

The Peclet number is an important parameter in calculating the dust collection efficiency according to the diffusion deposition mechanism (η_D).

$$Pe = \frac{d_m U_o}{D} \quad (3.9)$$

D: Particle Diffusion Coefficient: 2.806×10^{-12} (m^2/s)

$$Pe = \frac{1.593 \times 10^{-3} \times 0.1}{2.806 \times 10^{-12}} = 5.677 \times 10^7$$

It is shown in Equation 3.11 that

$$\eta_D = \left(\frac{8}{3\pi} \right) \left(\frac{2}{Pe} \right)^{\frac{1}{2}} \quad (3.11)$$

Therefore
$$\eta_D = \left(\frac{8}{3\pi} \right) \left(\frac{2}{5.677 \times 10^7} \right)^{\frac{1}{2}} = 1.593 \times 10^{-4} \quad (5.6)$$

- Dust collection efficiency due to the effect of Gravitational Settling Deposition Mechanism (η_G)

Gravitational force of the earth is major cause of this deposition mechanism. Since gravity would affect movement of a dust particle by pulling it down vertically and collecting it, the dust collection efficiency related to gravitational settling (η_G) could be neglected in the design of this rice-husk packed bed dust collector, in which surface of rice husk media is not vertical and most of dust load in this process is fine dust. It appears that

$$\eta_G = 0.000 \quad (5.7)$$

Overall dust collection efficiency ($\eta_{\text{Media Particle}}$)

Since dust collection efficiencies of a single particle due to all four deposition mechanism are already calculated, the combined dust collection efficiency of a single media particle ($\eta_{\text{Media Particle}}$) could be found by Equation 3.12.

$$\eta_{\text{Media Particle}} = 1 - [(1 - \eta_I) * (1 - \eta_C) * (1 - \eta_D) * (1 - \eta_G)] \quad (3.12)$$

Replacing all individual collection efficiency in Equation 3.12, it is found that

$$\eta_{\text{Media Particle}} = 1 - [(1 - 5.000 * 10^{-3}) * (1 - 1.883 * 10^{-2}) * (1 - 1.593 * 10^{-4}) * (1 - 0.000)]$$

$$\eta_{\text{Media Particle}} = 2.389 * 10^{-2}$$

And it is shown in Equation 3.22 that

$$P = 1 - E = e^{\left(-1.5 * \left(\frac{\alpha * x}{d_m} \right) * \eta_{\text{Media Particle}} \right)} \quad (3.22)$$

Where

P : Penetration (-)

E : Overall dust collection efficiency (defined at 0.95)

$\eta_{\text{Medium Particle}}$: Dust collection efficiency of a single particle:
($2.389 * 10^{-2}$)

t : Minimum required thickness of media filter (m.)

d_m : Equivalent diameter of a single media particle:

($D_{EV} = 2.174 * 10^{-3}$ m)

$$P = 1 - 0.95 = e^{\left(-1.5 * \left(\frac{0.4 * t}{1.593 * 10^{-3}} \right) * 2.389 * 10^{-2} \right)}$$

$$t = 0.332 \text{ m.}$$

The required thickness of the filter media as calculated from Equation 3.22 is 0.332 m. It could be concluded that 0.332 m. of filter media is capable of screening dust particles, which is 10 micrometers in size, with the efficiency of 95%.

Similarly, required thicknesses of rice husk bed corresponding to other sizes of rice mill dust particles are shown in Table 5.1.

Table 5.1 Required thicknesses of filter media corresponding to each size of rice mill dust particles.

Considered size of rice mill dust particles	Collection efficiency due to Interception (η_c)	Collection efficiency due to Inertial impaction (η_i)	Collection efficiency due to Diffusion (η_D)	Single particle efficiency ($\eta_{\text{Media particle}}$)	Required media thickness (m.)
10	1.883×10^{-2}	5.000×10^{-3}	1.593×10^{-4}	2.389×10^{-2}	3.32×10^{-1}
8	1.507×10^{-2}	0.000	1.786×10^{-4}	1.524×10^{-2}	5.21×10^{-1}
5	9.416×10^{-3}	0.000	2.275×10^{-4}	9.643×10^{-3}	8.24×10^{-1}
3	5.650×10^{-3}	0.000	2.959×10^{-4}	5.944×10^{-3}	1.34
1	1.883×10^{-3}	0.000	5.207×10^{-4}	2.403×10^{-3}	3.31
0.5	9.416×10^{-4}	0.000	7.439×10^{-4}	1.685×10^{-3}	4.721
0.1	1.883×10^{-4}	0.000	1.703×10^{-3}	1.891×10^{-3}	4.207

It should be noted that diameter of rice husk collector is equivalent diameter relied on volume basis, filtration velocity is steady at 0.1 m/s, and density of rice mill dust particles is assumed equal to pure silica at $2,330 \text{ kg/m}^3$.

It is clear from Table 5.1 that the thicker the media filter is, the higher performance the media filter possesses. Since the dimension of the dust collector would directly depend on the thickness of media filter, it is not practical to assign more than 1 meter to the thickness of media filter. So the expected dust collection efficiency responding to 1 meter of media thickness is listed in Table 5.2.

สถาบันวิทยบริการ
จุฬาลงกรณ์มหาวิทยาลัย

Table 5.2 Overall dust collection efficiencies, corresponding to 1 meter of media filter.

Considered size of rice mill dust particles	Collection efficiency due to Interception (η_C)	Collection efficiency due to Inertial impaction (η_I)	Collection efficiency due to Diffusion (η_D)	Single particle efficiency ($\eta_{\text{Media particle}}$)	Overall filtration efficiency (η_{overall})
10	1.883×10^{-2}	5.000×10^{-3}	1.593×10^{-4}	2.389×10^{-2}	99.99
8	1.507×10^{-2}	0.000	1.786×10^{-4}	1.524×10^{-2}	99.68
5	9.416×10^{-3}	0.000	2.275×10^{-4}	9.643×10^{-3}	97.35
3	5.650×10^{-3}	0.000	2.959×10^{-4}	5.944×10^{-3}	89.34
1	1.883×10^{-3}	0.000	5.207×10^{-4}	2.403×10^{-3}	59.55
0.5	9.416×10^{-4}	0.000	7.439×10^{-4}	1.685×10^{-3}	46.98
0.1	1.883×10^{-4}	0.000	1.703×10^{-3}	1.891×10^{-3}	50.94

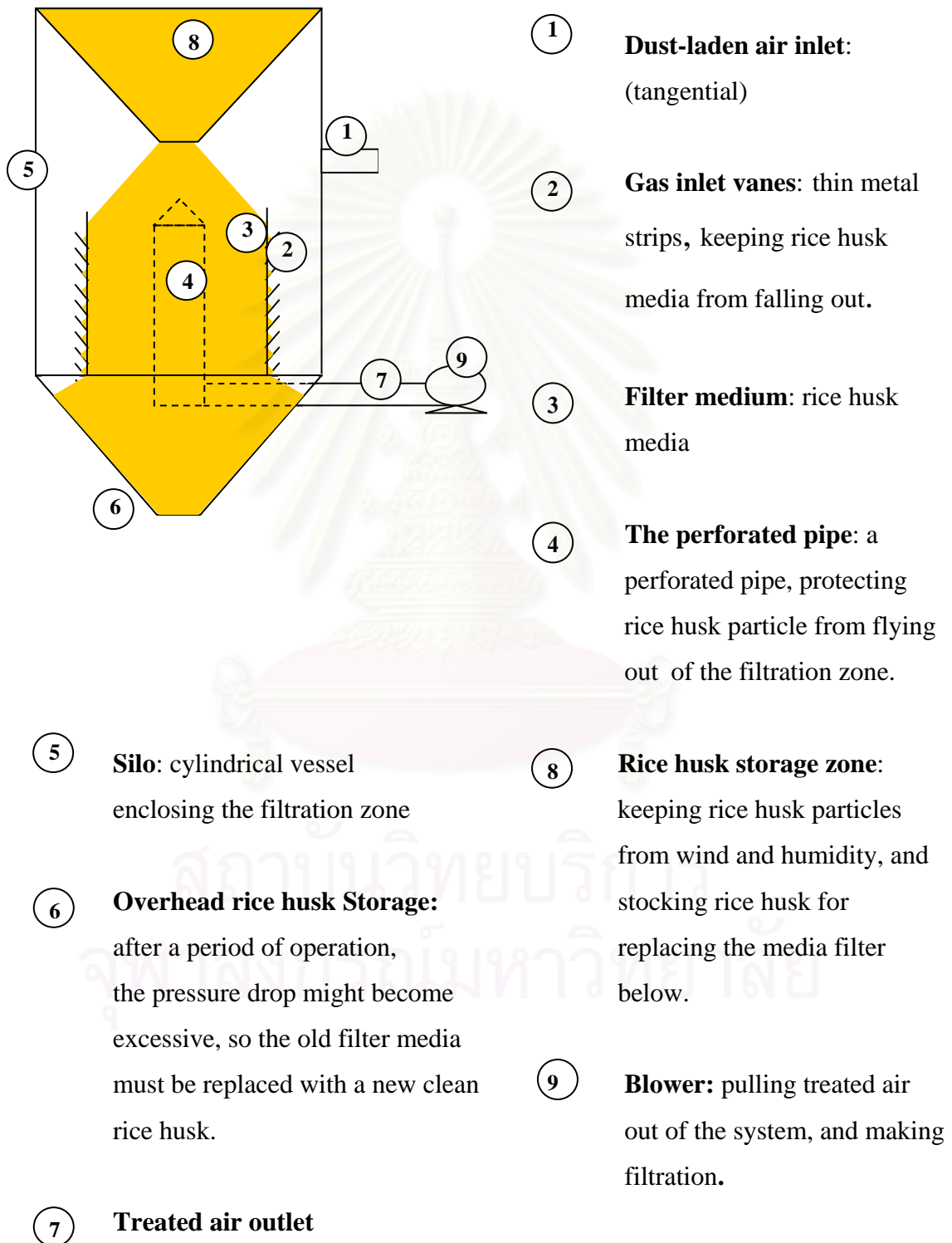
5.2 Dimension designation

Once the thickness of media filter is chosen as 1 meter, the various dimensions of the dust collector could be designed and sketched. Basically, the rice-husk packed bed dust collector is planned to imitate the shape of an ordinary silo, equipped with a filtration zone, of which rice husk bed is applied as a media filter. When the filtration process begins, dust particles in the dust-laden air would be screened and gradually piled up to become a dust cake layer, covering the filtration surface. Because the void spaces between the screened dust particles, accumulated as dust cake layer, are much smaller than the void spaces between the rice husk media or even the size of dust particle itself, the dust cake layer possesses higher dust collection efficiency than the media filter.

In Figure 5.1, first of all, the dust-laden air comes through the inlet port located tangentially (indicated as number 1) into the cylindrical silo (number 5). As the dust-laden air is suctioned down through the porous perforated pipe (number 4) by the pull force of a blower (number 9), the air is filtrated by the packed bed of rice husk media filter (number 3), supported by gas inlet vane (number 2). Finally, the clean filtrated air would flow out through the air outlet (number 7). However, once the pressure drop across the media filter, due to formation and accumulation of dust cake layer, reaches a maximum allowable point, the partially clogged media filter

must be discharged (number 6) and the bed is replaced by clean rice husk media, stored in an overhead rice husk storage (number 8).

Figure 5.1 Schematic diagram of the dust collector



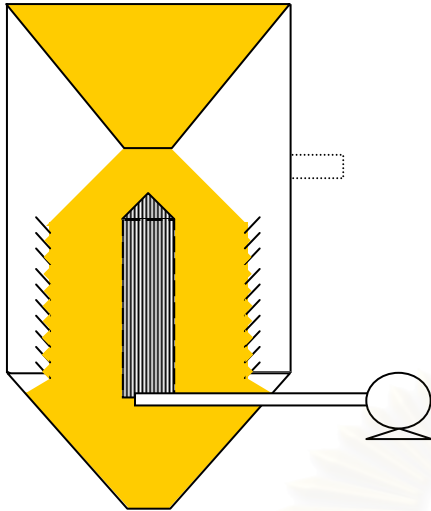


Figure 5.2 Schematic diagram of the dust collector (2)

The rice mill owner was interviewed and he recommended that *an ordinary silo should not exceed 4 meters in diameter. And the maximum horse power of a blower that the rice mill felt comfortable to afford should not exceed 20 HP.*

5.2.1 Dimension of perforated pipe

Basically, the air transport velocity in a pipe line should not exceed 15 m/s. [2] Since the filtration velocity is only around 0.17 m/s, the air velocity in the perforated pipe is controlled at 7 m/s.

$$Q = U_0 A_p \quad (5.8)$$

Q: Flow rate of dust-laden air (m³/s)

A_p: Projected area of perforated pipe (m²)

U₀: Face velocity (m/s)

Substitution of into the equation (5.8), we obtain

$$2.4 \text{ m}^3/\text{s} = \frac{7 * \pi * D_F^2}{4} \quad (5.9)$$

The exact diameter of the perforated pipe, calculated by equation 5.9, is 0.66 m. Practically, the perforated pipe is chosen as 0.7 m. of diameter.

5.2.2 Appropriated thickness of media filter and void spaces

As of now, the total diameter of the silo is selected at 4 m. and the size of the perforated pipe is set at 0.7 m. in diameter. When empty spaces around the dust collection system are considered, it is possible to determine an appropriate thickness of the filter media. 0.65 m. of void space is spared on each side of the silo, in order to collect data, investigate dust filtration phenomena, and modify or fix internal parts. The thickness of the filter media could be found by solving equation 5.10.

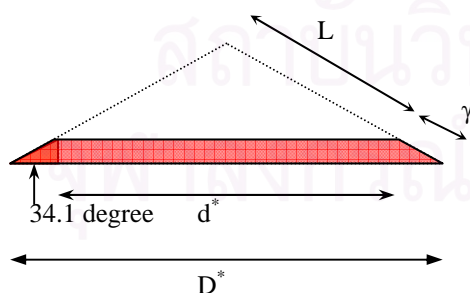
$$4 = (0.65*2) + (t*2) + 0.7 \quad (5.10)$$

It is obvious from Equation 5.10 that the appropriate thickness of the filter media is limited at 1 m., which is equal to the required thickness of media filter chosen in Table 5.5. According to the calculation results expressed in Table 5.2, 1 m. of rice husk media is capable of collecting 3-micrometer dust particles with an efficiency of almost 90 %. (It is worth noting from our experimental results that that 0.5 m. rice husk bed was capable in filtrating 2 μ m. dust particles with the filtration efficiency of over 90 %)

5.2.3 Dimension of storeys of media filter

The number of gas inlet vanes is chosen to be 10 storeys, between which the face velocity is 0.1 m/s. Referring to Figure 5.2, the filter media is piled up and naturally set up at the “angle of repose”, measured by the powder tester as 34.1 degree (Appendix A1). According to its definition, the angle of repose is the maximum angle at which a pile of unconsolidated material can remain stable, the so-called stable angle. The angle the soil panel makes with the pile itself must be more than the angle of repose, so that the pile of rice husk, or media filter, could be simply released from the dust collector.

Figure 5.3 One storey of media filter



As mentioned in section 5.1.1, the total required filtration surface area is 24 m². Since there are 10 storeys of gas inlet vanes, each storey must possess 10% or 2.4 m² of the filtration area.

According to Figure 5.3, we have

$$A_i = \frac{\pi * D^* * (L + \gamma)}{2} - \frac{\pi * d^* * (L)}{2} \quad (5.11)$$

A_i : Filtration area of one storey: 2.4 m²

D^* : Wider diameter of media filter:

$$(4 - (0.65*2)) = 2.7 \text{ m.}$$

d^* : Shorter diameter of media filter:

$$D^* - [2 * \gamma * \text{Cos}(34.1)]$$

Substitute all available data into equation 5.11 to obtain

$$A_i = \frac{\pi * D^{*2}}{(4 * \text{Cos}(34.1))} - \frac{\pi * \left(\frac{D^{*2}}{2} - (\gamma * \text{Cos}(34.1)) \right)^2}{\text{Cos}(34.1)}$$

$$A_i = \frac{\pi}{(4 * \text{Cos}(34.1))} * \left[D^{*2} - \left(\frac{D^{*2}}{2} - (\gamma * \text{Cos}(34.1)) \right)^2 \right] \quad (5.12)$$

Finally, set $A_i = 2.4 \text{ m}^2$ and $D^* = 2.7 \text{ m}$. of equation 5.12 to obtain $\gamma = 0.313 \text{ m}$. In case that the gas inlet vane located at 35 degree with the horizontal line, a little bit more than the angle of repose is, dimension of media filter is expressed as shown in Figure 5.4.

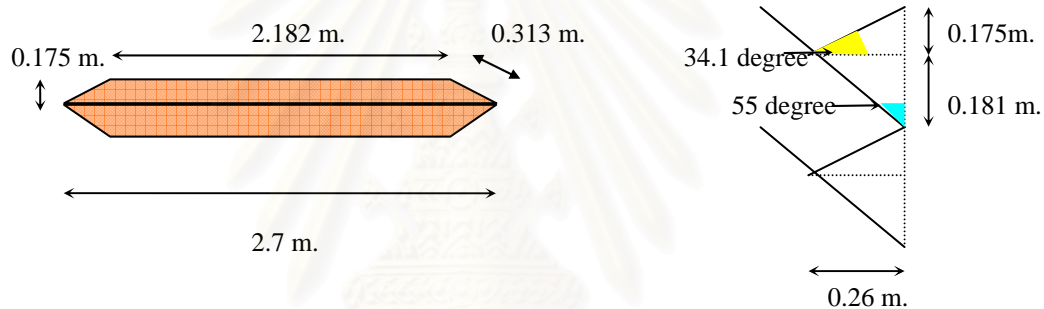


Figure 5.4 Dimensions of one storey of media

Then, it is revealed that height of each storey of media filter is 0.357 m.

However, it is not technically practical to construct a circular sheet of gas inlet vane, since it would take too much effort during the construction process, and might not be economical to manufacture. Then, the circular gas inlet vanes were replaced as octagonal, which is the combination of 8 pieces of trapezoidal sheets in each storey of the filter media.

In figure 5.4, the narrower side of media filter was 2.7 m. in diameter, and the gas inlet vanes make an angle of 35 degree with the horizontal axis. Assuming that 8 trapezoidal sheets were arranged in octagonal shape around the narrower side of media filter, as shown on the left side of Figure 5.5. Each of 8 triangles combining in the octagonal is similar to each other. Then, it is gained that

$$\tan(22.5) = \frac{\left(\frac{X'}{2}\right)}{\left(\frac{2.182}{2}\right)} \quad (5.13)$$

$X' = 0.904$ m. is obtained from Equation (5.13)

Next, as shown in the right hand side of Figure 5.4, the difference between the wider side to the narrower side of the filter media is 0.26 m. However, for safety reason, the vane for influent gas vane is extended to 0.30 m. long.

$$X'' \sin(55) = 0.30 \quad (5.14)$$

$X'' = 0.366$ m. is obtained from Equation 5.14

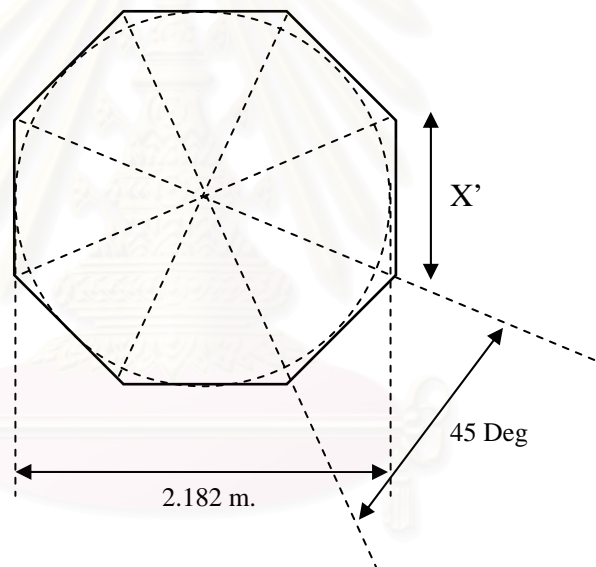


Figure 5.5 Eight pieces of dust inlet vane were arranged in octagonal shape.

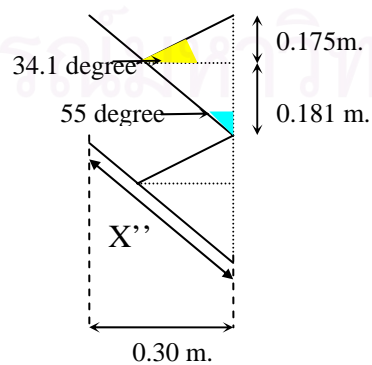


Figure 5.6 Model for the calculation of inlet vane

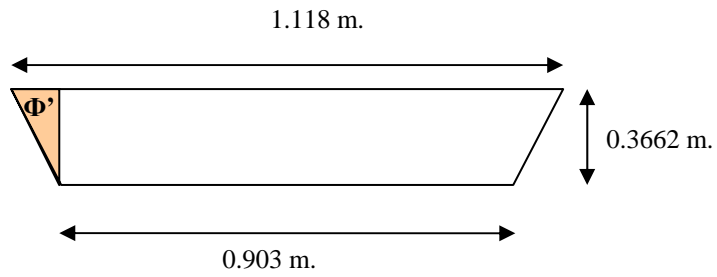


Figure 5.7 Model for the calculation of trapezoidal sheet

Figure 5.7 shows that

$$\begin{aligned} \tan(\Phi') &= \frac{0.3662}{\left[\frac{(1.118 - 0.903)}{2} \right]} & (5.15) \\ \Phi' &= 73.64 \text{ Degree} \end{aligned}$$

Therefore, the dimension of trapezoidal sheet is concluded in Figure 5.8

สถาบันวิทยบริการ
จุฬาลงกรณ์มหาวิทยาลัย

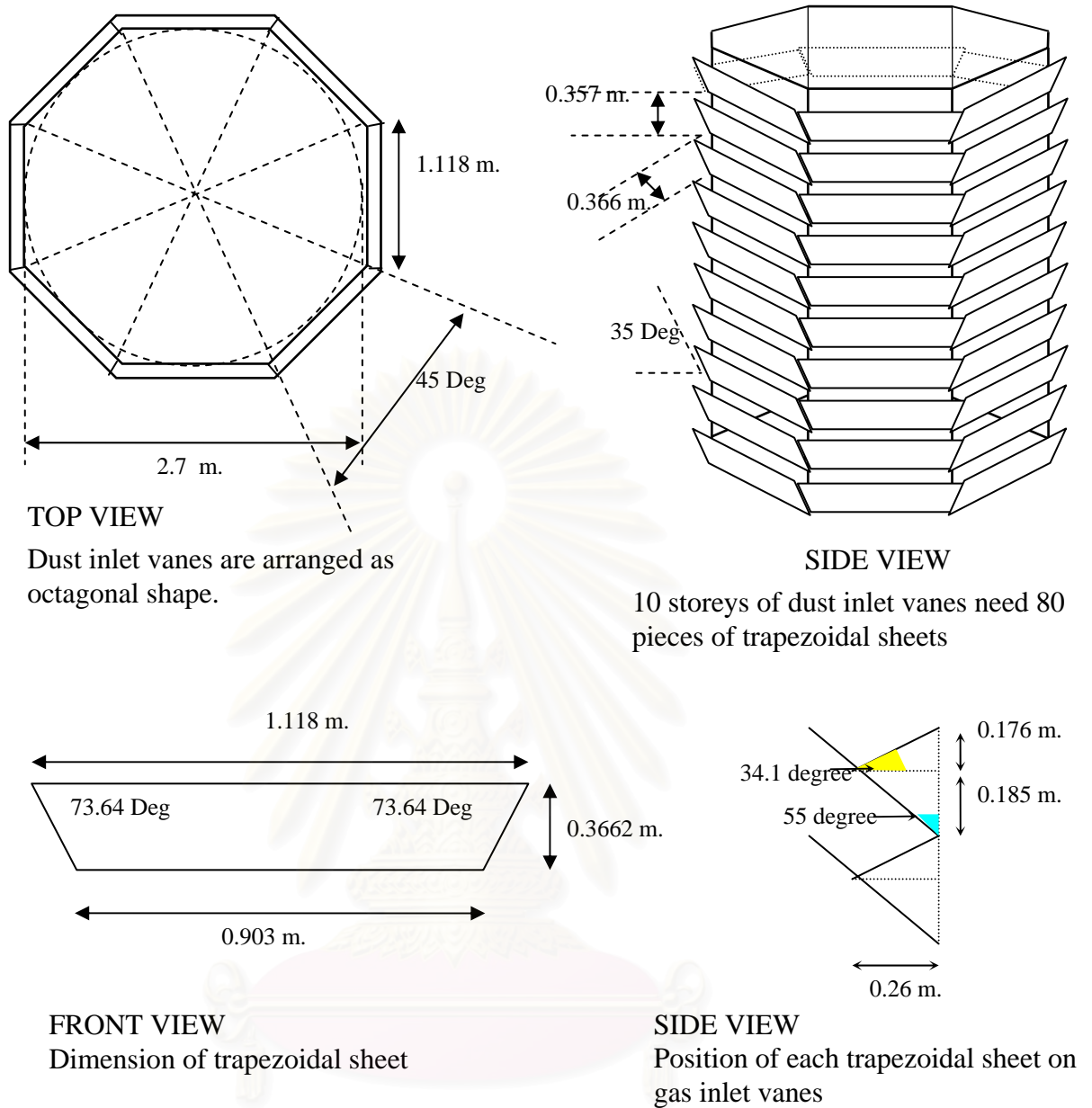


Figure 5.8 Dimension of gas inlet vanes and trapezoidal sheet.

5.2.4 Dimension of Silo

As mentioned above, the angle the bottom floor of silo make with the horizontal axis must be steeper than the angle of repose of rice husk pile. To make sure that rice husk media would be easily moved out from the dust collector, the angle the bottom floor of silo makes with the horizontal axis is set at 50 degree.

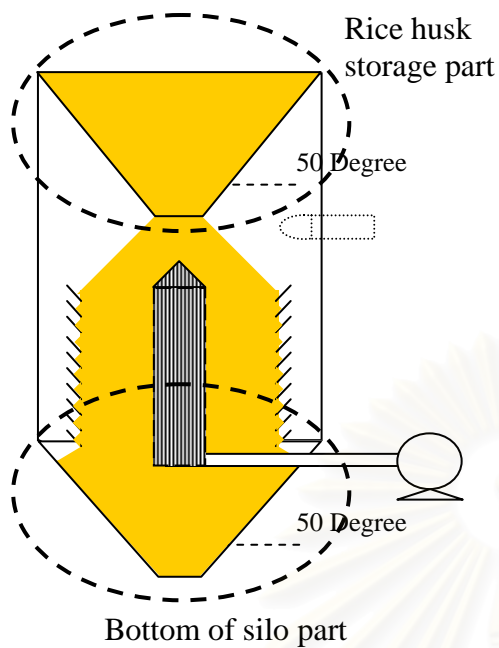


Figure 5.9 Schematic diagram of the dust collector (3)

Open holes located at bottom of silo part and rice husk storage part are equal in size, 0.6 m. in diameter. Up to this point, dimension of bottom part and rice husk storage part could be calculated.

According to figure 5.10, it was interpreted that

$$H = (2) * \tan(50) - (0.3) * \tan(50) \quad (5.16)$$

So, we get that $H = 2.026 \text{ m}$.

In addition, the total height of the dust collector includes height due to the bottom part of the silo, the rice husk storage part, the filtration zone, and the distance between the filtration zone and rice husk storage zone. The last one could be theoretically calculated as shown below.

Likewise, the slope of rice husk storage part is set at 50 degree, to make sure that clean rice husk media would freely move to replace the used media below.

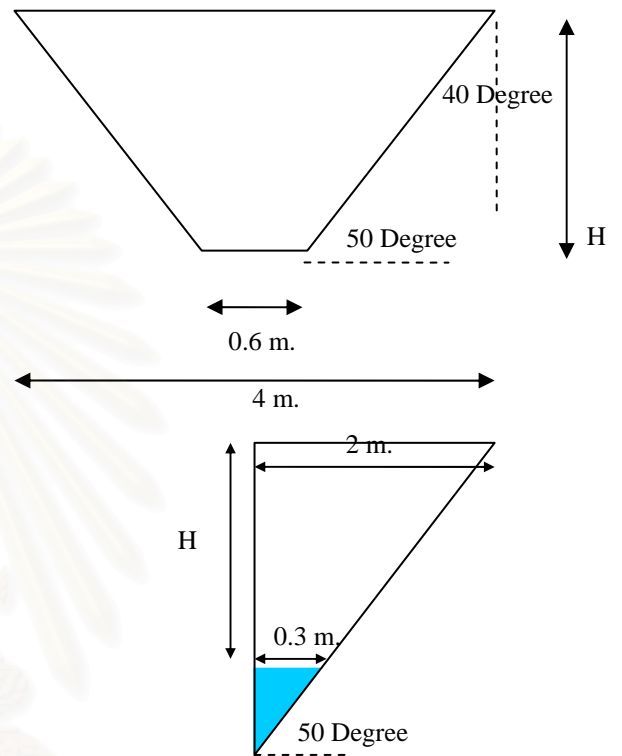
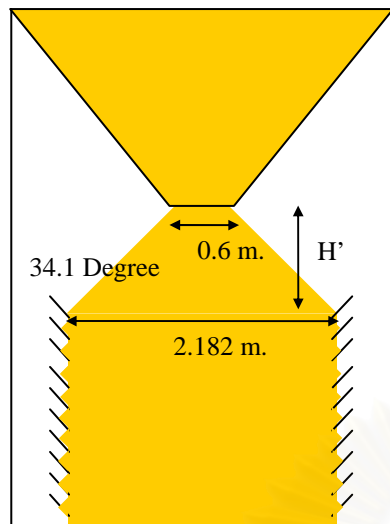


Figure 5.10 Model for the calculation of bottom part and rice husk storage part



$H' =$

$$\left(\frac{2.182}{2} \right) * \tan (34.1) - \left(\frac{-0.6}{2} \right) * \tan (34.1) \quad (5.17)$$

Then, $H' = 0.536$ m.

Now that the dimensions of all major parts are identified, the schematic diagram of the dust collector could be illustrated as shown in Figure 5.12.

Figure 5.11 Model for the calculation of distance between rice husk storage and filtration zone

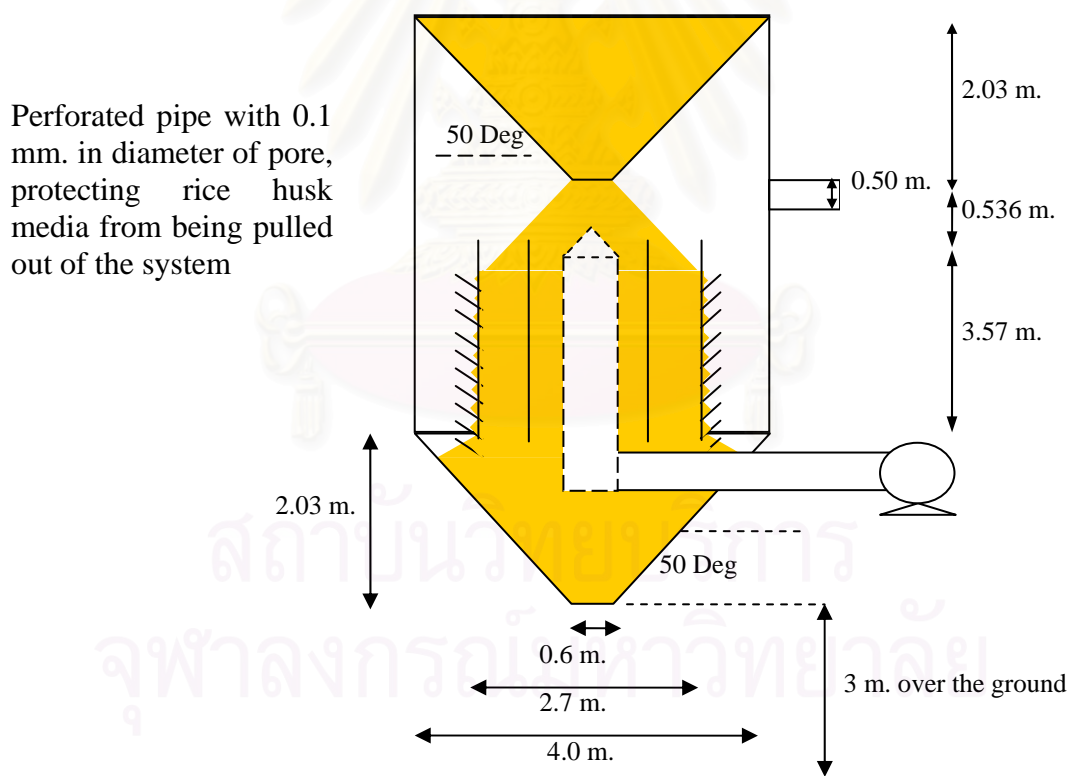


Figure 5.12 Schematic diagram of the dust collector with dimensions

5.3 Calculation of pressure drop over clean and used media filter

After the dimensions of the dust collector are identified, the next step is to estimate the power of blowers needed and to find appropriated time period for a cycle of operation before replacing the filter media. Overall pressure drop across the media filter and pipeline system must be included to estimate the tolerable flow resistance accumulated in the system, so that the required power of blowers and time period can be found.

Firstly, the cycle time of media replacement is assumed to be 24 hours or more from a practical viewpoint considering that once-in-a-day changing of the filter media is not too much burden for a rice mill. Total pressure drop generated in the system consists of three major parts- pipe line, media filter, and dust cake layer, which would be considered individually.

5.3.1 Pressure drop due to the effect of pipeline system

When clean or dust-laden air moves through the pipeline, it encounters flow resistance, better known as pressure drop, slowing down the air flow. Pressure drop corresponding to the effect of pipeline could be separated into two main parts, the perforated pipe, and the pipeline.

Pressure drop caused by the perforated pipe

As described in section 5.1.3, the diameter of the perforated pipe is designed at 0.7 m., and it possesses short 0.1-mm.-wide slits along the length. Each slit would look like a triangle shape with a lopped off apex. A top view of the pipe cross section is shown in Figure 5.16.

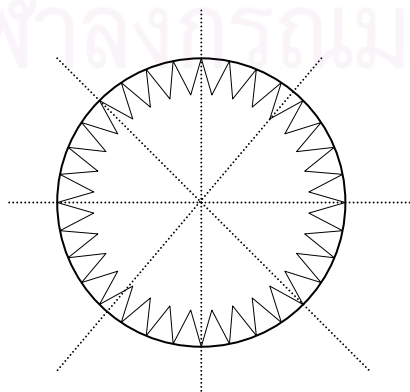


Figure 5.13 Top view of perforated pipe

To estimate the pressure drop, caused by the perforated pipe, the slits would be considered as orifice opening, covering 15 percent of the whole external surface area of the pipe. Since a 3.7 m. long pipe is used, the surface area covered by the slits could be calculated as shown below.

(Percent of surface area covered by slits)*(Whole surface area of perforated pipe)

$$= (0.15)*(\pi*D*L) = (0.15*\pi*0.7*3.7) = 1.22 \text{ m}^2.$$

The flow rate the de-dusted air passing through the perforated pipe is $2.4 \text{ m}^3/\text{s}$, which could be changed to the linear velocity as $(2.4/1.22) = 1.967 \text{ m/s}$. Because all slits are assumed as orifice, the pressure drop across them could be calculated with Equation (5.18).

$$U = \left(\frac{C}{\sqrt{1-B^4}} \right) * \sqrt{\frac{2 * g_c \Delta P}{\rho}} \quad (5.18)$$

Where

U_O : Linear velocity passing through the slits: 1.967 m/s

B : Ratio of slit width to the perimeter of pipe: close to zero (0).

C : Orifice coefficient: 0.61

ρ : Air density (27°C): 1.3 kg/m^3

Rearrange Equation (5.18), to get

$$\Delta P_{\text{ORIFICE}} = \left(\frac{U^2}{C^2} \right) * (1-B^4) * \frac{\rho}{2g_c} \quad (5.19)$$

Substitute the above values into Equation (5.34) to get

$$\Delta P_{\text{ORIFICE}} = \left(\frac{1.967^2}{0.61^2} \right) * (1-0^4) * \left(\frac{1.3}{2} \right)$$

$$\Delta P_{\text{ORIFICE}} = 6.756 \text{ Pa, or } 6.756 * 10^{-3} \text{ KPa} \quad (*)$$

In addition, there is pressure drop caused by another flow resistance in perforated pipe. It is the pressure drop due to the length of the pipe, and it was calculated by Fanning equation.

Fanning equation,
$$\Delta P_{\text{Perforated pipe}} = (4 * f) * \left(\frac{L}{D}\right) * \left(\frac{U^2}{2}\right) * \rho \quad (5.20)$$

f: Fanning factor: $f = 16/\text{Re}$ for laminar flow

, and $f = \left(\frac{0.0791}{\text{Re}^{0.25}}\right)$ for turbulent flow

Check Reynolds number:

$$\text{Re} = \left(\frac{\rho * U * D}{\mu}\right) = \left(\frac{1.3 * 1.967 * 0.7}{1.81 * 10^{-5}}\right)$$

$$\text{Re} = 98,893.37 \text{ -----} \rightarrow \text{Turbulent flow}$$

L: Total length of perforated pipe: 3.7 m.

D: Diameter of perforated pipe: 0.7 m.

U: Linear velocity of air: 1.967 m/s

Substituting all values into Fanning equation, we get

$$\Delta P_{\text{Perforated pipe}} = \left(4 * \left(\frac{0.0791}{98,893.37^{0.25}}\right)\right) * \left(\frac{3.7}{0.7}\right) * \left(\frac{1.967^2}{2}\right) * (1.3)$$

$$\Delta P_{\text{Perforated pipe}} = 0.237 \text{ Pa} = 2.372 * 10^{-4} \text{ KPa} \quad (**)$$

Total pressure drop, caused by the perforated pipe becomes

$$\begin{aligned} \Delta P_{\text{Total Perforated pipe}} &= \Delta P_{\text{ORIFICE}} + \Delta P_{\text{Perforated pipe}} &= 6.756 * 10^{-3} + 2.372 * 10^{-4} \\ & &= 6.993 * 10^{-3} \text{ KPa} \end{aligned}$$

สถาบันวิทยบริการ
จุฬาลงกรณ์มหาวิทยาลัย

Pressure drop caused by the exhaust pipe

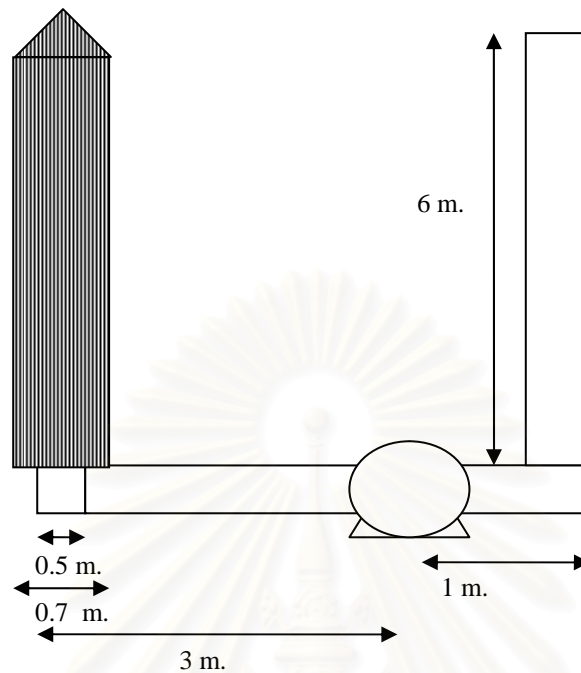


Figure 5.14 Line of exhaust pipe

Location of pipeline is illustrated in Figure 5.14. Effect of flow resistance is the combination of 10 m. of total length, one surface convergence, and two elbow turns.

Likewise, pressure drop due to effect of pipe length could be found by Fanning equation (equation 5.20)

$$\Delta P_{\text{Pipe length}} = (4 * f) * \left(\frac{L}{D}\right) * \left(\frac{U^2}{2}\right) * \rho \quad (5.20)$$

f: Fanning factor: $f = 16/\text{Re}$ for laminar flow

, and $f = 0.0791/\text{Re}^{0.25}$ for turbulent flow

Check Reynolds number:

$$\text{Re} = \left(\frac{\rho * U * D}{\mu}\right) = \left(\frac{1.3 * 12.22 * 0.5}{1.81 * 10^{-5}}\right)$$

$$\text{Re} = 438,839.78 \text{ -----} > \text{Turbulent flow}$$

L: Length of perforated pipe: 10 m.

D: Diameter of pipe: 0.5 m.

U: Air velocity: 12.22 m/s

$$\Delta P_{\text{Pipe length}} = \left(4 * \left(\frac{0.0791}{438,839.78^{0.25}} \right) \right) * \left(\frac{10}{0.5} \right) * \left(\frac{12.22^2}{2} \right) * 1.3$$

$$\Delta P_{\text{Pipe length}} = 23.864 \text{ Pa} = 0.0234 \text{ KPa} \quad (***)$$

Moreover, two elbow turns could cause flow resistance as shown in equation 5.21

$$\Delta P_{\text{Elbow turn}} = \left(\frac{K * U^2}{2 * g_c} \right) \quad (5.21)$$

K: flow resistance coefficient: $0.75(D)^{-0.81}$, for elbow turn

U: Air velocity: 12.22 m/s

$$\Delta P_{\text{Elbow turn}} = \left(\frac{0.75 * (0.5^{-0.81}) * 12.22^2}{2} \right) * 2 \quad (\text{Note two elbow turns})$$

$$\Delta P_{\text{Elbow turn}} = 196.353 \text{ Pa} = 0.196 \text{ KPa} \quad (****)$$

The last flow resistance blocked in pipe line is pressure drop due to change in pipe diameter, as the pipe diameter converts from 0.7 m. to 0.5 m.

$$\Delta P_{\text{Conversion}} = \left(\frac{K * U^2}{2 * g_c} \right) \quad (5.22)$$

K: flow resistance coefficient:

$$K = 0.5 - 0.167 * \left(\frac{D_2}{D_1} \right) - 0.125 * \left(\frac{D_2}{D_1} \right)^2 - 0.208 * \left(\frac{D_2}{D_1} \right)^3$$

U: Air velocity: 12.22 m/s

$$\Delta P_{\text{Conversion}} = \left[0.5 - 0.167 * \left(\frac{0.5}{0.7} \right) - 0.125 * \left(\frac{0.5}{0.7} \right)^2 - 0.208 * \left(\frac{0.5}{0.7} \right)^3 \right] * \left(\frac{12.22^2}{2} \right)$$

$$\Delta P_{\text{Conversion}} = 18.004 \text{ Pa} = 0.018 \text{ KPa} \quad (*****)$$

Therefore, total pressure drop over the pipe line system is the summation of (*), (**), (***), (****), and (*****).

$$\begin{aligned}\Delta P_{\text{PIPE Total}} &= \Delta P_{\text{Perforated Pipe}} + \Delta P_{\text{Pipe length}} + \Delta P_{\text{Elbow turn}} + \Delta P_{\text{Conversion}} \\ \Delta P_{\text{PIPE Total}} &= 0.0070 + 0.0234 + 0.196 + 0.018 = 0.2444 \text{ KPa}\end{aligned}$$

5.3.2 Pressure drop due to the effect of clean rice husk media

To estimate the flow resistance of filter media, it is practical to use the well-known Ergun equation as already mention in section 4.3.

$$\left(\frac{\Delta P_m}{t}\right) = \rho * \left(\frac{S_p}{V_p}\right) * \left(\frac{1-\varepsilon}{\varepsilon^3}\right) * \left[\left(\frac{150 * \mu * U_0 * (1-\varepsilon)}{36}\right) * \left(\frac{S_p}{\rho * V_p}\right)\right] + \left(\frac{1.75 * U_0^2}{6}\right) \quad (4.2)$$

where ΔP_m : Pressure drop across the filter media: [Pa]

t : Media thickness: 1 [m.]

μ : Air viscosity: $1.81 * 10^{-5}$ [kg/ms],

(Based on the viscosity of clean air at 27° C)

ρ : Air density: 1.3 [kg/m³]

(Based on the density of clean air at 27° C)

ε : Porosity of media [-]: 0.6

U_0 : Face velocity: 0.1 [m/s]

S_p : Surface area of a media particle: $\pi * \left(\frac{D_m^2}{4}\right)$

V_p : Volume of a media particle: $\pi * \left(\frac{D_m^3}{6}\right)$

D_m : Equivalent diameter of media particle: 1.593 mm. (D_{EV})

After substituting all values into equation (5.31), we get

$$\begin{aligned}\left(\frac{\Delta P_m}{t}\right) &= \\ (1.3) * \left(\frac{1.5}{1.593 * 10^{-3}}\right) * \left(\frac{1-0.6}{0.6^3}\right) * \left[\left(\frac{150 * (1.81 * 10^{-5}) * 0.1 * (1-0.6)}{36}\right) * \left(\frac{1.5}{1.3 * 1.593 * 10^{-3}}\right)\right] &+ \left(\frac{1.75 * (0.1^2)}{6}\right)\end{aligned}$$

$$\left(\frac{\Delta P_m}{t}\right) = 105.70, \quad \text{but } t = 1 \text{ m.}$$

$$\Delta P_m = 1.057 * 10^{-1} \text{ KPa}$$

Flow resistance caused by the clean rice husk media is calculated as $1.057 * 10^{-1}$ KPa

5.3.3 Pressure drop caused by the dust cake layer

As dust particles are filtrated over the surface of rice husk media, dust particles would be packed together and gradually build up to become dust cake layer, thereby giving higher dust collection efficiency than the rice husk media itself. However, since dust cake layer can cause huge flow resistance, it is important to optimize the thickness of dust cake layer from during each cycle, so that a reasonable power of the blower used could be selected.

According to equation (4.2),

$$\left(\frac{\Delta P_m}{t}\right) = \rho * \left(\frac{S_p}{V_p}\right) * \left(\frac{1-\varepsilon}{\varepsilon^3}\right) * \left[\left(\left(\frac{150 * \mu * U_0 * (1-\varepsilon)}{36}\right) * \left(\frac{S_p}{\rho * V_p}\right)\right) + \left(\frac{1.75 * U_0^2}{6}\right)\right] \quad (4.2)$$

where

ΔP_c : Pressure drop across the dust cake layer: [Pa]

t : Thickness of dust cake layer: x [m.]

μ : Air viscosity: $1.81 * 10^{-5}$ [kg/ms],

(Based on the viscosity of clean air at 27° C)

ρ : Air density: 1.3 [kg/m³]

(Based on the density of clean air at 27° C)

ε : Porosity of dust cake layer: 0.35 [-]

U_0 : Face velocity: 0.1 [m/s]

S_p : Surface area of a media particle: $\left(\frac{\pi * D_p^2}{4}\right)$

V_p : Volume of a media particle: $\left(\frac{\pi * D_p^3}{6}\right)$

D_p : Average diameter of dust particle: $7 * 10^{-6}$ m.

(Assume average diameter of dust particles)

After substituting all values into equation (5.31)

$$\left(\frac{\Delta P_c}{t}\right) =$$

$$(1.3) * \left(\frac{1.5}{5 * 10^{-6}}\right) * \left(\frac{1-0.35}{0.35^3}\right) * \left[\left(\left(\frac{150 * (1.81 * 10^{-5}) * (0.1) * (1-0.35)}{36}\right) * \left(\frac{1.5}{1.3 * 5 * 10^{-6}}\right)\right) + \left(\frac{1.75 * (0.1^2)}{6}\right)\right]$$

$$\Delta P_c/t = 3,424,846.79$$

but t is still an unknown variable and is defined at x m.

$$\Delta P_c = 3,424.85x \text{ KPa}$$

Total pressure drop calculated over the direction of air flow, while filtration process is taking place, is

$$\Delta P_{TOT} = \Delta P_{PIPE \text{ Total}} + \Delta P_m + \Delta P_c = \Delta P_{PIPE \text{ Total}}$$

$$\Delta P_{TOT} = 0.244 + 0.105 + 3,424.85x$$

$$\Delta P_{TOT} = 0.35 + 3,424.85x \text{ KPa} \quad (5.23)$$

It is obvious from Equation (5.23) that total the pressure drop of the system is dominated on the variable x . Here it is considered that replacing the filter media once every 24 hours is not too much burden for the rice mill operator.

As measured in Section 1.2.3, the dust concentration of dust-laden air carried to the dust collection system is 1.353 g/m^3 . Firstly, dust-laden air would be treated with the cyclone dust collector, which is not effective enough to collect all on-coming fine dust carried to. So, fine dust particles are passed to be further filtrated by the rice-husk packed bed dust collector. Here it is assumed that dust collection efficiency of an ordinary cyclone dust collector is 80%.

$$[0.2] * [1.353 \text{ g/m}^3] = 0.2706 \text{ g/m}^3$$

Therefore, 0.2706 grams per cubicmeter of dust particles are sent to the rice-husk packed bed dust collector.

For future expansion, the designed flow rate of dust-laden air is double to $2.4 \text{ m}^3/\text{s}$ in the calculation.

$$[0.2706 \text{ g/m}^3] * [2.4 \text{ m}^3/\text{s}] = 0.649 \text{ g/s}$$

In short, 0.649 grams of rice-mill dust particles must be treated in one second, or 56.112 kg of fine dust must be filtrated within 24 hours.

Next 90% by mass of fine dust particles is assumed to be captured by the secondary dust collector. Then, it could be concluded that 50.5 kg of dust particles are accumulated and form dust cake layer over the rice husk media within 24 hours of

operation. Separately, The Powder Tester (Appendix A) revealed that the packed density of dust particles is 0.471 grams per cubic centimeters. Then, 50.5 kilograms by mass of dust particle could be translated to 0.1072 m^3 by volume. When those dust particles cover the surface of rice husk media (24 m^2), the thickness of dust cake layer form on the filter media is $4.467 \times 10^{-3} \text{ m}$.

Inserting 0.0223 m. of thickness of dust cake layer into equation (5.23), we get total pressure drop, ΔP_{TOT} , as calculated by Ergun Equation equal to 15 KPa, which is excessively large flow resistance.

However, the experimental results, described in Chapter 4, reveal that “screened dust particles did not really form cake layer convering over the media filter, but, in reality, they penetrated and filled empty spaces between media particles”. So, it is not suitable to use the Ergun Equation to evaluate the pressue drop caused by the dust cake layer.

For example, according to the experimental results shown in Chapter 4 when face velocity is steady at 0.22 m/s, dust particles are captured after penetration into rice husk media, forming a “media+dust cake layer”. The difference between experimental pressure drops across clean and used media (at $t_1 = 0$, and $t_2 = 2$ hours) is about 800 – 900 Pa at 0.22 m/s of face velocity. Since inlet concentration of dust laden air is about 1.89 g/m^3 , it could be estimated that

$$[1.89 \text{ g/m}^3] * [0.22 \text{ m/s}] * [0.2 * 0.2 \text{ m}^2] * [2 \text{ hr}] * [3600 \text{ s/1 hr}] = 119.750 \text{ grams}$$

of Turbo1 dust particles are carried to be treated in the rice husk media within 2 hours. Based on 2 micrometers in average diameter, and 1.264 g/cm^3 in packed density of Turbo1 dust particles the thickness of an independent dust cake layer could be found as follows.

$$[119.750 \text{ g}] * [1/1.264 \text{ cm}^3/\text{g}] * [10^{-6} \text{ m}^3/\text{cm}^3] / [0.2 * 0.2 \text{ m}^2] = 2.368 * 10^{-3} \text{ m}.$$

*The corresponding pressure drop, predicted by Ergun equation, for $2.368 * 10^{-3} \text{ m}$ thick dust cake layer, with $2 \mu\text{m}$. in average diameter becomes 218.274 KPa, which is very huge and differed too much from the experimental value.*

However, if 2.368×10^{-3} m. of Turbo1 cake layer (2 μm in average diameter of dust particle) contributed to additional 900 Pa in pressure drop (interpreted from experimental results), *it could be roughly estimated that 4.467×10^{-3} m. of rice-mill dust cake layer (7 μm in average diameter of dust particle) could not cause more than 2 KPa.*

Referring to Equation (5.23)

$$\Delta P_{\text{TOT}} = 0.35 + 3,424.85x \quad \text{KPa} \quad (5.23)$$

The latter group is pressure drop corresponding to the layer of dust cake. Substituting the latter group with 2 KPa, *it is found that the total pressure drop is 2.35 KPa.* Since efficiency of a blower is generally accepted at 60%, the required power of a blower could be simply calculated.

$$\begin{aligned} \text{Power of blower} &= [2.35 \times 1000 \text{ kg/ms}^2] \times [2.4 \text{ m}^3/\text{s}] \times [1.341/1000] / [0.6] \\ &= 12.61 \text{ HP (9.4 inH}_2\text{O)} \end{aligned}$$

It is shown that 15 HP of blower should suffice in this rice-husk packed bed dust collection system.

In conclusion, the packed bed dust collection system should be capable in continually filtrating dust-laden air coming from cyclone dust collector, and need to be regenerated every 24 hours of operation. Filtrated dust particles would be accumulated and work along with media filter in capturing other dust particles with increasingly higher dust collection efficiency.

5.4 The maximum dust collection efficiency

According to Tables 5.2, the clean rice husk media is expected to possess the maximum dust collection efficiency when the thickness of dust cake layer reaches its maximum value at 4.5×10^{-3} m., and the predicted maximum efficiencies are listed in Tables 5.3.

Table 5.3 The maximum dust collection efficiencies of the rice-husk packed bed dust collection system. (rice husk bed with formation of cake)

Diameter of dust particles, d_p ($\mu\text{m.}$)	Ratio of dust particles smaller than d_p (%by mass)*	Dust collection efficiency at each d_p (-)		Average dust collection efficiencies between two particle sizes (-)		%By mass of each size range of dust particles escaping from the dust collection system
		4.5 mm. thick dust cake layer	1 m. thick rice husk filter media	4.5 mm. thick dust cake layer	1 m. thick rice husk filter media	
0.1	0	100	99.99	100	99.84	0
0.5	0	99.96	99.68	100	98.52	0
1	1.5	100	97.35	100	93.35	0
3	5.0	100	89.34	100	74.45	0
5	7.0	100	59.55	100	53.27	0
8	10.0	100	46.98	100	48.96	0
10	12.0	100	50.94			
% By mass of escaped rice-mill dust particle						0.0000

* *Theses results were based on the theory of deposition mechanisms.*

It is obvious from Table 5.3 that the dust cake layer could provide quite impressive dust collection efficiency at the expense of reasonable amount of energy consumption.

The key dimensions of rice-husk packed bed dust collector are already illustrated in Figure 5.12.

REFERENCES

- [1] นภาพร พานิช และคณะ. ตำราระบบบำบัดมลพิษอากาศ. กรมโรงงานอุตสาหกรรม: ศูนย์บริการวิชาการแห่งจุฬาลงกรณ์มหาวิทยาลัย, 2547.
- [2] ศิริกัลยา สุวจิตตานนท์, วิวัฒน์ ตัณฑะพานิชกุล. มลภาวะอากาศ. พิมพ์ครั้งที่ 2. กรุงเทพมหานคร: สำนักพิมพ์มหาวิทยาลัยเกษตรศาสตร์, 2544.
- [3] Carter, G. W. Properties of brick incorporating unground rice husk. Building and Environment 17(1982): 285-291.
- [4] Tzong-Hong Liou. Preparation and characterization of nano-structured silica from rice husk. Journal of Materials Science & Engineering A364 (2004): 313-323.
- [5] Wong, KK. , et al. Removal of Cu and Pb from electroplating wastewater using tartaric acid modified rice husk. Journal of Process Biochemistry 39 (2003): 437-445.
- [6] Guise, M.T. , et al. An experimental investigation of aerosol collection utilizing packed beds of silica aerogel microspheres. Journal of Non-Crystalline Solids 285(2001): 317-322.
- [7] Endo Yoshiyuki, et al. Bimodal aerosol loading and dust cake formation on air filter. Filtration & Separation 35(1998): 191-195.
- [8] Endo Yoshiyuki, et al. Theoretical consideration of permeation resistance of fluid through a particle packed bed layer. Powder Technology 124 (2002): 119-126.
- [9] Kim, H. T. Diffusional filtration of polydispersed aerosol particles by fibrous and packed-bed filters. Filtration & Separation 37(2000): 37-42.
- [10] Lee, K-C. , et al. Granular-bed filtration assisted by filter-cake formation 1. Exploring a new mode of soil failure for renewal of filtration surfaces in a panel bed. Powder Technology 155(2005): 5-16.

- [11] Lee, K-C. , et al. Granular-bed filtration assisted by filter-cake formation 2. The panel bed gas filter with puffback renewal of gas-entry surfaces. Powder Technology 155(2005): 52-61.
- [12] Lee, K-C. , et al. Granular-bed filtration assisted by filter-cake formation 3. Penetration of filter cakes by a monodispersed aerosol. Powder Technology 155(2005): 62-73.
- [13] William C. Hinds. Aerosol Technology. New York: John Wiley & Sons Inc, 1999.
- [14] Pan, R. Pressure Drop and Slug Velocity in Low-velocity Pneumatic Conveying of Bulk Solid. Powder Technology 94(1997): 123-132.
- [15] Strauss, W. Industrial Gas Cleaning. International Series in Chemical Engineering: Pergamon Press, 1975.
- [16] Warren L. McCabe. Unit Operation of Chemical Engineering. 5th ed: McGraw-Hill Inc, 1993.
- [17] Robert H. Perry. Perry's Chemical Engineers' Handbook. 7th ed: McGraw-Hill Inc, 1997.
- [18] Igor J. Karassik. Pump Handbook. 2nd ed: McGraw-Hill, 1986.
- [19] Iinoya Koichi. Powder Technology Handbook. USA: Marcel Dekker, Inc, 1991.
- [20] ชีเกะฟูมิ ฟุจิตะ. คู่มืออุปกรณ์การผลิตในอุตสาหกรรมเคมี. แปลโดย วิวัฒน์ ตันทะพานิชกุล. กรุงเทพมหานคร: สมาคมส่งเสริมเทคโนโลยี (ไทย-ญี่ปุ่น), 2533.

สถาบันวิทยบริการ
จุฬาลงกรณ์มหาวิทยาลัย



APPENDICES

สถาบันวิทยบริการ
จุฬาลงกรณ์มหาวิทยาลัย

APPENDIX A1

Table A1 Properties of rice husk sample (Tested by Powder Tester)

Properties	Number	Results	Average Results
Aerated bulk density	1 2 3	0.083 g/cc. 0.087 g/cc. 0.086 g/cc.	0.085 g/cc.
Tapping packed density	1 2 3	0.114 g/cc. 0.110 g/cc. 0.110 g/cc.	0.111 g/cc.
Compressibility	1 2 3	27.1 % 24.1 % 23.4 %	37.30 %
Angle repose	1 2 3	32.5 degree 35.2 degree 34.7 degree	34.1 degree
Angle of fall	1 2 3	20.8 degree 26.6 degree 20.6 degree	22.7 degree
Angle of different	1 2 3	11.7 degree 10.1 degree 11.4 degree	11.1 degree
Angle of spatula	1 2 3	39.9 degree 42.2 degree 35.6 degree	40.23 degree
Dispersibility	1 2 3	33.0 % 27.3 % 32.4 %	30.9 %
Total Index	1 2 3	Flow index = 76 , Degree = Good Flood index = 77 , Degree = Fairly good Flow index = 80 , Degree = Fairly good Flood index = 73 , Degree = Fairly good Flow index = 80 , Degree = Fairly good Flood index = 70 , Degree = Fairly good	

It can be concluded from Table A1 that rice husk is easy to flow and flood. It is able to simply be fluidized in air, and is light weight.



Figure A1 A photo of Powder Tester

สถาบันวิทยบริการ
จุฬาลงกรณ์มหาวิทยาลัย

APPENDIX A2

Table A2 Properties of rice mill dust particles (Tested by Powder Tester)

Properties	Number	Results	Average Results
Aerated bulk density	1 2 3	0.253 g/cc. 0.254 g/cc. 0.254 g/cc.	0.254 g/cc.
Tapping packed density	1 2 3	0.470 g/cc. 0.469 g/cc. 0.474 g/cc.	0.471 g/cc.
Compressibility	1 2 3	46.1 % 45.8 % 46.4 %	46.1 %
Angle repose	1 2 3	49.1 degree 46.9 degree 48.8 degree	48.3 degree
Angle of fall	1 2 3	38.5 degree 32.4 degree 38.6 degree	36.5 degree
Angle of different	1 2 3	10.6 degree 14.5 degree 10.2 degree	11.77 degree
Angle of spatula	1 2 3	73.1degree 75.3 degree 72.7 degree	73.7 degree
Dispersibility	1 2 3	40.8 % 33.2 % 33.9 %	35.97 %
Total Index	1 2 3	Flow index = 36 , Degree = Bad Flood index = 34 , Degree = Bad Flow index = 36 , Degree = Bad Flood index = 61 , Degree = Fairly high Flood index = 61 , Degree = Fairly high Flood index = 57.5 , Degree = Fairly high	

In Table A2, it was found that rice mill dusts possess low flowability index, but high floodability index, referring that rice mill dusts were not easy to flow, but tend to be easily flooded and fluidized. Moreover, rice mill dust particles were found small in size and light weight, which make them possess high dispersibility and tend to suspend in air.



สถาบันวิทยบริการ
จุฬาลงกรณ์มหาวิทยาลัย

APPENDIX A3

Table A3 Properties of Turbo 1 dust particles (Tested by Powder Tester)

Properties	Number	Results	Average Results
Aerated bulk density	1	0.714 g/cc.	0.742 g/cc.
	2	0.771 g/cc.	
Tapping packed density	1	1.264 g/cc.	1.302 g/cc.
	2	1.339 g/cc.	
Compressibility	1	43.5 %	42.95 %
	2	42.4 %	
Angle repose	1	53.2 degree	51.05 degree
	2	48.9 degree	
Angle of fall	1	37.8 degree	38.7 degree
	2	39.6 degree	
Angle of different	1	15.4 degree	12.35 degree
	2	9.3 degree	
Angle of spatula	1	60.1 degree	61.6 degree
	2	63.1 degree	
Dispersibility	1	18.7 %	27.55 %
	2	36.4 %	
Total Index	1	Flow index = 66 , Degree = Normal	
	2	Flood index = 70.5 , Degree = Fairly High Flow index = 63 , Degree = Normal Flood index = 70.5 , Degree = Fairly High	

In Table A3, Turbo 1 showed moderate flowability index, but high floodability index. It could be explained that Turbo 1 dust particles were able to simply flow, but tended to be easily flooded and fluidized. Moreover, Turbo 1 particles were loosely agglomerated and kind of heavy, since they provided not much dispersibility characteristic.

APPENDIX B

Data of time that a particle dropped naturally with terminal velocity in a distance of 1.3 m. were recorded, as shown in Table B.1

Table B.1

Number of experiments	Time (s)	Number of experiments	Time (s)
1	0.65	39	0.65
2	0.87	40	0.84
3	0.75	41	0.81
4	0.72	42	0.63
5	0.79	43	0.62
6	0.56	44	0.72
7	0.72	45	0.91
8	0.81	46	0.78
9	0.57	47	0.75
10	0.5	48	0.72
11	0.72	49	1
12	0.63	50	1.09
13	0.81	51	1.02
14	0.66	52	0.69
15	0.63	53	0.53
16	0.72	54	0.57
17	0.47	55	0.54
18	0.69	56	0.65
19	0.6	57	0.72
20	0.7	58	1.03
21	0.68	59	0.63
22	0.62	60	1.06
23	0.56	61	1.29
24	0.66	62	0.72
25	0.75	63	0.84
26	0.87	64	0.75
27	0.88	65	0.81
28	0.62	66	0.69
29	0.87	67	1
30	0.75	68	0.87
31	0.62	69	0.72
32	0.66	70	1.19
33	0.75	71	0.44
34	0.62	72	0.81
35	0.66	73	0.63
36	0.75	74	0.75
37	0.56	75	0.69
38	0.78	76	0.71

Table B.1 (Continue)

Number of experiments	Time (s)	Number of experiments	Time (s)
77	1.22	115	1.19
78	0.88	116	0.97
79	1.1	117	0.97
80	0.75	118	0.88
81	0.97	119	0.81
82	0.47	120	0.91
83	0.97	121	0.69
84	0.53	122	0.88
85	1.03	123	0.84
86	0.85	124	0.88
87	0.75	125	0.78
88	0.65	126	0.85
89	0.78	127	0.72
90	1.05	128	0.78
91	0.9	129	0.97
92	0.68	130	0.72
93	1.09	131	0.88
94	0.81	132	1.03
95	0.78	133	0.84
96	0.88	134	0.65
97	0.53	135	0.7
98	0.96	136	0.68
99	0.94	137	0.78
100	1.25		
101	0.75		
102	1.18		
103	0.91		
104	0.94		
105	0.59		
106	0.75		
107	0.81		
108	0.84		
109	0.75		
110	0.69		
111	0.85		
112	0.81		
113	0.88		
114	0.97		

Average time a rice husk particle used in falling through 1.3-m.-long pipe was found from Table A.1 as about 0.8098 seconds. So, the average terminal velocity was 1.605 m/s.

To determine the equivalent diameter of a rice husk particle, Iteration method was applied.

The Iteration Processes

Step1 According to Table 3.3 in “Aerosol Technology” [1], equivalent diameter of water droplet responding with 1.605 m/s of terminal velocity was 0.400 mm. This could be used as the initial value for iteration process.

Step2 The iterating was begun with 0.400 mm. of equivalent diameter (D_E).

Step3 Next, Reynolds number was calculated by equation (B.1).

$$Re = \frac{D_E * V_{TS} * \rho_{Air}}{\eta_{Air}} \quad (B.1)$$

where, D_E : Equivalent diameter [m]
 V_{TS} : Terminal settling velocity [m/s]
 ρ_{Air} : Air density [kg/m^3]
 η_{Air} : Air viscosity [kg/ms]

Step4 Replace Reynolds number earned from (B.1) to equation (B.2).

$$C_D = [24/Re] * [1 + (0.15 * Re^{0.687})] \quad (B.2)$$

Step5 From force balance of the system, terminal settling velocity (V_{TS}) was provided as

$$V_{TS} = \frac{[4 * \rho_p * d_p * g]^{0.5}}{[3 * C_D * \rho_g]^{0.5}} \quad (B.3)$$

Replace C_D value earned from equation (B.2) and all parameters into (B.3) to get back the V_{TS} . So, the new V_{TS} calculated by (B.3) must be compared with 1.605 m/s of terminal settling velocity in step1. If the different in those two terminal settling velocities was more than acceptable tolerance, D_{eq} must be re-adjusted and the iteration process must be continued from step 2 to step 5 again and again, until the different between those terminal settling velocities was accepted.

Due to the iterating method process, equivalent diameter was shown at 0.237 mm.

APPENDIX C1

Rice mill dust particles are tested by Mastersizer S long Bed. The results are shown in Figure C1 – C2.

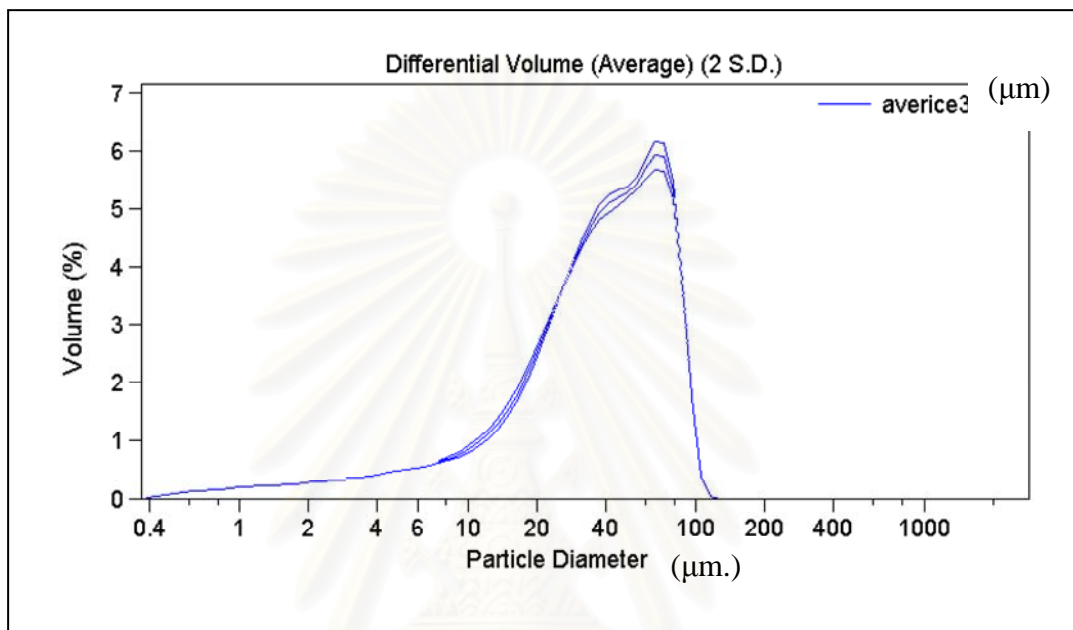


Figure C1 Size distribution curve of rice mill dust particles

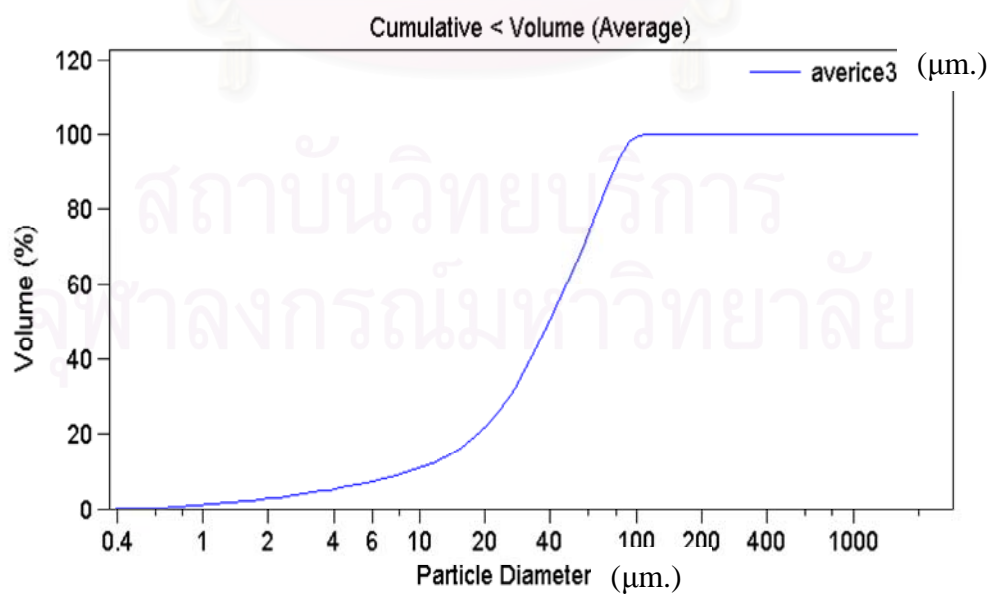


Figure C2 Cumulative size distribution curve of rice mill dust particles

APPENDIX C2

Size distribution curve of Turbo 1 dust particles are provided by Mastersizer S long Bed. The results are shown in Figure C3.

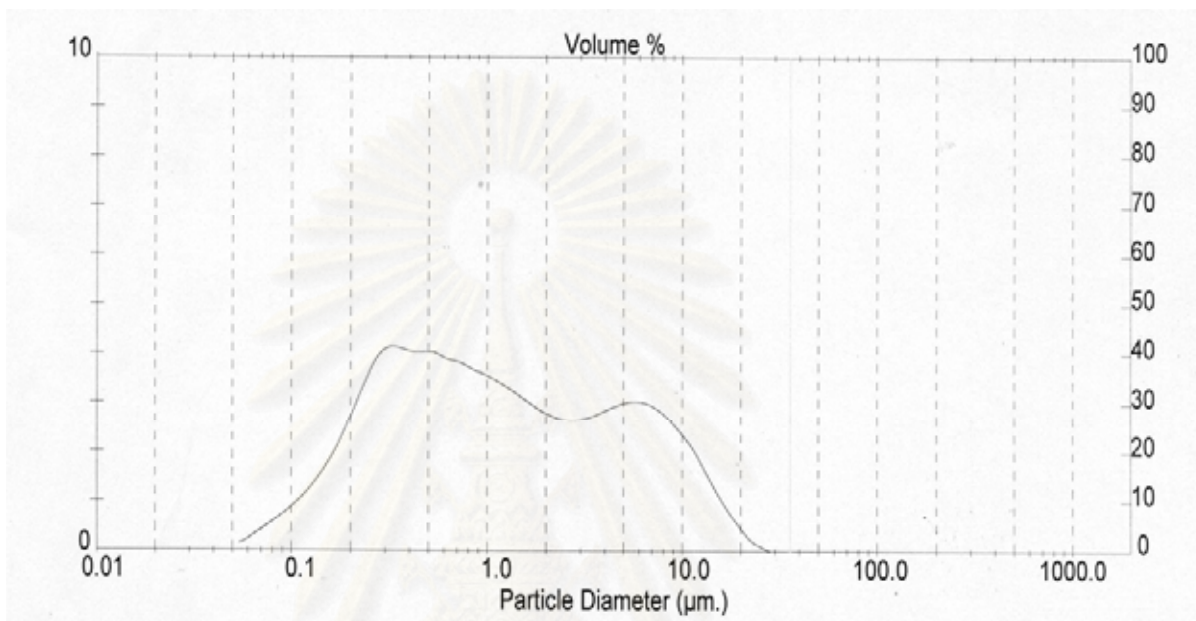


Figure C3 Size distribution curve of Turbo1 dust particles

It is noted that density of calcium carbonate is 2.7 g/cm^3 and surface area of Turbo 1 is $4.2755 \text{ m}^2/\text{g}$.

สถาบันวิทยบริการ
จุฬาลงกรณ์มหาวิทยาลัย

APPENDIX D1

When a liquid or gas is passed at very low velocity up through a bed of solid particles, particles might not move; however, once the fluid velocity increases and reaches an appropriate point, particles would start to move and suspended in the fluid. [16] The term fluidization is used to describe the condition of fully suspended particles. In this experiment, glass beads are fluidized to ensure the mixing quality of air stream and calcium carbonate dust particles to become dust-laden air in the fluidization zone (Mixing zone).

Based on the well-known Ergun equation, a quadratic equation for the minimum fluidization velocity, V_{OM} , is derived as shown below.

$$\left(\frac{150 * \mu * V_{OM} * (1 - \varepsilon_M)}{\Phi^2 * D_p^2 * \varepsilon_M^3} \right) + \left(\frac{1.75 * \rho * V_{OM}^2 * (1 - \varepsilon_M)}{\Phi * D_p * \varepsilon_M^3} \right) = g * (\rho_p - \rho) \quad (D1.1)$$

, Where

- μ : Air viscosity: [1.81*10⁻⁵ kg/ms]
- ρ : Density of air: [1.3 kg/m³]
- ρ_p : Density of glass bead: [2500 kg/m³]
- V_{OM} : Minimum fluidization velocity: [m/s]
- Φ : Sphericity of glass bead: [-]
- D_p : Diameter of glass bead: [m.]
- ε_M : Porosity of glass bead bed: [0.45]

Firstly, round sphere glass beads ($\Phi = 1$), with the diameter of 0.5, 1, and 2 mm. are applied, and it is responded from equation D1.1 that the minimum fluidization velocity are 0.303, 0.716 and 1.247 m/s respectively.

Since fluidized bed is generally operated at 10 – 20 times of the minimum fluidization velocity [16] and very low filtration velocity is necessary for packed bed filtration [2], it is highly recommended that the glass beads with 0.5 mm. in diameter is applied as a fluidized material for the fluidization zone.

APPENDIX D2

According to section 4.4, it was assumed that there existed the “saturated zone”, the mixing zone of media bed and dust particles, in which porosity of the zone was higher than clean rice husk bed. To predict the average filtration efficiency, it was practical to estimate that dust load accumulating in the first 15 minutes of operation affecting performance of filter media all over the first 30 minutes.

For example, in condition 1, 0.125 m. of media thickness and 0.22 m/s of face velocity was set, and dust feed rate was kept steady at 1.89 g/m³. Dust load coming into the system over the first 15 minutes was

$$= (15 \text{ min}) * (1.89 \text{ g/m}^3) * (0.0088 \text{ m}^3/\text{s}) * \left(\frac{60 \text{ s}}{1 \text{ min}} \right) = 14.969 \text{ g.}$$

If the bulk density was applied to the dust cake forming in the void spaces of filter media, volume of dust cake was

$$= \left(\frac{14.969 \text{ g.}}{0.714 \frac{\text{g}}{\text{cm}^3}} \right) = 20.965 \text{ cm}^3$$

Thickness of saturated zone, or the distance that most of dust particles penetrate into filter media and were captured, was firstly estimated at 0.002 m. It was known that surface area of filtration was 0.04 m². Then, the volume of saturated zone was

$$= (0.04 \text{ m}^2) * (0.002 \text{ m}) = 8 * 10^{-5} \text{ m}^3$$

It was noted that porosity of clean filter media was 0.6.

Volume possessed by media particles was = $(0.4 * 8 * 10^{-5}) \text{ m}^3$

Volume possessed by media particles and dust cake was

$$= (0.4 * 8 * 10^{-5}) + \left(\frac{20.965}{10^6} \right) = 5.297 * 10^{-5} \text{ m}^3$$

Over the first 30 minutes of operation, average porosity of 0.002 m. saturated zone was

$$= \left(\frac{\text{Volume possessed by media particles and dust cake}}{\text{Volume of saturated zone}} \right) = \left(\frac{5.297 * 10^{-5} \text{ m}^3}{8 * 10^{-5} \text{ m}^3} \right)$$

$$= 0.662$$

Filtration efficiency corresponded to saturated zone and clean media zone were calculated separately based on the same deposition mechanism process appeared in section 5.1.2. And, it was revealed from calculation process that filtration efficiency related to saturated zone and clean media zone were 3.01 and 72.16 percent by mass respectively. Filtration efficiencies of these two filter zone could be combined as

$$= (1 - (1-0.0301)*(1-0.7216))*100 = 73.00 \%$$

However, the experimental results at condition 1 revealed that the overall filtration efficiency was equal to 90.56%. *Therefore, the relative error between calculation and experimental result was determined as 19.393 %*



สถาบันวิทยบริการ
จุฬาลงกรณ์มหาวิทยาลัย

VITA

Mister Sira Srinives was born on December 3rd, 1979 in Samutsakorn province, Thailand, before moved, with his family, to Nakornpathom in 1986. He studied elementary school at Kasetsart Demonstration School (Kamphaengsaen campus), and secondary school at Prapathom Vittayalai School. After that, he spent another four years to finish Bachelor Degree of Engineering (Chemical Engineering) from Kasetsart University. His senior project was dealing with correlation of diameter of dispersed phase in liquid-liquid extraction column. When he continued to study for the Master degree at Chulalongkorn University, his research topic was in the field of dust collection and was entitled as “Development of Rice Mill Dust Collection System Using Rice Husk Bed”



สถาบันวิทยบริการ
จุฬาลงกรณ์มหาวิทยาลัย